



Volume 2 Issue 1 2022

ISSN (Print): 2767-6412
ISSN (Online): 2767-3308

International Journal of Grey Systems

www.thescienceinsight.com **Science
Insight**

International Journal of Grey Systems is devoted to advancing the theory and practice of Grey System Theory as a novel mathematical approach to soft computing and computational intelligence. The journal is particularly interested in manuscripts that are backed by theory rather than tradition and can lead us to develop a scientifically rigorous body of knowledge on the Grey System Theory. Innovative ideas to manage uncertain systems that have the potential to create a debate are also of interest. Being the first open-access journal on the Grey System Theory, it is hoped to play a decisive role in mainstreaming the Grey System Theory by improving its understanding and global outreach. The journal seeks to foster communications between young and seasoned scholars and between scholars and practitioners with a view to aid data analysts, problem solvers, and decision-makers in handling complex problems objectively.

EDITOR-IN-CHIEF

Saad Ahmed Javed, Ph.D.

Nanjing University of Information Science and Technology, China

Email: drsaj@nuist.edu.cn

HONORARY EDITOR

Sifeng Liu, Ph.D.

Nanjing University of Aeronautics and Astronautics, China

EDITORIAL ASSISTANT

Yehuan Zhao,

Editorial Office, China

Email: 2497415255@qq.com

ASSOCIATE EDITORS

Delcea Camelia, Ph.D.

Bucharest University of Economic Studies, Romania

Erdal Aydemir, Ph.D.

Suleyman Demirel University, Turkey

Muhammad Ikram, Ph.D.

Al Akhawayn University, Morocco

Muhammad Nawaz, Ph.D.

National College of Business Administration & Economics, Pakistan

Wenjie Dong, Ph.D.

Nanjing University of Aeronautics and Astronautics, China

For colored images, please consult the electronic version of the journal.

For marketing, sales, and advertisement-related queries, please write to the publisher.

For collaboration or partnership, write to the Editorial Assistant or the publisher

For the proposals for Special Issues, please write to Editorial Assistant or Editor-in-chief.

For submitting a manuscript, please click on "Make A Submission" on the journal's website.

For reviewing manuscripts, please register at the journal's website.

For reading past issues, visit the website or write to the publisher.

All content published in the journal is subject to Creative Commons Attribution-NonCommercial 4.0 International.

No responsibility is accepted for the accuracy of information contained in the text, tables, illustrations or advertisements. The opinions expressed in the articles are not necessarily those of the Editor or the publisher.

For further information, please visit publish.thescienceinsight.com

Cover Image: Karma by Do Ho Suh
©unsplash.com/photos/tKgcMR8saYA
Cover Designer: Yehuan Zhao

PUBLISHER

Iqra Javed,

Science Insight, Florida, U.S.A.

Email: manager@thescienceinsight.com

ISSN (Print): 2767-6412

ISSN (Online): 2767-3308

© 2022 Science Insight

International Journal of Grey Systems

ISSN (Print) 2767-6412
ISSN (Online) 2767-3308
Volume 2
Issue 1
2022

Editor-in-chief
Saad Ahmed Javed

Editorial Advisory Board	3
A Conformable Fractional Discrete Grey Model CFDGM (1,1) and its Application <i>Wenqing Wu, Xin Ma, Hui Zhang, Xue Tian, Gaoxun Zhang and Peng Zhang</i>	5
Modeling and Grey Relational Multi-response Optimization of Chemical Additives and Engine Parameters on Performance Efficiency of Diesel Engine <i>Johnson Kehinde Abifarin and Joseph Chukwuka Ofodu Clifford Septian Candra</i>	16
Mechanical Properties Optimization and Modeling of Palm Kernel Shell Ash Reinforced Al-Mg-Si Composite using Grey Relational Analysis <i>Elijah Oyewusi Oyedeji, Muhammed Danda, Shehu Aliyu Yaro and Malik Abdulwahab</i>	33
Evaluation of Barriers to Electric Vehicle Adoption in Indonesia through Grey Ordinal Priority Approach <i>Clifford Septian Candra</i>	38

In the memory of Professor Deng Julong (1933 - 2013),
the founder of Grey System Theory

EDITORIAL ADVISORY BOARD

Arjab Singh Khuman, De Montfort University, UK

Bo Zeng, Chongqing Technology and Business University, China

Dan Cudjoe, Nanjing University of Information Science and Technology, China

Delcea Camelia, Bucharest University of Economic Studies, Romania

Ehsan Javanmardi, Nanjing University of Aeronautics and Astronautics, China

Erdal Aydemir, Suleyman Demirel University, Turkey

Hafeez Ullah, Shanghai Jiaotong University, China

Halis Bilgil, Aksaray University, Turkey

Izhar Mithal Jiskani, China University of Mining and Technology, China

Liangyan Tao, Nanjing University of Aeronautics and Astronautics, China

Lifeng Wu, Hebei University of Engineering, China

Mirjana Grdinić-Rakonjac, University of Montenegro, Montenegro

Moses Olabhele Esangbedo, Northwestern Polytechnical University, China

Muhammad Ikram, Al Akhawayn University, Morocco

Muhammad Nawaz, National College of Business Administration & Economics, Pakistan

Naiming Xie, Nanjing University of Aeronautics and Astronautics, China

Pourya Pourhejazy, National Taipei University of Technology, Taiwan

Rafal Mierzwiak, Poznań University of Technology, Poland

Syed Mithun Ali, Bangladesh University of Engineering and Technology, Bangladesh

Wanli Xie, Nanjing Normal University, China

Wenjie Dong, Nanjing University of Aeronautics and Astronautics, China

Xiaopeng Deng, Southeast University, China

Xin Ma, Southwest University of Science and Technology, China

Yong Liu, Jiangnan University, China

Yusuf Sahin, Burdur Mehmet Akif Ersoy University, Turkey

This Page Intentionally Left Blank

A Conformable Fractional Discrete Grey Model CFDGM (1,1) and its Application

Wenqing Wu^{1,*} | Xin Ma^{1,2,*} | Hui Zhang^{1,3} | Xue Tian¹
Gaoxun Zhang^{1,2} | Peng Zhang¹

¹School of Science, Southwest University of Science and Technology, Mianyang, 621010, P.R. China

²School of Economics & Management, Southwest University of Science and Technology, Mianyang, 621010, P.R. China

³School of Computer Science and Technology, Southwest University of Science and Technology, 621010, Mianyang, P.R. China

*Corresponding authors: wwqing0704@163.com; cauchy7203@gmail.com

Received 17 December 2021; Revised 21 January 2022; Accepted 22 January 2022

Abstract: An accurate forecast of the area of drought disaster is vitally important for the government to take appropriate measures to prevent disaster. In the current study, a new conformable fractional discrete grey model is applied to study the trend of the area affected by drought disasters. Firstly, the new model, abbreviated as CFDGM(1,1), is proposed with the definitions of the conformable fractional operator and the classical GM(1,1) model. Then the recursive expression of the time response function is obtained by the grey basic form, and the linear system parameters are confirmed by the linear least squares method. Further, the Salp Swarm Algorithm is chosen to determine the optimal conformable fractional order. Finally, the area of drought disaster is studied by the new model and others, where the results show the new model has a good performance among these models.

Keywords: Drought disaster; grey forecast model; conformable fractional operator; salp swarm algorithm

1. Introduction

Drought as a natural disaster happens due to climate variability under different climatic conditions on all continents and has a disastrous impact on the ecosystems, agricultural production, and economic and social conditions. Drought disaster is a serious problem in China, and the causes of drought disasters in various parts of China can be roughly summarised into three aspects. The first aspect is the precipitation, where the precipitation is lower than average in most places. The second aspect is the water resources because of the imbalance of water resources in different regions in China. The third aspect is the socio-economic factors such as the increasing water consumption in industrial and agricultural production in China in recent years. Due to these factors, the drought disasters happened, and the area of the drought disaster was also influenced.

To study the area of drought disaster, the current study uses the grey forecasting models. The grey theory was proposed by professor Deng (1982), and the grey system refers to an incomplete information system with partially clear and partially unclear information. The grey predicting theory is an important part of the grey system, and it does not require a lot of data for modeling to achieve

accurate results. The first-order univariate grey forecasting model GM(1,1) is the core of grey forecasting models, where the time response function is derived by its whitening differential equation and the system parameters are derived by the grey basic form. To improve the precision of the GM(1,1) model, Javed and Cudjoe (2022) considered DGM(1,1, α) model and applied to forecast the emissions in four industries sectors of China and India. Gou *et al.* (2022) proposed a new high-performance grey prediction model FDGM(1,1, \sqrt{k} , r) for wastewater discharge prediction. Gao *et al.* (2022) studied a novel grey Gompertz model FAGGM(1,1) for carbon emission forecasting in the American industrial sector. Ma *et al.* (2020) first proposed a new conformable fractional grey model CFGM(1,1), in which the conformable fractional operator is used for the pretreatment of raw data. The conformable fractional operator is much easier for theoretical analysis and applications than the classical fractional operator. With a series of numerical examples, the results demonstrate that the new model is more efficient in non-smooth time series prediction and longer-term forecasting than the classical fractional grey model FGM(1,1) proposed by Wu *et al.* (2013). Subsequently, Wu *et al.* (2020) studied a conformable fractional non-homogeneous grey model and used it to forecast the carbon dioxide emissions of BRICS countries. The results obtained by the newly constructed model are compared with the models NGM(1,1,k,c), NGMO(1,1,k,c), FGM(1,1), FANGM(1,1,k,c) and showed that the model CFNGM(1,1,k,c) outperformed others in terms of forecast accuracy.

Xie *et al.* (2020a) proposed a continuous conformable fractional grey model CCFGM(1,1) with the definition of conformable fractional derivative and then applied it to the domestic energy consumption of China and the domestic coal consumption of China. Xie *et al.* (2020b) studied the annual electricity consumption of China by a CFGOM(1,1) with the opposite direction. Zheng *et al.* (2021) proposed a conformable fractional non-homogeneous grey Bernoulli model to study natural gas production and consumption. Liu *et al.* (2021) considered Jiangsu's electricity consumption with two types of conformable fractional grey interval models. Due to the conformable fractional operator being simple and easy to implement, there have been considerable pieces of literature on conformable fractional grey models during the last two years, see Wu *et al.* (2022a; 2022b; 2019), Xie *et al.* (2021; 2020c), and Xu *et al.* (2020). These works enriched and improved the conformable fraction grey models in theory and applications.

In the CFGM(1,1) model (Ma *et al.*, 2020), the time response function is obtained by solving the whitening differential equation, and the linear system parameters are derived by the grey basic form. However, the whitening differential equation and the grey basic form of the CFGM(1,1) model are inconsistent because the background values are deduced with the help of the trapezoidal approximation formula. This treatment may cause large errors in some applications. Therefore, inspired by the above research work, this study introduces the conformable fractional accumulation and difference into the classical univariate discrete grey model to construct a new grey model called CFDGM(1,1) and then applies it to the area of drought disaster.

The rest of this paper is organised as follows. The next section systematically studies the CFDGM(1,1) model. We first give the definition of the conformable fractional accumulation and difference and then give the definition of the new model. With the theory of the ordinary differential equations, the least squares estimation method, and the salp swarm algorithm, the expressions of the time response function and system parameters are determined. Section 3 studies the area of drought disaster in China. Conclusions are drawn in the last section.

2. The conformable fractional discrete grey model

The definition of the conformable fractional operator, and the properties of the proposed models are discussed in this section.

2.1 The conformable fractional operator

This subsection introduces the definition of the conformable fractional operator, including the conformable fractional accumulation and conformable fractional difference.

DEFINITION 1 (Wu et al., 2020). The expression of the conformable fractional accumulation is given by

$$\nabla^{\alpha} f(k) = \sum_{i=1}^k \binom{k-i+\lceil \alpha \rceil - 1}{k-i} \frac{f(i)}{i^{\lceil \alpha \rceil - \alpha}}, \alpha > 0, \quad (1)$$

where the combine number $\binom{k-i+\lceil \alpha \rceil - 1}{k-i} = \frac{(k-i+\lceil \alpha \rceil - 1)!}{(k-1)!(\lceil \alpha \rceil - 1)!}$, and $\lceil \alpha \rceil$ is the smallest integer greater than or equal to α .

DEFINITION 2 (Wu et al., 2020). The expression of the conformable fractional difference is given by

$$\Delta^{\alpha} f(k) = k^{\lceil \alpha \rceil - \alpha} \binom{\lceil \alpha \rceil}{k-i} f(i), \alpha > 0, \quad (2)$$

where $\binom{\lceil \alpha \rceil}{k-i} = \frac{\lceil \alpha \rceil!}{(\lceil \alpha \rceil - k + 1)!(k-i)!}$.

DEFINITION 3 (Ma et al., 2020). Let sequence be $X^{(0)} = (x^{(0)}(1), x^{(0)}(2), \dots, x^{(0)}(n))$, the α^{th} conformable fractional accumulation (α -CFA) sequence is $X^{(\alpha)} = (x^{(\alpha)}(1), x^{(\alpha)}(2), \dots, x^{(\alpha)}(n))$, and the α^{th} conformable fractional difference (α -CFD) sequence is $X^{(-\alpha)} = (x^{(-\alpha)}(1), x^{(-\alpha)}(2), \dots, x^{(-\alpha)}(n))$. The expression of them are outlined as follows.

$$x^{(\alpha)}(k) = \sum_{i=1}^k \binom{\lceil \alpha \rceil}{k-i} \frac{1}{i^{\lceil \alpha \rceil - \alpha}} x^{(0)}(i), \alpha > 0 \quad (k=1, 2, \dots, n), \quad (3)$$

$$x^{(-\alpha)}(k) = k^{\lceil \alpha \rceil - \alpha} \sum_{i=1}^k \binom{-\lceil \alpha \rceil}{k-i} x^{(0)}(i), \alpha > 0 \quad (k=1, 2, \dots, n). \quad (4)$$

2.2 The CFDGM (1, 1) model

DEFINITION 4. With the classical grey prediction model GM (1,1) and the conformable fractional accumulation, the whitening differential equation of the new model is

$$\frac{dx^{(\alpha)}(t)}{dt} + b_1 x^{(\alpha)}(t) = b_2, \quad (5)$$

where b_1 is the development coefficient, b_2 is the grey action quantity, and α is the conformable fractional order accumulation.

Integrating both sides of the whitening differential Eq. (5) on the interval $[k-1, k]$, it can calculate that

$$\int_{k-1}^k dx^{(\alpha)}(t) + b_1 \int_{k-1}^k x^{(\alpha)}(t) dt = b_2 \int_{k-1}^k dt. \quad (6)$$

Solving Eq. (6) with the trapezoidal approximation formula, it can be simplified that

$$x^{(\alpha)}(k) - x^{(\alpha)}(k-1) + b_1 \frac{x^{(\alpha)}(k) + x^{(\alpha)}(k-1)}{2} = b_2, \quad (7)$$

which also arrivals

$$(2 + b_1)x^{(\alpha)}(k) - (2 - b_1)x^{(\alpha)}(k-1) = 2b_2. \quad (8)$$

Thus, it is obvious that

$$x^{(\alpha)}(k) - \frac{2-b_1}{2+b_1}x^{(\alpha)}(k-1) = \frac{2b_2}{2+b_1}, \quad (9)$$

which is the grey basic form of the whitening differential equation. And then, we will deduce the expression of the model with Eq. (9), which is called conformable fractional discrete grey model CFDGM(1,1).

THEOREM 1. The recursive formula of the time response function of the CFDGM(1,1) model is

$$x^{(\alpha)}(k) = \left(\frac{2-b_1}{2+b_1}\right)^{k-1} x^{(\alpha)}(1) + \frac{b_2}{b_1} \left[1 - \left(\frac{2-b_1}{2+b_1}\right)^{k-1}\right], \quad k = 2, 3, \dots, \quad (10)$$

and the restored values are

$$x^{(-\alpha)}(k) = k^{\lceil \alpha \rceil - \alpha} \sum_{i=1}^k \left[\frac{-\lceil \alpha \rceil}{k-i} \right] x^{(0)}(i), \quad \alpha > 0, \quad k = 1, 2, \dots, n. \quad (11)$$

PROOF 1. It follows from the grey basic form of the CFDGM(1,1) model that

$$\begin{aligned} x^{(\alpha)}(k) - \frac{2-b_1}{2+b_1}x^{(\alpha)}(k-1) &= \frac{2b_2}{2+b_1}, \\ x^{(\alpha)}(k-1) - \frac{2-b_1}{2+b_1}x^{(\alpha)}(k-2) &= \frac{2b_2}{2+b_1}, \\ x^{(\alpha)}(k-2) - \frac{2-b_1}{2+b_1}x^{(\alpha)}(k-3) &= \frac{2b_2}{2+b_1}, \\ &\vdots \\ x^{(\alpha)}(2) - \frac{2-b_1}{2+b_1}x^{(\alpha)}(1) &= \frac{2b_2}{2+b_1}. \end{aligned}$$

Multiplying factors $\left(\frac{2-b_1}{2+b_1}\right)^i$ ($i = 0, 1, \dots, k-2$) on both sides of this equations, we obtain

the following set of equations

$$\begin{aligned} \left(\frac{2-b_1}{2+b_1}\right)^0 \left[x^{(\alpha)}(k) - \frac{2-b_1}{2+b_1}x^{(\alpha)}(k-1) \right] &= \left(\frac{2b_2}{2+b_1}\right) \left(\frac{2-b_1}{2+b_1}\right)^0, \\ \left(\frac{2-b_1}{2+b_1}\right)^1 \left[x^{(\alpha)}(k-1) - \frac{2-b_1}{2+b_1}x^{(\alpha)}(k-2) \right] &= \left(\frac{2b_2}{2+b_1}\right) \left(\frac{2-b_1}{2+b_1}\right)^1, \\ \left(\frac{2-b_1}{2+b_1}\right)^2 \left[x^{(\alpha)}(k-2) - \frac{2-b_1}{2+b_1}x^{(\alpha)}(k-3) \right] &= \left(\frac{2b_2}{2+b_1}\right) \left(\frac{2-b_1}{2+b_1}\right)^2 \end{aligned}$$

$$\begin{aligned} & \vdots \\ & \left(\frac{2-b_1}{2+b_1} \right)^{k-2} \left[x^{(\alpha)}(2) - \frac{2-b_1}{2+b_1} x^{(\alpha)}(1) \right] = \left(\frac{2b_2}{2+b_1} \right) \left(\frac{2-b_1}{2+b_1} \right)^{k-2}, \end{aligned}$$

then we add these equations together to produce the following results

$$x^{(\alpha)}(k) = \left(\frac{2-b_1}{2+b_1} \right)^{k-1} x^{(\alpha)}(1) + \frac{b_2}{b_1} \left[1 - \left(\frac{2-b_1}{2+b_1} \right)^{k-1} \right], \quad k = 2, 3, \dots,$$

and then we complete this proof by the conformable fractional operator.

It can be seen that the system parameters b_1 and b_2 in Eqs. (10) and (11) are unknown and needs to be determined. Thus the following theorem gives the expression of system linear parameters b_1 and b_2 .

THEOREM 2. The system linear parameters b_1 and b_2 of the CFDGM (1, 1) model can be expressed as follows.

$$(b_1, b_2)^T = (B^T B)^{-1} (B^T Y), \quad (12)$$

where the matrices B and Y are

$$B = \begin{pmatrix} \frac{x^{(\alpha)}(1) + x^{(\alpha)}(2)}{2} & -1 \\ \frac{x^{(\alpha)}(2) + x^{(\alpha)}(3)}{2} & -1 \\ \vdots & \vdots \\ \frac{x^{(\alpha)}(r-1) + x^{(\alpha)}(r)}{2} & -1 \end{pmatrix}, \quad Y = \begin{pmatrix} x^{(\alpha)}(1) - x^{(\alpha)}(2) \\ x^{(\alpha)}(2) - x^{(\alpha)}(3) \\ \vdots \\ x^{(\alpha)}(r-1) - x^{(\alpha)}(r) \end{pmatrix}.$$

PROOF 2. Integrating the whitening differential Eq. (5) and organising it, we obtain

$$\int_{k-1}^k dx^{(\alpha)}(t) + b_1 \int_{k-1}^k x^{(\alpha)}(t) dt = b_2 \int_{k-1}^k dt.$$

Applying the trapezoid approximation formula $\int_{k-1}^k x^{(\alpha)}(t) dt = \frac{x^{(\alpha)}(k) + x^{(\alpha)}(k-1)}{2}$, so it yields that

$$x^{(\alpha)}(k) - x^{(\alpha)}(k-1) + b_1 \frac{x^{(\alpha)}(k) + x^{(\alpha)}(k-1)}{2} = b_2. \quad (12)$$

It is easily to achieve that

$$b_1 \frac{x^{(\alpha)}(k) + x^{(\alpha)}(k-1)}{2} - b_2 = x^{(\alpha)}(k) - x^{(\alpha)}(k-1).$$

Considering $k = 2, 3, \dots, r$ in the above equation, and writing them in matrix form, it arrives that

$$\begin{pmatrix} \frac{x^{(\alpha)}(1) + x^{(\alpha)}(2)}{2} & -1 \\ \frac{x^{(\alpha)}(2) + x^{(\alpha)}(3)}{2} & -1 \\ \vdots & \vdots \\ \frac{x^{(\alpha)}(r-1) + x^{(\alpha)}(r)}{2} & -1 \end{pmatrix} \begin{pmatrix} b_1 \\ b_2 \end{pmatrix} = \begin{pmatrix} x^{(\alpha)}(1) - x^{(\alpha)}(2) \\ x^{(\alpha)}(2) - x^{(\alpha)}(3) \\ \vdots \\ x^{(\alpha)}(r-1) - x^{(\alpha)}(r) \end{pmatrix},$$

and then the expression of system linear parameters of the new model is computed by

$$(b_1, b_2)^T = (B^T B)^{-1} (B^T Y).$$

2.3 The Salp Swarm Algorithm for optimal conformable fractional order

This subsection outlines the details of the search process for the optimal conformable fractional order α . At first, some measures are provided to show the feasibility and accuracy of grey forecasting models: the absolute percentage error (APE) and the mean absolute percentage error (MAPE). The mathematical formulas of them are produced below.

The absolute percentage error (APE)

$$APE(k) = \left| \frac{\hat{x}^{(0)}(k) - x^{(0)}(k)}{x^{(0)}(k)} \right| \times 100\%, (k = 2, 3, \dots). \quad (14)$$

The mean absolute percentage error (MAPE)

$$MAPE = \frac{1}{n} \sum_{k=1}^n \left| \frac{\hat{x}^{(0)}(k) - x^{(0)}(k)}{x^{(0)}(k)} \right| \times 100\%, (k = 2, 3, \dots). \quad (14)$$

It can be seen from the above analysis that the values of parameters b_1 and b_2 can be calculated by the least squares estimation method, and the remaining task is to find the value of the conformable fractional order. Thus an optimisation problem where α is a decision variable is constructed, where the corresponding objective function is given below.

$$\begin{aligned} MAPE_{\alpha} &= \frac{1}{r} \sum_{k=1}^r \left| \frac{\hat{x}^{(0)}(k) - x^{(0)}(k)}{x^{(0)}(k)} \right| \times 100\%, k = 2, 3, \dots, \\ \text{s.t.} \quad &\begin{cases} (b_1, b_2)^T = (B^T B)^{-1} (B^T Y), \\ x^{(\alpha)}(k) = \left(\frac{2-b_1}{2+b_1} \right)^{k-1} x^{(\alpha)}(1) + \frac{b_2}{b_1} \left[1 - \left(\frac{2-b_1}{2+b_1} \right)^{k-1} \right], k = 2, 3, \dots, \\ x^{(0)}(k) = k^{\lceil \alpha \rceil - \alpha} \sum_{i=1}^k \left[\frac{-\lceil \alpha \rceil}{k-i} \right] x^{(\alpha)}(i), \alpha > 0, k = 1, 2, \dots, n. \end{cases} \end{aligned}$$

It is known that it's an arduous task to derive the closed-form expression of the optimal conformable fractional order because this optimisation problem is highly nonlinear and complex. Therefore, the nature-inspired algorithm called Salp Swarm Algorithm (SSA) (Mirjalili et al., 2017) is adapted to numerically find α . This algorithm is a new type of bionic swarm intelligence

algorithm. The algorithm has some advantages, such as fewer adjustment parameters, easy-to-understand concepts, less difficulty in programming, and good directionality in optimisation. The pseudo-code of the Salp Swarm Algorithm is presented below.

```

Initialise the salp population  $x_i(i=1,2,\dots,n)$  considering upper bound  $ub$  and lower bound  $lb$  of  $\alpha$ .
While (end condition is not satisfied)
  Calculate the fitness of each search agent (salp)
  F=the best search agent

  Update  $c_1$  by  $c_1 = 2e^{-\left(\frac{4l}{L}\right)^2}$ 

  for each salp ( $X_i$ )
    if ( $i == 1$ )
      Update the position of the leading salp by
      
$$x_j^1 = \begin{cases} F_j + c_1((ub_j - lb_j)c_2 + lb_j) & c_3 \geq 0 \\ F_j - c_1((ub_j - lb_j)c_2 + lb_j) & c_3 < 0 \end{cases}$$

    else
      Update the position of the follower salp by  $x_j^i = \frac{1}{2}(x_j^i + x_j^{i-1})$ 
    end
  end
  Amend the salps based on the upper and lower bounds of variables
end
return F

```

3. Applications

This application section discusses the area of drought disaster in China by different grey forecasting models, including the DGM(1,1), FDGM(1,1) and CFDGM(1,1) models. The raw data of the area of drought disaster of China are all collected from the website of the National Bureau of Statistics (<https://data.stats.gov.cn/easyquery.htm?cn=C01>) and is presented in Table 1. These data are divided into two parts, the first part from the year 2010 to 2016 is used for modelling, and the second part from 2017 to 2019 is used for out-of-sample testing.

It is known that the whole modelling process can be established when system parameters b_1 , b_2 and α are determined. Here the detailed modeling process of the CFDGM(1,1) model is shown. According to Table 1, the raw data on the area of drought disaster in China is

$$X^{(0)} = (13258.6, 16304.2, 9339.8, 1410.4, 12271.7, 10609.7, 9872.7, 9874.8, 7711.8, 7838.0).$$

Firstly, according to the Salp Swarm Algorithm and the raw data of the year from 2010 to 2016, we obtain the system nonlinear parameter $\alpha = 0.9188$. Then on the base of Theorem 2, the values of B and Y can be given as follows.

$$B = \begin{pmatrix} 20964.7125 & -1 \\ 32942.3244 & -1 \\ 43513.7163 & -1 \\ 55198.0466 & -1 \\ 65169.3050 & -1 \\ 73971.2518 & -1 \end{pmatrix}, \quad Y = \begin{pmatrix} -15412.2249 \\ -8542.9990 \\ -12599.7846 \\ -10768.8760 \\ -9173.6408 \\ -8430.2527 \end{pmatrix}.$$

Table 1. The raw data of the area of drought disaster of China (thousand hectares)

Year	2010	2011	2012	2013	2014
Data	13258.6	16304.2	9339.8	14100.4	12271.7
Year	2015	2016	2017	2018	2019
Data	10609.7	9872.7	9874.8	7711.8	7838.0

It follows from formula $(b_1, b_2)^T = (B^T B)^{-1} (B^T Y)$ that $b_1=0.0944$, $b_2=15413.6863$. And then the expression of grey model CFDGM(1,1) can be written as

$$x^{(\alpha)}(k) = 0.9098^{k-1} x^{(\alpha)}(1) + 163207.9470 [1 - 0.9098^{k-1}], \quad k = 2, 3, \dots,$$

and the restored values of the CFDGM(1,1) model are easily computed. Actually, the other grey forecasting models DGM(1,1) and FDGM(1,1) can also be established. The computational results and errors are tabulated in Table 2 and Figure 1, and all results are reported to two decimal places.

It follows from Table 2 and Figure 1 that the three discrete grey models successfully catch the trend of the area of the drought disaster in China. The MAPE_{simu}, MAPE_{pred} and MAPE_{all} of the DGM(1,1) model are 12.54%, 6.87% and 10.65%, those of the FDGM(1,1) model are 12.37%, 6.19%, 10.31%, and those of the CFDGM(1,1) model are 12.31%, 6.18% and 10.27%, respectively. It is seen that the CFDGM(1,1) model obtains better results than the other discrete grey models. However, it must be admitted that their accuracy is basically the same, and they are all suitable for the area of drought disaster of China.

To further study the accuracy of the three grey discrete models, we consider the following two cases.

Case 1: The raw data from 2010 to 2015 are used for modelling, and the raw data from 2016 to 2019 are used for out-of-sample testing ($r = 6$).

Case 2: The raw data from 2010 to 2017 are used for modelling, and the raw data from 2018 to 2019 are used for out-of-sample testing ($r = 8$).

The computational results and corresponding errors are listed in Table 3 and Figure 2, and Table 4 and Figure 3, respectively.

It follows from Table 3 and Figure 2 that the MAPE_{simu}, MAPE_{pred} and MAPE_{all} of the DGM(1,1) model are 14.85%, 6.39% and 11.09%, those of the FDGM(1,1) model are 13.53%, 99.93%, 51.93%, and those of the CFDGM(1,1) model are 14.70%, 6.01% and 10.84%, respectively. It is obvious that the FDGM(1,1) model is inapplicable in the area of drought disasters in China.

It can be seen in Table 4 and Figure 3 that the MAPE_{simu}, MAPE_{pred} and MAPE_{all} of the DGM(1,1) model are 11.62%, 10.86% and 11.45%, those of the FDGM(1,1) model are 11.04%, 19.73%, 12.97%, and those of the CFDGM(1,1) model are 11.62%, 10.86% and 11.45%,

Table 2. The computational results of the DGM(1,1), FDGM(1,1) and CFDGM(1,1) models

Year	Data	DGM(1,1)	APE	FDGM(1,1)	APE	CFDGM(1,1)	APE
				<i>fractional order=0.9185</i>		<i>fractional order=0.9188</i>	
2010	13258.6	13258.60	0.00	13258.60	0.00	13258.60	0.00
2011	16304.2	14372.39	11.85	14231.56	12.71	14305.58	12.26
2012	9339.8	13366.88	43.12	13467.11	44.19	13450.93	44.02
2013	14100.4	12431.71	11.83	12555.11	10.96	12527.01	11.16
2014	12271.7	11561.97	5.78	11626.16	5.26	11605.59	5.43
2015	10609.7	10753.08	1.35	10725.76	1.09	10716.38	1.01
2016	9872.7	10000.78	1.30	9872.70	0.00	9872.70	0.00
2017	9874.8	9301.11	5.81	9074.57	8.10	9080.23	8.05
2018	7711.8	8650.39	12.17	8333.56	8.06	8340.70	8.16
2019	7838.0	8045.20	2.64	7649.10	2.41	7653.69	2.35
MAPE _{simu}			12.54		12.37		12.31
MAPE _{pred}			6.87		6.19		6.18
MAPE _{all}			10.65		10.31		10.27

Table 3. The computational results of the DGM(1,1), FDGM(1,1) and CFDGM(1,1) models (case 1)

Year	Data	DGM(1,1)	APE	FDGM(1,1)	APE	CFDGM(1,1)	APE
				<i>fractional order</i> =1.6157		<i>fractional order</i> =0.8579	
2010	13258.6	13258.60	0.00	13258.60	0.00	13258.60	0.00
2011	16304.2	14326.53	12.13	16304.20	0.00	14299.76	12.29
2012	9339.8	13361.47	43.06	11324.73	21.25	13520.58	44.76
2013	14100.4	12461.42	11.62	11114.39	21.18	12571.67	10.84
2014	12271.7	11622.00	5.29	11760.07	4.17	11582.65	5.62
2015	10609.7	10839.12	2.16	12842.73	21.05	10609.70	0.00
2016	9872.7	10108.98	2.39	14256.47	44.40	9679.65	1.96
2017	9874.8	9428.02	4.52	15976.41	61.79	8805.30	10.83
2018	7711.8	8792.94	14.02	18009.50	133.53	7992.02	3.63
2019	7838.0	8200.63	4.63	20379.47	160.01	7241.06	7.62
MAPE _{simu}			14.85		13.53		14.70
MAPE _{pred}			6.39		99.93		6.01
MAPE _{all}			11.09		51.93		10.84

Table 4. The computational results of the DGM(1,1), FDGM(1,1) and CFDGM(1,1) models (case 2)

Year	Data	DGM(1,1)	APE	FDGM(1,1)	APE	CFDGM(1,1)	APE
				<i>fractional order</i> =1.1497		<i>fractional order</i> =1.0000	
2010	13258.6	13258.60	0.00	13258.60	0.00	13258.60	0.00
2011	16304.2	14268.10	12.49	14767.29	9.43	14268.10	12.49
2012	9339.8	13339.12	42.82	13109.57	40.36	13339.12	42.82
2013	14100.4	12470.63	11.56	12124.66	14.01	12470.63	11.56
2014	12271.7	11658.68	5.00	11397.32	7.13	11658.68	5.00
2015	10609.7	10899.60	2.73	10809.91	1.89	10899.60	2.73
2016	9872.7	10189.94	3.21	10311.38	4.44	10189.94	3.21
2017	9874.8	9526.48	3.53	9874.80	0.00	9526.48	3.53
2018	7711.8	8906.22	15.49	9484.17	22.98	8906.22	15.49
2019	7838.0	8326.35	6.23	9129.22	16.47	8326.35	6.23
MAPE _{simu}			11.62		11.04		11.62
MAPE _{pred}			10.86		19.73		10.86
MAPE _{all}			11.45		12.97		11.45

respectively. These results show the FDGM(1,1) model is also inapplicable in the area of drought disasters in China. Moreover, we can see the optimal conformable fractional order of the CFDGM(1,1) model $\alpha = 1.0000$, and then it reduces to the classical DGM(1,1) model and has the same results in this case. It can also conclude that the CFDGM(1,1) model is suitable for the area of drought disasters in China.

4. Conclusion

In the current study, the area of China affected by the drought disaster is studied by using three discrete grey models, namely, the DGM(1,1) model, the FDGM(1,1) model, and the CFDGM(1,1) model. The optimal conformable fractional order is determined by the salp swarm algorithm. And we considered three different cases to study the accuracy of different grey models. The computational results show that the CFDGM(1,1) model performs better than the other discrete grey models, where the mean absolute prediction error MAPE_{pred} in the three cases are 6.18%, 6.01%, and 10.86%, respectively. Moreover, it can be seen from Tables 2 – 4 and Figures 1 – 3 that the fractional order of the FDGM(1,1) model ranges from 0.9185 to 1.6157, and the conformable fractional order of the CFDGM(1,1) model ranges from 0.8579 to 1.0000. This means the CFDGM(1,1) model needs a narrower range of conformable fractional order and obtains higher accuracy results than the FDGM(1,1) in China's drought disaster.

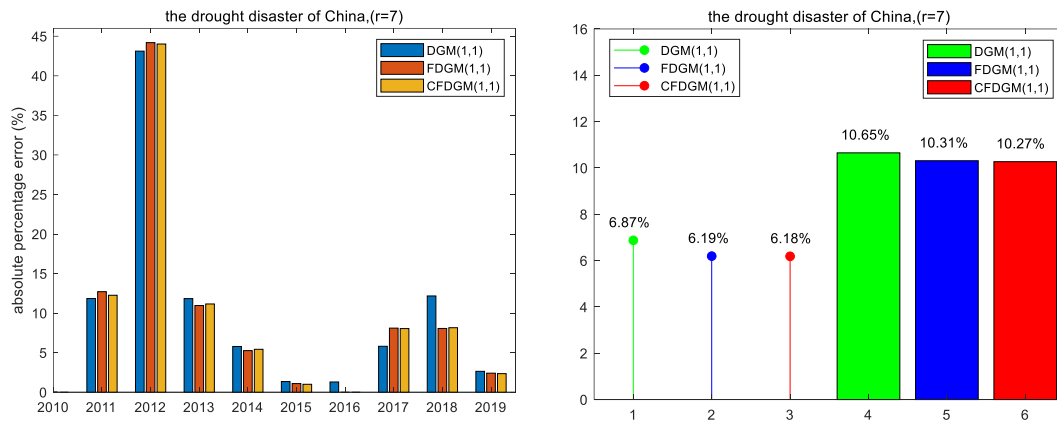


Fig 1. Results among the DGM(1,1), FDGM(1,1) and CFDGM(1,1) models

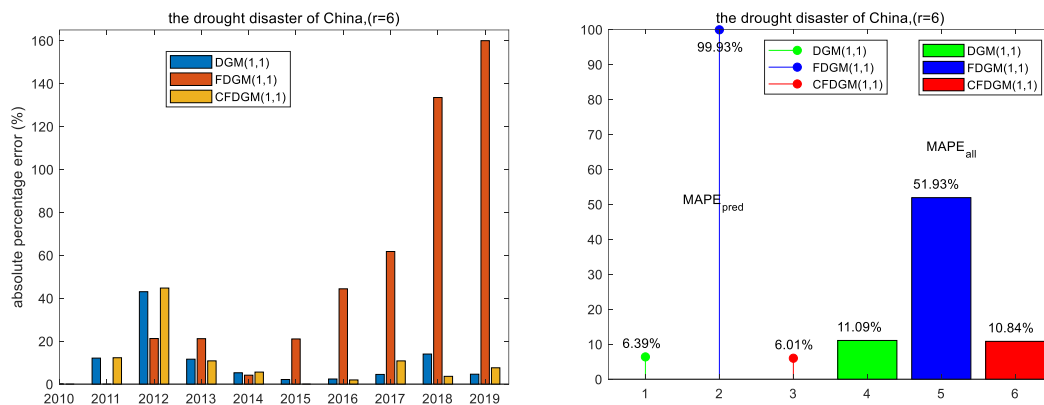


Fig 2. Results among the DGM(1,1), FDGM(1,1) and CFDGM(1,1) models (case 1)

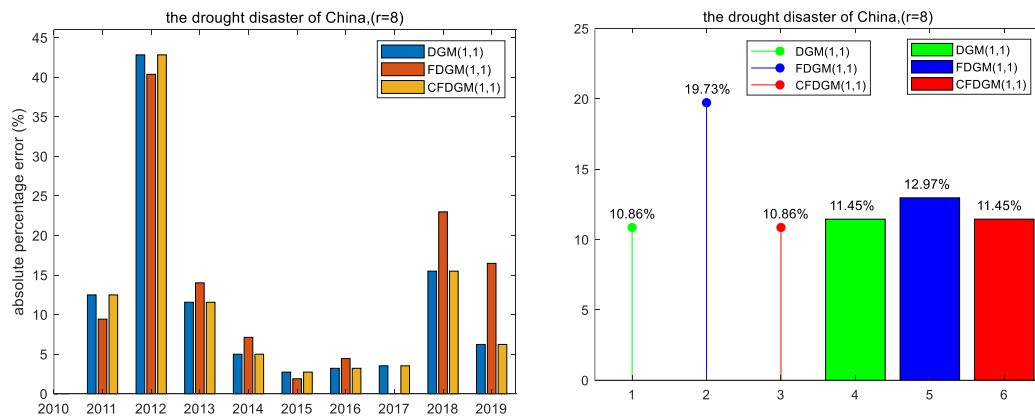


Fig 3. Results among the DGM(1,1), FDGM(1,1) and CFDGM(1,1) models (case 2)

Actually, the accuracy of the CFDGM(1,1) model has much room for improvement owing to the best $MAPE_{pred}$ is 6.01% in the area of drought disaster in China. On the one hand, the raw data of China's drought disaster exhibits considerable variation, while the CFDGM(1,1) model is a linear model and cannot depict the data's fluctuation features. On the other hand, it is infeasible to consider other factors, such as population, and meteorological, which affect the current situation of China's drought disaster in the newly proposed model owing to the CFDGM(1,1) model is univariate. In the future, some nonlinear grey forecasting models or multivariate grey forecasting models with conformable fractional order can be considered and applied to the area of drought disaster in China.

Acknowledgement

This work is supported by the National Natural Science Foundation of China (No.72001181, 71901184), the funding of V.C. & V.R. Key Lab of Sichuan Province (SCVCVR2020.01VS), the Key R&D projects of Sichuan Science and Technology Department (No.2021YFG0031), and the fund of the provincial scientific research institutes' achievement transformation project of the science and technology department of Sichuan Province (2022JDZH0035).

References

- Deng, J.-L. (1982). Control problems of grey systems. *Systems & Control Letters*, 1(5), 288-294. [https://doi.org/10.1016/S0167-6911\(82\)80025-X](https://doi.org/10.1016/S0167-6911(82)80025-X)
- Gao, M.-Y., Yang, H.-L., Xiao Q.-Z., & Goh, M. (2022). A novel method for carbon emission forecasting based on Gompertz's law and fractional grey model: evidence from American industrial sector. *Renewable Energy*, 181, 803-819. <https://doi.org/10.1016/j.renene.2021.09.072>
- Gou, X.-Y., Zeng, B., & Gong, Y. (2022). Application of the novel four-parameter discrete optimised grey model to forecast the wastewater discharged in Chongqing China. *Engineering Applications of Artificial Intelligence*, 107, 104522. <https://doi.org/10.1016/j.engappai.2021.104522>
- Javed, S.A., & Cudjoe, D. (2022). A novel grey forecasting of greenhouse gas emissions from four industries of China and India. *Sustainable Production and Consumption*, 29, 777-790. <https://doi.org/10.1016/j.spc.2021.11.017>
- Liu, Y.-T., Xue, D.-Y., & Yang, Y. (2021). Two types of conformable fractional grey interval models and their applications in regional electricity consumption prediction. *Chaos, Solitons & Fractals*, 153, 111628. <https://doi.org/10.1016/j.chaos.2021.111628>
- Ma, X., Wu, W.-Q., Zeng B., Wang, Y., & Wu, X.-X. (2020). The conformable fractional grey system model. *ISA Transactions*, 96, 255-271. <https://doi.org/10.1016/j.isatra.2019.07.009>
- Mirjalili, S., Gandomi, A.-H., Mirjalili, S.-Z., Saremi, S., Faris, H., & Mirjalili, S.-M. (2017). Salp Swarm Algorithm: A bio-inspired optimiser for engineering design problems. *Advances in Engineering Software*, 114, 163-191. <https://doi.org/10.1016/j.advengsoft.2017.07.002>
- Wu, L.-F., Liu, S.-F., Yao, L.-G., Yan, S.-L., & Liu, D.-L. (2013). Grey system model with the fractional order accumulation. *Communications in Nonlinear Science and Numerical Simulation*, 18(7), 1775-1785. <https://doi.org/10.1016/j.cnsns.2012.11.017>
- Wu, W.-Q., Ma, X., Zhang, Y.-Y., Li, W.-P., & Wang, Y. (2020). A novel conformable fractional non-homogeneous grey model for forecasting carbon dioxide emissions of BRICS countries. *Science of the Total Environment*, 707, 135447. <https://doi.org/10.1016/j.scitotenv.2019.135447>
- Wu, W.-Q., Ma, X., Zeng, B., Zhang, H., & Zhang, P. (2022a) A novel multivariate grey system model with conformable fractional derivative and its applications, *Computers & Industrial Engineering*, 164, 107888. <https://doi.org/10.1016/j.cie.2021.107888>
- Wu, W.-Z., Jiang, J.-M., & Li, Q. (2019). A novel discrete grey model and its application. *Mathematical Problems in Engineering*, 2019, 9623878. <https://doi.org/10.1155/2019/9623878>
- Wu, W.-Z., Xie, W.-L., Liu, C., & Zhang T. (2022b). A novel fractional discrete nonlinear grey Bernoulli model for forecasting the wind turbine capacity of China. *Grey Systems: Theory and Application*, 12 (2), 357-375. <https://doi.org/10.1108/GS-08-2020-0113>
- Xie, W.-L., Liu, C.-X., Wu, W.-Z., Li, W.-D., & Liu, C. (2020a). Continuous grey model with conformable fractional derivative. *Chaos, Solitons & Fractals*, 139, 110285. <https://doi.org/10.1016/j.chaos.2020.110285>
- Xie, W.-L., Wu, W.-Z., Liu, C., & Zhao, J.-J. (2020b). Forecasting annual electricity consumption in China by employing a conformable fractional grey model in opposite direction. *Energy*, 202, 117682. <https://doi.org/10.1016/j.energy.2020.117682>
- Xie, W.-L., & Yu, G.-X. (2020c) A novel conformable fractional nonlinear grey Bernoulli model and its application. *Complexity*, 2020, 9178098. <https://doi.org/10.1155/2020/9178098>
- Xie, W.-L., Wu, W.-Z., Liu, C., Zhang, T., & Dong, Z.-J. (2021). Forecasting fuel combustion-related CO₂ emissions by a novel continuous fractional nonlinear grey Bernoulli model with grey wolf optimiser, *Environmental Science and Pollution Research*, 28, 38128-38144. <https://doi.org/10.1007/s11356-021-12736-w>
- Xu, Z.-C., Dun, M., & Wu, L.-F. (2020) Prediction of air quality based on hybrid grey double exponential smoothing model. *Complexity*, 2020, 9427102. <https://doi.org/10.1155/2020/9427102>
- Zheng, C.-L., Wu, W.-Z., Xie W.-L., & Li, Q. (2021). A MFO-based conformable fractional non-homogeneous grey Bernoulli model for natural gas production and consumption forecasting, *Applied Soft Computing*, 99, 106891. <https://doi.org/10.1016/j.asoc.2020.106891>

Modeling and Grey Relational Multi-response Optimization of Chemical Additives and Engine Parameters on Performance Efficiency of Diesel Engine

Johnson Kehinde Abifarin^{1,*} | Joseph Chukwuka Ofodu²

¹Department of Mechanical Engineering, Ahmadu Bello University, Zaria, Nigeria

²Department of Mechanical Engineering, University of Port Harcourt, Nigeria

*Corresponding author: jkabifarin@abu.edu.ng

Received 28 October 2021; Revised 24 December 2021; Accepted 17 January 2022

Abstract: Singular optimization of engine conditions for better engine performance have been studied extensively. However, in the practical sense, more than one performance characteristics are essential in the optimization of engine conditions. The current study investigates the effect, optimization, and modeling of engine conditions on multi-characteristics of a single cylinder-dual direct injection-water cooled diesel engine with the help of Taguchi-grey relational and regression analyses. The engine conditions employed are engine load, hydrogen, multi-walled carbon nanotubes (MWCNTs), ignition pressure, and ignition timing, at four different levels. The engine performance characteristics analyzed were brake thermal efficiency (BTE), brake specific fuel consumption (BSFC), hydrocarbons (HC), nitrogen oxide (NO_x), carbon monoxide (CO), and carbon dioxide (CO₂). The results showed that there was a similar behavioral pattern of the effect of engine conditions on engine performance, except for ignition timing. The optimal settings for better engine performance were obtained at 25% engine load, 20% hydrogen, 50 ppm MWCNTs, 220 bar ignition pressure, and 21 obTDC ignition timing. Interestingly, the discovered optimal did not fall within the considered experimental runs, however, the predicted optimal engine performance was within 95% confidence bounds. It is recommended that the experimental work based on the obtained optimal settings should be conducted to elucidate the efficacy of the confirmation analysis. The analysis of variance showed that the engine load was the most significant factor on the overall engine performance, having a contribution of 71.47%, followed by hydrogen and MWCNTs. Also, the ignition pressure and timing were not significant on the overall engine performance, which showed a need to place more attention on the significant factors for better engine performance. The mathematical and graphical modeling showed the efficacy of the design analysis, while the interaction plots showed broader detailed factor settings for better engine performance.

Keywords: Grey relational optimization; diesel engine; brake thermal efficiency; fuel consumption; emissions

1. Introduction

In ongoing many years, all-out overall energy utilization has been expanded essentially. It prompts unnatural weather change and brings about higher temperatures on the earth (Masoudi &

Zaccour, 2017) and undermines energy security (Wallington *et al.*, 2013). This effect is detrimental to human well-being and the ecosystem (Lin *et al.*, 2011; Arbab *et al.*, 2013). A lot of researches have shown that fossil fuels contribute significantly to ozone layer depletion (Oparanti *et al.*, 2022). The pace of energy utilization has been reported by International Energy Organization (IEA) to reach about 53% by 2030 (Taufiqurrahmi & Bhatia, 2011). Meaning, the adverse effect of the utilization of fossil fuels on ozone layers depletion by 2030 is likely to be unbearable. Several pieces of research have been conducted on the several ways to mitigate these challenges. Abu-Jrai *et al.* (2009) researched the likelihood of improving performance efficiency and reducing combustion emissions of a single-cylinder-direct injection-diesel engine. In their work, simulated reformer product gas was added to a typical ultra-low Sulphur diesel (ULSD) and a replacement ultra-clean synthetic GTL (gas-to-liquid) fuel to research engine performance, combustion, and emissions at different operating conditions. They concluded that an optimal combination of GTL and simulated reformer product gas significantly improved both NO_x and smoke emissions. Ren *et al.* (2008) investigated combustion and emissions of a diesel direct engine injection (DI) powered by diesel-oxygenate blends. They observed that there was a discount in smoke concentration no matter the kinds of oxygenating additives, however, the smoke reduced when oxygen mass fraction within the blends was increased without increasing the NO_x and engine thermal efficiency. Conversely, it had been noticed that CO and HC concentrations reduced with a rise in oxygen mass fraction within the blends. Li *et al.* (2015) fueled an immediate injection diesel with pentanol to research the combustion and emissions of the compression ignition of the engine. It had been discovered that NO_x and soot emissions were significantly reduced for pentanol with comparable efficiencies under one injection strategy without exhaust gas recirculation (EGR). It had been also observed that the employed pentanol fuel offered obvious characteristics to realize a smoother heat release rate with reduced peak pressure-rise rate in contrast to the diesel oil. Prabhu and Ramanan (2020) studied the effect of emission and performance characteristics in an unmodified diesel powered by pentanol-diesel mixtures at different ratios. They found that pentanol acted as a catalyst (oxidizing) thereby reducing the carbon monoxide gas and hydrocarbon emissions. It had been also discovered that there was a substantial reduction in NO_x emission and also a discount in fuel consumption which increased the brake thermal efficiency of the engine. Kalam *et al.* (2011) investigated the emissions and performance characteristics of an indirect ignition diesel fueled with a waste vegetable oil. They found that there was a discount in brake power compared with ordinary diesel oil. However, a discount in exhaust emissions like unburned hydrocarbon (HC), smoke, carbon mono-oxide (CO), and nitrogen oxides (NO_x) was generated by the blended fuels.

Furthermore, many studies are conducted on the optimization of input parameters on the emissions and performance efficiency of diesel engines. Sivaramakrishnan and Ravikumar (2014) optimized some operation parameters on the performance and emissions of a diesel fueled with biodiesel. It had been found that a compression ratio of 17.9, 10 you look after fuel blend, and 3.81 kW of power were the optimum parameters for the test engine. Leung *et al.* (2006) optimized engine parameters namely; injection pressure, injection timing, and fuel pump plunger diameter. Their findings showed that that individual setting of the engine parameters couldn't cause an honest balance between PM and NO_x emissions, but multiparameter settings with the consideration of their cross-interactive effects could reduce particulate matters and hydrocarbon without increasing NO_x emission and trading off fuel combustion efficiency. Koten *et al.* (2014) discovered the optimum operating conditions for a diesel when it had been fueled with compressed biogas (CBG) and pilot diesel dual-fuel. Their findings showed that there have been significantly lower NO_x emissions emitted under dual-fuel operation for all cases compared to single-fuel mode in the least engine load conditions. Ramachander *et al.* (2021) optimized the emission and combustion characteristics of diesel engines operating under the reactivity-controlled compression ignition mode. The operating parameters investigated were fuel injection system timings, injection pressure, and variable engine load, using Box-Behnken-based response surface methodology. Manigandan *et al.* (2020) administered optimization on the engine conditions of one cylinder-dual direct injection-water cooled diesel fueled under hydrogen, multiwall carbon nanotubes (MWCNTs), ignition

pressure, and ignition timing. Their findings reflected that there's an improvement in brake power by 13% and a discount in brake-specific fuel consumption by 8% at full engine load conditions. It had been also added in their findings that there was a big emission reduction.

Taguchi design of experiment (DOE) has to do with the reduction of robust laboratory work or experiment to determine the effect of processing parameters or variables on the response of a system, product, or process (Taguchi & Phadke, 1989; Taguchi *et al.*, 2000; Taguchi *et al.*, 2005). However, Taguchi is only capable of optimizing a singular response of a process, product, or system. However, the Taguchi DOE method with the assistance of grey relational analysis (GRA) can optimize multiple responses. In other words, when there is a complex situation or uncertainty, like in the case of a need to optimize more than one characteristic of a system, product, or process, GRA can be employed to simplify the situation for possible optimization (Julong 1989; Javed *et al.*, 2019). GRA is employed to convert multiple response characteristics into a singular response understood by the Taguchi DOE technique. GRA has been explored in several applications in the past studies. Tosun (2006) employed GRA for the optimization of multi-responses in drilling operations. Hamzaçebi and Pekkaya (2011) determined stock investments using GRA. Li *et al.* (2019) employed GRA in combination with the incremental capacity analysis technique in the application of accurate battery state-of-health (SOH) monitoring for the safe and reliable operation of electric vehicles. Wu *et al.* (2020) incorporated TRIZ, AD, fuzzy, and GRA design as a novel design approach in the designing and manufacturing of a product. Senthilkumar *et al.* (2021) blended and optimized a transformer oil with vegetable oil using the Taguchi-GRA technique. This review shows that GRA has applications in invariably all areas of endeavors.

Having discussed the state of the art of the subject matter, it is important to state that several studies have considered the optimization of engine conditions for better engine performance and reduced emissions. These studies mostly considered the optimization of singular performance characteristics, which is an actual sense, there is a need to consider optimization of engine conditions for all the important performance characteristics of an engine, such as engine conditions, fuel blends, etc. This will lead to efficient optimization. Multiple performance characteristics optimization is complicated because all the design of experiment (DOE) techniques can optimize singular performance characteristics of a system, process, or product. Due to this challenge, Manigandan *et al.* (2020) evaluated all the multiple performance characteristics of a diesel engine using the Taguchi DOE technique. They optimized those characteristics individually, which is somewhat not good enough for efficient optimization (Ofodu & Abifarin, 2022). Hence, this study identified the gap by employing grey relational analysis (GRA) to assist the Taguchi DOE technique for multiple performance characteristics of a single cylinder-dual direct injection-water cooled diesel engine. GRA technique is employed to assist the Taguchi design technique because the engine performance conditions were complex to optimize due to incomplete and uncertain information present in this study. GRA has been proven to mitigate this very challenge (Javed 2019; Javed *et al.*, 2019; Abifarin, 2021; Abifarin *et al.*, 2022a).

2. Research design and methodology

2.1 Experimental data curation and research design

This study followed the study of Manigandan *et al.* (2020). The experimental data was obtained from their work for analysis. Tables 1, 2, and 3 show the experimental factors considered, the experimental runs, and the corresponding data, respectively for the analysis in this study. The Taguchi design and modeling were done using Minitab 16 software, while interaction plots and other plots were done using Origin 19 software.

2.2 Research methodology and data analysis

Grey relational analysis was conducted on the experimental data presented in Table 3. The data was first normalized using grey relational generation. The brake thermal efficiency (BTE) was normalized using the higher-the-better normalization condition, as giving in Equation 1.

Table 1. Experimental factors and levels

Factors	Engine load (%)	Hydrogen (%)	MWCNTs (ppm)	Ignition pressure (bar)	Ignition timing (°bTDC)
Factors symbols	A	B	C	D	E
Level 1	25	0	0	180	21
Level 2	50	10	30	200	23
Level 3	75	20	50	220	27
Level 4	100	30	80	240	31

Table 2. Experimental runs

Exp. runs	Engine load (%)	Hydrogen (%)	MWCNTs (ppm)	Ignition pressure (bar)	Ignition timing (°bTDC)
1	25	0	0	180	21
2	25	10	30	200	23
3	25	20	50	220	27
4	25	30	80	240	31
5	50	0	30	220	31
6	50	10	0	240	27
7	50	20	80	180	23
8	50	30	50	200	21
9	75	0	50	240	23
10	75	10	80	220	21
11	75	20	0	200	31
12	75	30	30	180	27
13	100	0	80	200	27
14	100	10	50	180	31
15	100	20	30	240	21
16	100	30	0	220	23

Table 3. Experimental multiple responses of the tested diesel engine

Exp. runs	BTE	BSFC	HC	NOx	CO	CO ₂
1	32.65	755	8.65	120	0.09	2.61
2	33.88	735	8.5	112	0.08	2.55
3	37.3	708	8	108	0.05	2.1
4	35.25	715	8.25	105	0.06	2.32
5	33.95	662	10.8	210	0.128	4.05
6	32.15	625	10.2	235	0.125	3.95
7	34.35	539	9.4	210	0.12	3.8
8	36.98	468	9.2	198	0.1	3.52
9	33.55	490	13.05	265	0.135	5.52
10	35.12	452	12.19	265	0.149	4.32
11	33.84	485	11.95	280	0.14	4.25
12	34.5	435	11.25	242	0.132	4.15
13	33.56	375	14.68	365	0.158	7.25
14	34.1	355	13.72	315	0.155	6.75
15	35.95	348	12.68	298	0.145	4.45
16	35.05	368	15.66	338	0.151	6.2

The reason for the higher-the-better normalization is that break thermal efficiency is required as high as possible. Then, the rest of the data, namely; break specific fuel consumption (BSFC), hydrocarbons (HC), nitrogen oxide (NOx), carbon monoxide (CO), and carbon dioxide (CO₂) were normalized using the smaller-the-better normalization condition, as shown in Equation 2. The smaller-the-better normalization condition was chosen because we require those characteristics as low as possible. A comparison was done with an ideal sequence, $x_o(k)$ ($k = 1, 2, \dots, 16$) for the six performance characteristics.

$$x_i(k) = \frac{y_i(k) - \min y_i(k)}{\max y_i(k) - \min y_i(k)} \quad (1)$$

$$x_i(k) = \frac{\max y_i(k) - y_i(k)}{\max y_i(k) - \min y_i(k)} \quad (2)$$

$x_i(k)$ is the data being preprocessed for the i^{th} experiment, and $y_i(k)$ is the initial sequence of the mean of the responses. The deviation sequence (Equation 3) was subsequently calculated to enable the determination of grey relational coefficient (GRC). The grey relational generation and the deviation sequence of the six experimental data are shown in Table 4.

$$\Delta_{oi}(k) = |x_o(k) - x_i(k)| \quad (3)$$

where $\Delta_{oi}(k)$, $x_o(k)$, and $x_i(k)$ are the deviation, reference sequence, and normalized data, respectively. The GRC values were calculated using Equation 4. The GRC values show the relationship between the expected and obtained experimental data.

$$\xi_i(k) = \frac{\Delta_{min} + \zeta \Delta_{max}}{\Delta_{oi}(k) + \zeta \Delta_{max}} \quad (4)$$

where $\xi_i(k)$ is the GRC value of the individual experimental data, computed as a function of Δ_{min} and Δ_{max} , the minimum and the maximum deviations of each experimental data. ζ is the distinguishing coefficient, whose value is widely assumed to be 0.5 (Mahmoudi *et al.*, 2020; Abifarin *et al.*, 2021a).

Lastly, the grey relational grade (GRG) was calculated using Equation 5. The GRC, GRG, and signal to noise (S/N) ratios are displayed in Table 5. The GRG (the converted singular response) gives the overall multiple performance characteristics for the six experimental data, which made it possible for Taguchi DOE technique to analyze. As always require in GRA Optimization, the higher-the-better signal to noise ratio is considered for the Taguchi DOE analysis (Taguchi & Phadke, 1989; Taguchi *et al.*, 2000; Taguchi *et al.*, 2005; Abifarin, 2021; Abifarin *et al.*, 2021b; Abifarin *et al.*, 2022b; Awodi *et al.*, 2021).

$$\gamma_i = \frac{1}{n} \sum_{i=1}^n \xi_i(k) \quad (5)$$

γ_i is the GRG value obtained for the i^{th} experiment and n is the number of performance characteristics.

Table 4. Grey relational generation and deviation sequence

	Generation						Deviation sequence					
	BTE	BSFC	HC	NOx	CO	CO2	BTE	BSFC	HC	NOx	CO	CO2
1	0.097	0	0.915	0.942	0.630	0.901	0.903	1	0.085	0.058	0.370	0.099
2	0.336	0.049	0.935	0.973	0.722	0.913	0.664	0.951	0.0653	0.027	0.278	0.087
3	1	0.116	1	0.989	1	1	0	0.885	0	0.012	0	0
4	0.602	0.098	0.967	1	0.907	0.957	0.398	0.902	0.033	0	0.093	0.043
5	0.350	0.229	0.635	0.596	0.278	0.621	0.651	0.772	0.366	0.404	0.722	0.379
6	0	0.319	0.713	0.5	0.306	0.641	1	0.681	0.287	0.5	0.694	0.359
7	0.427	0.531	0.817	0.596	0.352	0.670	0.573	0.469	0.183	0.404	0.648	0.330
8	0.938	0.705	0.843	0.642	0.537	0.724	0.062	0.295	0.157	0.358	0.463	0.276
9	0.272	0.651	0.341	0.385	0.213	0.336	0.728	0.349	0.659	0.615	0.787	0.664
10	0.577	0.745	0.453	0.385	0.083	0.569	0.423	0.256	0.547	0.615	0.917	0.431
11	0.328	0.663	0.484	0.327	0.167	0.582	0.672	0.337	0.516	0.673	0.833	0.418
12	0.456	0.786	0.576	0.473	0.241	0.602	0.544	0.214	0.424	0.527	0.759	0.398
13	0.274	0.934	0.128	0	0	0	0.726	0.066	0.872	1	1	1
14	0.379	0.983	0.253	0.192	0.028	0.097	0.621	0.017	0.747	0.808	0.972	0.903
15	0.738	1	0.389	0.258	0.120	0.544	0.262	0	0.611	0.742	0.880	0.456
16	0.563	0.951	0	0.104	0.065	0.204	0.437	0.049	1	0.896	0.935	0.796

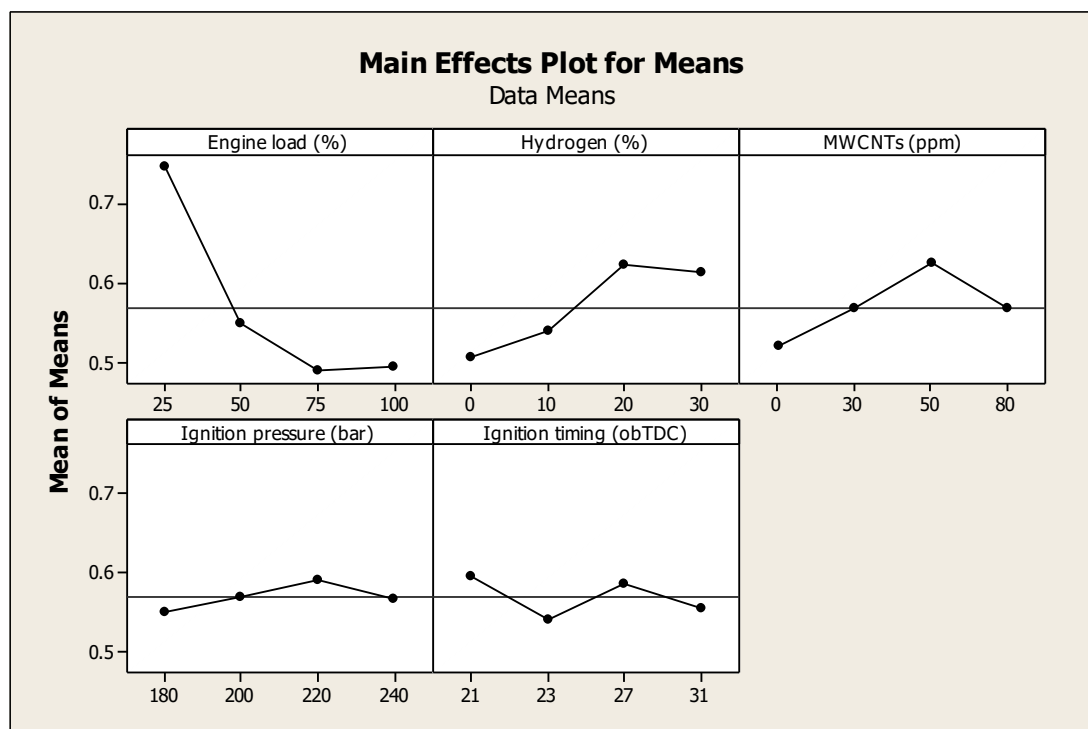
Table 5. Grey relational coefficient (GRC), grey relational grade (GRG) and S/N ratio

Exp. Runs	GRC						GRG	S/N ratio
	BTE	BSFC	HC	NO _x	CO	CO ₂		
1	0.356	0.333	0.855	0.897	0.575	0.835	0.642	-3.853
2	0.430	0.345	0.885	0.949	0.643	0.851	0.684	-3.304
3	1	0.361	1	0.977	1	1	0.890	-1.015
4	0.557	0.357	0.939	1	0.844	0.921	0.770	-2.275
5	0.435	0.393	0.578	0.553	0.409	0.569	0.490	-6.205
6	0.333	0.424	0.635	0.5	0.419	0.582	0.482	-6.338
7	0.466	0.516	0.732	0.553	0.436	0.602	0.551	-5.179
8	0.890	0.629	0.761	0.583	0.519	0.645	0.671	-3.464
9	0.407	0.589	0.431	0.448	0.389	0.430	0.449	-6.956
10	0.542	0.662	0.478	0.448	0.353	0.537	0.503	-5.965
11	0.427	0.598	0.492	0.426	0.375	0.545	0.477	-6.427
12	0.479	0.701	0.541	0.487	0.397	0.557	0.527	-5.566
13	0.408	0.883	0.364	0.333	0.333	0.333	0.443	-7.082
14	0.446	0.967	0.401	0.382	0.340	0.356	0.482	-6.339
15	0.656	1	0.450	0.403	0.362	0.523	0.566	-4.949
16	0.534	0.911	0.333	0.358	0.348	0.386	0.478	-6.406

3. Results and discussion

3.1 Effect and optimization of control factors on the engine multiple performance characteristics (GRG)

The effect of control factors on the multiple performance characteristics (GRG) of the diesel engine has been illustrated in Figure 1. The results showed that there GRG value decreased with an increase in engine load, while there was an increase in GRG when hydrogen was increased to 20% before it dropped slightly at 30%. Similar to the effect of hydrogen on the GRG value, MWCNTs and ignition pressure, an increase in GRG value was noticed up to level 3, but dropped at level 4. But for ignition timing factor, there the value of GRG was inconsistent with the increase in ignition timing. In conclusion, the figure shows the optimal settings of those factors for better performance of the tested engine, which are 25% engine load, 20% hydrogen, 50 ppm MWCNTs, 220 bar ignition pressure, and 21 obTDC ignition timing.

**Fig 1.** Effect of control factors on multiple performance characteristics

3.2 Significance of control factors on multiple performance of the diesel engine

The variance analysis (ANOVA) of the engine performance is shown in Table 6. It displays the effect and weight of each factor on the resultant performance. It is found that engine load is the most significant factor, showing a contribution of 71.47%, followed by hydrogen (15.36%), and MWCNTs (8.66%). The other two factors reflected a very little contribution of ignition pressure and timing. Thus, much attention should be placed on the significantly influenced factors to achieve better engine performance efficiency.

3.3 Confirmation analysis

If γ_0 is the highest engine performance efficiency at optimal settings and γ_m is the average engine performance efficiency, while q is the number of the factors, then the predicted grey relational grade (engine performance efficiency) is

$$\gamma_{predicted} = \gamma_m + \sum_{i=1}^q \gamma_0 - \gamma_m \quad (6)$$

The predicted engine performance efficiency at optimal settings was known to be 0.8997, and thus confidence interval (CI) was obtained using probability distribution analysis of the various GRG values to check perhaps all the experimental GRG values and the predicted optimal GRG value are within 95% confidence bounds. The confidence bounds and the experimental GRG value (engine performance) are displayed in Figure 2. The graph shows the possibility that the predicted

Table 6. ANOVA for engine performance

Factors	Degree of Freedom (DF)	Adj SS	Adj MS	Contribution (%)	Remark
Engine load (%)	3	0.17646	0.05882	71.47	Most significant
Hydrogen (%)	3	0.03792	0.01264	15.36	Significant
MWCNTs (ppm)	3	0.02138	0.00713	8.66	Significant
Ignition pressure (bar)	3	0.00321	0.00107	1.30	Insignificant
Ignition timing (°bTDC)	3	0.00796	0.00265	3.22	Insignificant
Residual error	0				-
Total	15	0.24693	0.08231		

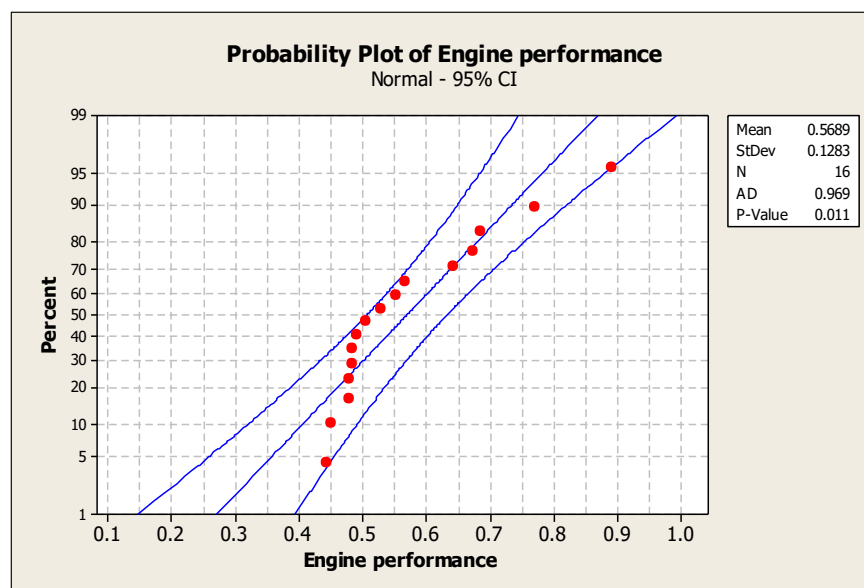


Fig 2. Confidence bounds of the engine performance (GRG)

optimal GRG value obtained fall within the 95% confidence bounds. However, further experimental work is recommended to be done considering the discovered optimal settings in this study. Because the discovered optimal settings were not among the experimental runs considered in the initial experimental work.

3.4 Modeling and interaction of chemical additives and engine parameters on engine performance

The Equation (7) shows the mathematical modeling of the engine performance (EP), while Figure 3 shows the experimental engine performance versus the modeled engine performance. The modeling was done using regression analysis with Mintab 16 software. Figure 3 shows that the predicted engine performance based on modeling followed the behavioral pattern of the experimental. This elucidates the validity of the design and model.

$$EP = 0.656 - 0.00329A + 0.00401B + 0.000716C + 0.000351D - 0.00174E \quad (7)$$

Figure 4 reflects the interaction plots of various factors on the engine performance. This explains the combination of factors settings for various engine performance efficiency. The figure shows the detailed combination of all the various factors levels to achieve engine performance as high as possible.

4. Conclusion

This study has successfully investigated the effect, optimization and modeling of engine conditions on multiple performance characteristics of a single cylinder-dual direct injection-water

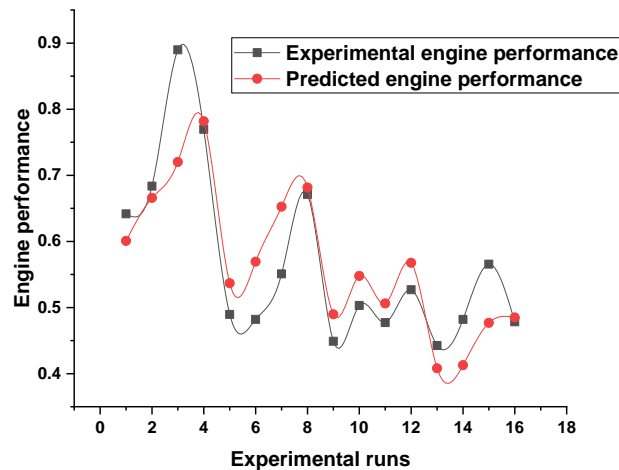


Fig 3. Experimental versus predicted engine performance

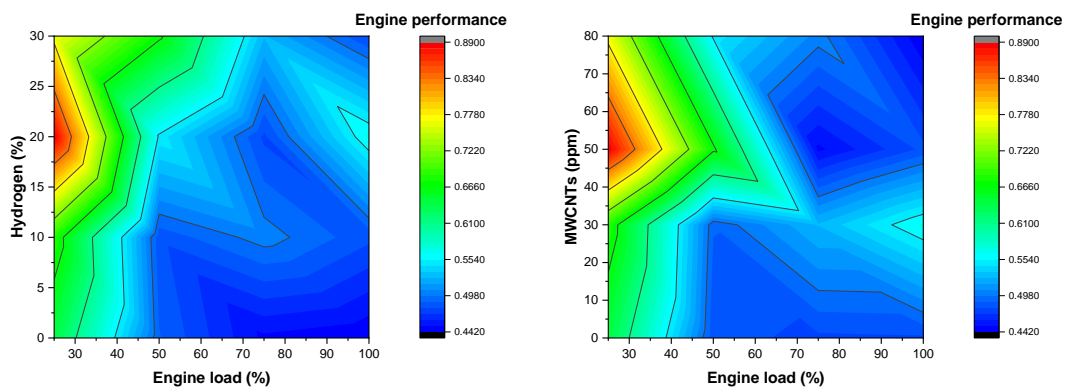


Fig 4. Interaction plots of parameters on engine performance

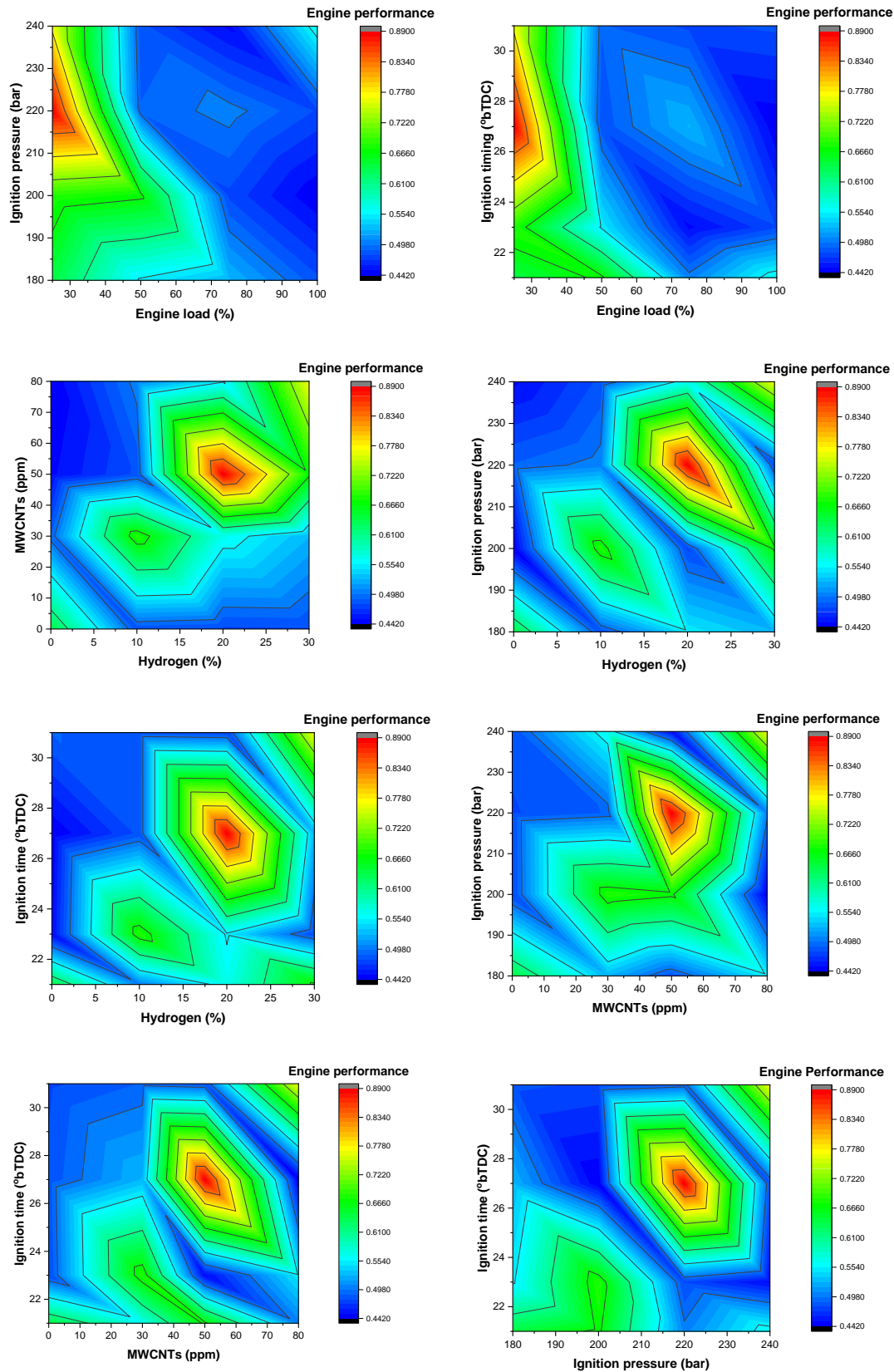


Fig 4. Interaction plots of parameters on engine performance (continued)

cooled diesel engine with the help of Taguchi grey relational and regression analysis. The multiple performance characteristics, namely; the break thermal efficiency (BTE), break specific fuel consumption (BSFC), hydrocarbons (HC), nitrogen oxide (NO_x), carbon monoxide (CO), and

carbon dioxide (CO₂) converted to a singular response, which made it feasible for Taguchi design technique to analyze. The results showed that there was similar behavioral pattern of the effect of engine conditions, except for ignition timing. The optimal settings for better engine performance were obtained to be 25% engine load, 20% hydrogen, 50 ppm MWCNTs, 220 bar ignition pressure, and 21 obTDC ignition timing. The discovered optimal settings for better engine performance did not fall within the experimental runs considered in the analysis. Although, confirmation analysis showed that there is possibility that the predicted optimal engine performance was within the confidence bound, however, there is a need to conduct experimental work based on the gotten optimal settings to elucidate the efficacy of the confirmation analysis. The analysis of variance (ANOVA) shows that engine load was the most significant factor with a contribution of 71.47%, followed by hydrogen and MWCNTs. The analysis revealed that the ignition pressure and timing were not significant on the overall engine performance. This shows that much attention is needed on the significant factors for better engine performance efficiency. The mathematical and graphical modeling of the overall engine performance were presented in this study. The modeling showed the efficacy of the design and analysis. Also, the interaction plots showed a broader detail of factor settings for better engine performance.

References

- Abifarin, J. K. (2021). Taguchi grey relational analysis on the mechanical properties of natural hydroxyapatite: effect of sintering parameters. *The International Journal of Advanced Manufacturing Technology*, 117, 49–57. <https://doi.org/10.1007/s00170-021-07288-9>
- Abifarin, J. K., Fidelis, F. B., Abdulrahim, M. Y., Oyediji, E. O., Nkwuo, T., & Prakash, C. (2022a). Response Surface Grey Relational Analysis On The Manufacturing of High Grade Biomedical Ti-13Zr-13Nb. *Research Square*. <https://doi.org/10.21203/rs.3.rs-1225030/v1>
- Abifarin, J. K., Obada, D. O., Dauda, E. T., & Oyediji, E. O. (2021a). Taguchi grey relational optimization of the multi-mechanical characteristics of kaolin reinforced hydroxyapatite: effect of fabrication parameters. *International Journal of Grey Systems*, 1(2), 20-32. <https://doi.org/10.52812/ijgs.30>
- Abifarin, J. K., Prakash, C., & Singh, S. (2021b). Optimization and significance of fabrication parameters on the mechanical properties of 3D printed chitosan/PLA scaffold. *Materials Today: Proceedings*, 50 (Part 5), 2018-2025. <https://doi.org/10.1016/j.matpr.2021.09.386>
- Abifarin, J. K., Suleiman, M. U., Abifarin, E. A., Fidelis, F. B., Oyelakin, O. K., Jacob, D. I., & Abdulrahim, M. Y. (2022b). Fabrication of mechanically enhanced hydroxyapatite scaffold with the assistance of numerical analysis. *The International Journal of Advanced Manufacturing Technology*, 118, 3331–3344. <https://doi.org/10.1007/s00170-021-08184-y>
- Abu-Jrai, A., Rodríguez-Fernández, J., Tsolakis, A., Megaritis, A., Theinnoi, K., Cracknell, R. F., & Clark, R. H. (2009). Performance, combustion and emissions of a diesel engine operated with reformed EGR. Comparison of diesel and GTL fuelling. *Fuel*, 88(6), 1031-1041. <https://doi.org/10.1016/j.fuel.2008.12.001>
- Arbab, M. I., Masjuki, H. H., Varman, M., Kalam, M. A., Imtenan, S., & Sajjad, H. (2013). Fuel properties, engine performance and emission characteristic of common biodiesels as a renewable and sustainable source of fuel. *Renewable and Sustainable Energy Reviews*, 22, 133-147. <https://doi.org/10.1016/j.rser.2013.01.046>
- Awodi, E., Ishiaku, U. S., Yakubu, M. K., & Abifarin, J. K. (2021). Experimentally Predicted Optimum Processing Parameters Assisted by Numerical Analysis on the Multi-physicomechanical Characteristics of Coir Fiber Reinforced Recycled High Density Polyethylene Composites. *Research Square*. <https://doi.org/10.21203/rs.3.rs-591200/v1>
- Hamzaçebi, C., & Pekkaya, M. (2011). Determining of stock investments with grey relational analysis. *Expert Systems with Applications*, 38(8), 9186-9195. <https://doi.org/10.1016/j.eswa.2011.01.070>
- Javed, S. A. (2019). A novel research on grey incidence analysis models and its application in project management (PhD dissertation). *Nanjing University of Aeronautics and Astronautics*. Nanjing, PR China.
- Javed, S. A., Khan, A. M., Dong, W., Raza, A., & Liu, S. (2019). Systems evaluation through new grey relational analysis approach: an application on thermal conductivity—petrophysical parameters' relationships. *Processes*, 7(6), 348. <https://doi.org/10.3390/pr7060348>
- Julong, D. (1989). Introduction to Grey System Theory. *The Journal of Grey System*, 1(1), 1-24.
- Kalam, M. A., Masjuki, H. H., Jayed, M. H., & Liaquat, A. M. (2011). Emission and performance characteristics of an indirect ignition diesel engine fuelled with waste cooking oil. *Energy*, 36(1), 397-402. <https://doi.org/10.1016/j.energy.2010.10.026>

- Koten, H., Yilmaz, M., & Zafer Gul, M. (2014). Compressed biogas-diesel dual-fuel engine optimization study for ultralow emission. *Advances in Mechanical Engineering*, 6, 571063. <https://doi.org/10.1155/2014/571063>
- Leung, D. Y., Luo, Y., & Chan, T. L. (2006). Optimization of exhaust emissions of a diesel engine fuelled with biodiesel. *Energy & Fuels*, 20(3), 1015-1023. <https://doi.org/10.1021/ef050383s>
- Li, L., Wang, J., Wang, Z., & Liu, H. (2015). Combustion and emissions of compression ignition in a direct injection diesel engine fueled with pentanol. *Energy*, 80, 575-581. <https://doi.org/10.1016/j.energy.2014.12.013>
- Li, X., Wang, Z., Zhang, L., Zou, C., & Dorrell, D. D. (2019). State-of-health estimation for Li-ion batteries by combining the incremental capacity analysis method with grey relational analysis. *Journal of Power Sources*, 410, 106-114. <https://doi.org/10.1016/j.jpowsour.2018.10.069>
- Lin, L., Cunshan, Z., Vittayapadung, S., Xiangqian, S., & Mingdong, D. (2011). Opportunities and challenges for biodiesel fuel. *Applied Energy*, 88(4), 1020-1031. <https://doi.org/10.1016/j.apenergy.2010.09.029>
- Mahmoudi, A., Javed, S. A., Liu, S., & Deng, X. (2020). Distinguishing coefficient driven sensitivity analysis of GRA model for intelligent decisions: application in project management. *Technological and Economic Development of Economy*, 26(3), 621-641. <https://doi.org/10.3846/tede.2020.1189>
- Manigandan, S., Atabani, A. E., Ponnusamy, V. K., Pugazhendhi, A., Gunasekar, P., & Prakash, S. (2020). Effect of hydrogen and multiwall carbon nanotubes blends on combustion performance and emission of diesel engine using Taguchi approach. *Fuel*, 276, 118120. <https://doi.org/10.1016/j.fuel.2020.118120>
- Masoudi, N., & Zaccour, G. (2017). Adapting to climate change: Is cooperation good for the environment?. *Economics Letters*, 153, 1-5. <https://doi.org/10.1016/j.econlet.2017.01.018>
- Ofodu, J. C. & Abifarin, J. K. (2022). Employment of probability based multi-response optimization in high voltage thermofluids. *Military Technical Courier*, 70(2), 393-408. <https://doi.org/10.5937/vojtehg70-35764>
- Oparanti, S. O., Abdelmalik, A. A., Khaleed, A. A., Abifarin, J. K., Suleiman, M. U., & Oteikwu, V. E. (2022). Synthesis and characterization of cooling biodegradable nanofluids from non-edible oil for high voltage application. *Materials Chemistry and Physics*, 277, 125485. <https://doi.org/10.1016/j.matchemphys.2021.125485>
- Prabhu, A., & Ramanan, M. V. (2020). Emission and performance analysis of pentanol-diesel blends in unmodified diesel engine. *International Journal of Ambient Energy*, 41(6), 699-702. <https://doi.org/10.1080/01430750.2018.1490356>
- Ramachander, J., Gugulothu, S. K., Sastry, G. R. K., Panda, J. K., & Surya, M. S. (2021). Performance and emission predictions of a CRDI engine powered with diesel fuel: A combined study of injection parameters variation and Box-Behnken response surface methodology based optimization. *Fuel*, 290, 120069. <https://doi.org/10.1016/j.fuel.2020.120069>
- Ren, Y., Huang, Z., Miao, H., Di, Y., Jiang, D., Zeng, K., ... & Wang, X. (2008). Combustion and emissions of a DI diesel engine fuelled with diesel-oxygenate blends. *Fuel*, 87(12), 2691-2697. <https://doi.org/10.1016/j.fuel.2008.02.017>
- Senthilkumar, S., Karthick, A., Madavan, R., Moshi, A. A. M., Bharathi, S. S., Saroja, S., & Dhanalakshmi, C. S. (2021). Optimization of transformer oil blended with natural ester oils using Taguchi-based grey relational analysis. *Fuel*, 288, 119629. <https://doi.org/10.1016/j.fuel.2020.119629>
- Sivaramakrishnan, K., & Ravikumar, P. (2014). Optimization of operational parameters on performance and emissions of a diesel engine using biodiesel. *International Journal of Environmental Science and Technology*, 11(4), 949-958. <https://doi.org/10.1007/s13762-013-0273-5>
- Taguchi, G., & Phadke, M. S. (1989). Quality engineering through design optimization. In *Quality Control, Robust Design, and the Taguchi Method* (pp. 77-96). Springer, Boston, MA. https://doi.org/10.1007/978-1-4684-1472-1_5
- Taguchi, G., Chowdhury, S., Wu, Y., Taguchi, S., & Yano, H. (2005). *Taguchi's Quality Engineering Handbook*. Wiley-Interscience.
- Taguchi, G., Wu, Y., & Chodhury, S. (2000). *Mahalanobis-Taguchi System*. McGraw-Hill Professional.
- Taufiqurrahmi, N., & Bhatia, S. (2011). Catalytic cracking of edible and non-edible oils for the production of biofuels. *Energy & Environmental Science*, 4(4), 1087-1112. <https://doi.org/10.1039/C0EE00460J>
- Tosun, N. (2006). Determination of optimum parameters for multi-performance characteristics in drilling by using grey relational analysis. *The International Journal of Advanced Manufacturing Technology*, 28(5), 450-455. <https://doi.org/10.1007/s00170-004-2386-y>
- Wallington, T. J., Lambert, C. K., & Ruona, W. C. (2013). Diesel vehicles and sustainable mobility in the US. *Energy Policy*, 54, 47-53. <https://doi.org/10.1016/j.enpol.2011.11.068>
- Wu, Y., Zhou, F., & Kong, J. (2020). Innovative design approach for product design based on TRIZ, AD, fuzzy and Grey relational analysis. *Computers & Industrial Engineering*, 140, 106276. <https://doi.org/10.1016/j.cie.2020.106276>

Mechanical Properties Optimization and Modeling of Palm Kernel Shell Ash Reinforced Al-Mg-Si Composite using Grey Relational Analysis

Elijah Oyewusi Oyedeji^{1,2,*} | Muhammed Dauda^{1,3} |
Shehu Aliyu Yaro⁴ | Malik Abdulwahab^{4,5}

¹Department of Mechanical Engineering, Ahmadu Bello University, Zaria, Nigeria

²National Space Research and Development Agency (NASRDA), Abuja, Nigeria

³Provost office, Airforce Institute of Technology, Kaduna, Nigeria

⁴Department of Metallurgical and Materials Engineering, Ahmadu Bello University, Zaria, Nigeria

⁵Department of Metallurgical and Materials Engineering, Faculty of Air Engineering, Airforce Institute of Technology, Kaduna, Nigeria

*Corresponding author: foladeji1@gmail.com

Received 28 March 2022; Revised 22/27 April 2022; Accepted 29 May 2022

Abstract: There is relatively little information on the mechanical behavior and modeling of palm kernel shell ash reinforced Al-Mg-Si composite. Thus, this study investigates the mechanical behavior and modeling of Al-Mg-Si composite. Hardness, impact strength and modulus of rupture (MOR) of the composite were investigated and analyzed using Minitab 16 and Origin software. It was found that the mechanical properties of the composite are inconsistent with composition variation. The mathematical and graphical modeling of the composite mechanical properties of the composite have been presented. The modeling revealed that aside the composition, there are other factors responsible for the mechanical behavior of the composite which were not considered in the experimental analysis. Validation of the claim was also made with analysis. The study of the interaction between the two compositions on the resultant mechanical properties gave some specific compositions with better mechanical properties. However, this study strongly recommends conduction of further analysis on other important factors responsible for the mechanical response of the composite.

Keywords: Multi-objective optimization; mechanical properties; preferable probability; grey relational analysis; Al-Mg-Si composite

1. Introduction

Achieving both strength and flexibility in designing materials simultaneously is turning out to be progressively challenging. On account of lightweight Al composites, grain refinement utilizing grain refinement strategies such as high-pressure torsion, friction stir processing (FSP), and equal, which are key examples of plastic deformation strategies, have proved to produce ultrafine-grained (UFG) Al-composite with higher strength (Edalati *et al.*, 2012; Li *et al.*, 2018; Sanchez *et al.*, 2021). However,

ductility is reduced in the case of coarse-grained Al-composite due to the presence of low dislocation and disjointed coalesce, creating accumulating capabilities due to grain particle size and dispersion within the composition (Oyededeji *et al.*, 2021a; 2021b; 2021c). The presence of second-phase particles can significantly increase dislocation accumulation ability and resistance to dislocation sliding; therefore, adding some particles to the UFG matrix is one alternative. AA7075 has been cryogenically rolled (Kazemi-Navaee *et al.*, 2021), age-hardenable AA6063 (Engler, 2022), AA6082 alloys (Rakhmonov *et al.*, 2021), and in other cases, nano-particles have been used to reinforced Al composites (Chakravarthy *et al.*, 2020). All of these methods are some of the ways that the addition of second-phase particles has helped improve the strength and flexibility of Al-composite based on literature.

Aluminium is the third most plentiful element on the planet (Chaudhary & Tak, 2022). It has fundamentally supplanted ferrous components in the scope of uses because of its remarkable properties, which include low density that is responsible for its lightweight and resistance to corrosion as a result of its passivation characteristics. However, there are some disadvantages when Aluminum is used alone for some industrial applications (Kulekci, 2008; Sharma *et al.*, 2021). To fix and combat defects/imperfections/irregularities in pure aluminium, the combinations of the pure Al with other materials leading to the formation of another material known as Al-composite was found. An example of the Al-composite is the Al-Metallic Matrix Composite (MMC). An MMC is an intensified material made by joining two distinct parts to make a reinforced material. The constant material where the reinforcing material is consolidated, be it in the form of particles, textiles, or whiskers, is alluded to as the matrix of the MMC (Chou *et al.*, 1985). Furthermore, the reinforcing material can also be in the form of continuous or discontinuous particles. The term "hybrid metal matrix composite" (HMMC) refers to a material that contains more than one reinforcing element in addition to the matrix. MMCs assume a significant part in our day to day routines as materials that are mostly in use are made from MMCs. Some of the examples of reinforcing materials used in MMCs to develop mechanical structures are tungsten carbides, metallic binders, graphites, among others. When a typical material fails to fulfill the proper standards or specifications, it is usually used. The needed attribute to be reached with a base metal determines the metal matrix's reinforcement. MMCs in the form of Particulate Metal Matrix Composites (PMMCs) are a type of MMC (Kordijazi *et al.*, 2021; Miracle, 2005).

Scholars have used the Grey Relational Analysis (GRA) model to achieve optimum parameters in the production of optimized materials with superior mechanical properties for engineering applications such as aircraft, automobiles, and chemical plants, among others. For instance, Pandya and Rathod (2020) used the GRA and were able to find the ideal composition of agricultural reinforcement materials to build polymer-matrix composites with good mechanical properties. Sumesh and Kanthavel (2020) produced optimum parameters for agricultural reinforcing materials, using the GRA approach and an artificial neural network. GRA has also been employed to optimize mechanical properties (Reddy & Chalamalasetti, 2021; Soorya Prakash *et al.*, 2020). Thus, studies confirm the suitability of the GRA model for optimization problems (Yin, 2013).

The current study aims to learn about the mechanical behavior of Al-Mg-Si metal matrix reinforced by palm kernel shell ash (PKSA) produced through powder metallurgy using the GRA and statistical analysis. GRA was used to determine the ideal percentage weight composition of PKSA that gives the best mechanical qualities to obtain the best quality features. Section 1 contains the study's introduction and general background knowledge, section 2 contains materials and methods as they relate to this study, section 3 considers the study's experimental design, section 4 contains the experimental study's results and their discussions, and section 5 concluded the study.

2. Materials and methods

2.1 Materials and production

A palm oil processing plant in Nigeria, which is one of the major producers of oil palm, provided fresh palm kernel shells (Oyededeji *et al.*, 2021a; Oyededeji *et al.*, 2020). The fundamental Aluminum

6066 composite source was obtained from Shanghai Worldyang Chemical Co., Ltd., China, and comprised of unadulterated aluminum, manganese, silicon, chromium, magnesium, and copper powder. To act as reinforcement for the created aluminum matrix, the palm kernel shells were burned into ash. Details of the fabrication that took place between January 2020 and January 2021 exist in previous studies (Oyedepi *et al.*, 2022).

To optimize mechanical properties based on the influence of PKSA reinforcement, the grey relational approach was utilized, which assessed performance attributes and normalized them from zero to one. This technique is known as grey relational generation. Using the normalized data, the grey relational coefficient was calculated. The Grey relational grade was then calculated by averaging the grey relational coefficients. The grey relationship grade determines the full response. A multi-response optimization problem is reduced to a single-response optimization problem using this strategy. The grey relational grade is the objective function (Ramu *et al.*, 2018).

2.2 Mechanical Testing

2.2.1 Hardness: According to the ASTM E18-79 standard, the hardness of the composite was determined using the Rockwell hardness method with a force of 10 kgf.

2.2.2 Impact strength: The samples for the impact test were developed based on standard ISO-8256. Izod impact is a single point test that estimates material's resistance to impact from a pendulum. In this study, the Ceast Lot – Resil Impactor with Ceast NotchVIS was used. This test was carried out under standard conditions of relative air humidity and temperature of 50% and 23 °C respectively.

2.2.3 Modulus of rupture: The flexural strength test was performed by utilizing a Motorized Automatic Recording Tensometer. According to the ASTM D7028-07-201 standard, the samples were prepared, while the autographic recording drum of the machine was wrapped with the test graph sheet to record the readings of the test.

3. Experimental design

A palm oil processing plant in Nigeria, which is one of the major producers of oil palm, provided fresh palm kernel shells. The experiments are based on regression analysis, probability, and analysis of variance (ANOVA), with 11 experimental observations listed in Table 1.

3.1 Statistical analysis

The experimental mechanical properties were analyzed using regression analysis, analysis of variance (ANOVA), and interaction analysis with the help of Minitab (Version 16.1, Minitab Inc.) and Origin (Version 2020, OriginLab) software after the mechanical properties of the developed composites were evaluated. The percentage fluctuation in mechanical characteristics and the

Table 1. The experimental data

Experiment no.	PKSA	Al-Mg-Si	MOR (MPa)	Impact Strength (J)	Hardness
1	0	100	50.4	0.123	63.3
2	2.034	97.874	59.51	0.126	73
3	4.451	96.023	64.91	0.138	93
4	6.0323	93.9677	69.25	0.433	91
5	8.3902	82.7341	68.28	0.077	88
6	9.989	90.8879	56.32	0.138	91
7	12.781	88.0023	58.3	0.066	90.6
8	13.985	86.8745	64.84	0.111	73
9	15.997	83.9978	63.71	0.3	89
10	18.453	82.2348	56.81	0.21	82
11	20.0842	79.8765	60.07	0.013	0

descriptive statistical analysis of PKSA reinforcement on Al-Mg-Si alloy were computed in the study of Oyedede *et al.* (2021c).

3.2 Grey relational analysis

Grey relational analysis is a popular method for determining the degree of link between sequences based on the grey relational grade. In recent times, some researchers have utilized GRA optimization method to optimize input parameters resulting in outputs responses based on the Grey relational grade (GRG). GRA is usually used to incorporate all of the desired performance qualities that are being examined into a solitary number that can be utilized as the single quality optimized conditions (Abifarin *et al.*, 2021; Ramu *et al.*, 2018). Based on the form of values for each of the output responses, normalization of optimization responses can be classified into three types. They are the 'the smaller the better', the 'nominal the better', and the 'higher the better' values (Girish *et al.*, 2019).

For this study, the high values for MOR, Impact Strength and Hardness are desirable for overall mechanical properties of the composite. Hence, 'higher the better' normalization criteria of Grey relational analysis (GRA) was utilized in the experimental step to generate grey grades and establish the response between zero and one. The grey relational coefficient (GRC) was calculated using the set data to illustrate how near the expected response is to the actual response. A grey relational grade (GRG) represents the overall evaluation of all the individual performance parameters, which is produced by averaging GRCs of all the performance parameters for each sample treatment (Abifarin *et al.*, 2021; Ramu *et al.*, 2018). Optimizing a single grey relational grade, for example, entails balancing a complex set of various performance criteria, with the highest grey relational grade-level serving as the ideal level of this process parameter (Abifarin *et al.*, 2021).

Equation 1 is the linear data preprocessing approach used in this work for the mechanical properties of the investigated composite, and the larger the criteria, the better.

$$x_i(k) = \frac{y_i(k) - \min y_i(k)}{\max y_i(k) - \min y_i(k)} \quad (1)$$

where $x_i(k)$ is the preprocessed data, $\min y_i(k)$ is the lowest $y_i(k)$ response estimation, k^{th} , and $\max y_i(k)$ is the greatest $y_i(k)$ response estimation, k^{th} . The preprocessed data (grey relational generation sequences) from the experimental runs of the investigated composites are shown in Table 2.

Deng's grey relational analysis model was built to show the degree of grey relationship between two sequences $[x_o(k) \text{ and } x_i(k), i = 1, 2, 3, 4; k = 1, 2 \text{ \& } 3]$. The grey relational coefficient (GRC) is given by

$$\xi_i(k) = \frac{\Delta_{min} + \zeta \Delta_{max}}{\Delta_{oi}(k) + \zeta \Delta_{max}} \quad (2)$$

where the deviation sequence is,

Table 2. The preprocessed observation data

Experiment no.	MOR (MPa)	Impact Strength (J)	Hardness
1	0	0.261905	0.680645
2	0.483289	0.269048	0.784946
3	0.769761	0.297619	1
4	1	1	0.978495
5	0.948541	0.152381	0.946237
6	0.314058	0.297619	0.978495
7	0.419098	0.12619	0.974194
8	0.766048	0.233333	0.784946
9	0.706101	0.683333	0.956989
10	0.340053	0.469048	0.88172
11	0.512997	0	0

$$\Delta_{oi}(k) = \|x_o(k) - x_i(k)\| \quad (3)$$

$\Delta_{oi}(k)$ denotes the difference in absolute value between $x_o(k)$ and $x_i(k)$, $x_o(k)$ and $x_i(k)$ denote the reference and similarity arrangements, respectively, and ζ is the differentiating coefficient (0~1), which is generally allocated an equal weight of 0.5 to each parameter (Abifarin et al., 2021). The base of every reaction variable, as well as the majority of variations, are referred to as Δ_{min} and Δ_{max} . Table 3 presents the deviation sequence of the data in the experimental runs of the analyzed composites. The grey relationship coefficient (GRC), grey relational grade (GRG), and ranking are shown in Table 4 in which GRA was used to establish the GRG, and the respective value for each experiment number, ranking was carried out for the GRGs.

3.3 Probability-based multi-objective analysis

For aerospace applications, as previously stated in the GRA analysis, a considerable value of the mechanical qualities of the metallic composite is necessary; thus, the beneficial utility index technique was applied. In the computation, the index characteristic indicator contributes a linearly positive contribution to the partial preference probability (Ramu et al., 2018). Using Equation 4 and Equation 5, important parameters that relates to the partial probability index (denoted as P_{ij}) and the normalized factor of the j^{th} utility index (denoted as $\bar{\mu}_j$) were obtained to compute the performance characteristic indicator of the models.

$$P_{ij} = \bar{\mu}_j x_{ij}; i = 1, 2, \dots, n; j = 1, 2, \dots, m \quad (4)$$

$$\bar{\mu}_j = 1/(n\bar{x}_j) \quad (5)$$

Note that n and m are the sample number and utility indices of each sample respectively as it relate to this study, x_{ij} is the j^{th} sample's characteristic performance beneficial utility index measurement, and \bar{x}_j is the value of the sample characteristic performance indicator's arithmetic mean utility index.

Table 3. The deviation sequence observation data

Experiment no.	MOR (MPa)	Impact Strength (J)	Hardness
1	1	0.738095	0.319355
2	0.516711	0.730952	0.215054
3	0.230239	0.702381	0
4	0	0	0.021505
5	0.051459	0.847619	0.053763
6	0.685942	0.702381	0.021505
7	0.580902	0.87381	0.025806
8	0.233952	0.766667	0.215054
9	0.293899	0.316667	0.043011
10	0.659947	0.530952	0.11828
11	0.487003	1	1

Table 4. Grey relational coefficients, grades and ranks

Experiment no.	MOR (MPa)	Impact Strength (J)	Hardness	Samples	GRG	Rank
1	0.333333	0.403846	0.610236	C1	0.449139	10
2	0.491782	0.40619	0.699248	C2	0.532407	9
3	0.684708	0.415842	1	C3	0.700183	4
4	1	1	0.958763	C4	0.986254	1
5	0.906686	0.371025	0.902913	C5	0.726874	2
6	0.421606	0.415842	0.958763	C6	0.598737	5
7	0.462577	0.363951	0.95092	C7	0.592483	6
8	0.681243	0.394737	0.699248	C8	0.591743	7
9	0.629803	0.612245	0.920792	C9	0.720947	3
10	0.431054	0.484988	0.808696	C10	0.574913	8
11	0.506584	0.333333	0.333333	C11	0.391084	11

Finally, the analysis' decisive preferred probability is calculated as the product of each candidate sample's partial preferable probability. During the ranking process, the candidate sample with the best performance characteristics is also determined. The composites' preferred probability optimization and ranking are shown in Table 5.

4. Results and discussion

4.1 Micro hardness analysis

The experimental hardness of the various samples with different compositions are displayed in Table 6. The results revealed an inconsistent pattern as the compositions change. The mathematical modeling of the experimental hardness is shown in Equation 6 using regression analysis. The experimental hardness and the modeled hardness are also displayed in Figure 1. The figure revealed that the modeled hardness is inconsistent with its corresponding experimental result.

$$\text{Hardness} = 135 - 1.85 \text{ PKSA} - 0.46 \text{ Al} - \text{Mg} - \text{Si} \quad (6)$$

The modeled hardness revealed the fitness of the experimental design. This shows that there are some factors that influenced the experimental hardness results obtained. The inconsistency is further supported by the analysis of variance (ANOVA) of the data as shown in Table 7. The table showed that the residual error was 63.5% as compared to the modeled data. The implication is that lots of errors or some factors have not been accounted for and this could be responsible to the hardness data of the composite. This means that a substantive conclusion cannot be drawn on the behavioral pattern of the hardness of the composite as the compositions vary. Hence, it is recommended in this study that other factors that may be responsible for hardness of the fabricated composite should be investigated.

It is important to understand the behavior of the resultant hardness value, relative to the interaction between Al-Mg-Si and PKSA. The results showed that barely from 82-96% Al-Mg-Si mixed with 6-11% of PKSA will give relatively higher hardness value compared to other

Table 5. Preferable probability optimization

Experiment no.	MOR (MPa)	Impact Strength (J)	Hardness	Pt*1000	Rank
1	0.074955	0.070893	0.075908	0.403365	9
2	0.088504	0.072622	0.08754	0.562655	6
3	0.096535	0.079539	0.111524	0.856313	4
4	0.102989	0.249568	0.109126	2.804839	1
5	0.101547	0.04438	0.105528	0.475582	8
6	0.08376	0.079539	0.109126	0.727013	5
7	0.086704	0.03804	0.108646	0.358344	10
8	0.096431	0.063977	0.08754	0.540067	7
9	0.09475	0.172911	0.106727	1.748549	2
10	0.084488	0.121037	0.098333	1.00558	3
11	0.089337	0.007493	0	0	11

Table 6. Experimental hardness data

Experiment no.	PKSA	Al-Mg-Si	Hardness
1	0	100	63.3
2	2.034	97.874	73
3	4.451	96.023	93
4	6.0323	93.9677	91
5	8.3902	82.7341	88
6	9.989	90.8879	91
7	12.781	88.0023	90.6
8	13.985	86.8745	73
9	15.997	83.9978	89
10	18.453	82.2348	82
11	20.0842	79.8765	0

compositions. Also, it is seen that 82-84% Al-Mg-Si mixed with 12-18% give a relatively higher hardness value. In addition, to the findings made above, in some instances a particular hardness value is desired for a particular application. Thus, these interactions are shown in Figure 2 with the specific compositions required for some specific hardness value.

4.2 Impact strength analysis

Similar to hardness analysis, the experimental impact strength of the Al-Mg-Si-PKSA composites are presented in Table 8. It is noted that there is a gradient in impact strength of the composite as the composition varies. The mathematical modeling of the experimental impact strength is shown in Equation 7 obtained with the help of regression analysis. The experimental and the modeled impact strength are as shown in Figure 3. It is shown that the model impact strength does not follow the pattern of that of the experimental.

$$\text{Impact Strength (J)} = -0.67 + 0.0062 \text{ PKSA} + 0.0086 \text{ Al} - \text{Mg} - \text{Si} \quad (7)$$

The modeling revealed the unreliability of the repeatability of the experiment. The results showed that there are some factors responsible for the curation of the experimental impact strength of the composite that have been accounted for. ANOVA analysis (Table 9) further supports the inconsistency observed from the modeling. In the case of the contribution of the unaccounted factors on the experimental impact strength, the analysis revealed significant contribution of 81.7%. This is a pronounced contribution, which shows the necessity of further investigation of probable factors that may be responsible on the impact strength of the composite. These findings also showed that substantial conclusion cannot be drawn on the effect of the composition on the impact strength of the composite.

Figure 4 shows the interaction between Al-Mg-Si and PKSA relative to the resultant experimental impact strength. The results revealed that 92-95% Al-Mg-Si mixed with 4.5-6.5% of PKSA will give a relatively higher impact strength compared to other compositions. The presented interaction plot also highlights different compositions of Al-Mg-Si and PKSA with different resultant impact strength.

Table 7. Analysis of Variance for Hardness

Source	DF	SS	MS	% of Contribution
Modeled data	2	911.5	455.7	36.5
Residual Error	8	6344.6	793.1	63.5
Total	10	7256.0	1248.8	100

Table 8. Experimental impact strength

Experiment no.	PKSA	Al-Mg-Si	Impact Strength (J)
1	0	100	0.123
2	2.034	97.874	0.126
3	4.451	96.023	0.138
4	6.0323	93.9677	0.433
5	8.3902	82.7341	0.077
6	9.989	90.8879	0.138
7	12.781	88.0023	0.066
8	13.985	86.8745	0.111
9	15.997	83.9978	0.3
10	18.453	82.2348	0.21
11	20.0842	79.8765	0.013

Table 9. Analysis of variance for impact strength

Source	DF	SS	MS	% of Contribution
Regression	2	0.00741	0.00371	18.3
Residual Error	8	0.13239	0.01655	81.7
Total	10	0.1398	0.02026	

4.3 Modulus of rupture (MOR) analysis

The experimental MOR of the Al-Mg-Si-PKSA composites are presented in Table 10 as also done in the previously discussed mechanical properties. The result also showed variation in MOR of the composite as the composition changes. The mathematical modeling of the experimental MOR is displayed in Equation 8 obtained with the help of regression analysis. The experimental and the modeled impact strength are presented in Figure 5 and this modeling also revealed that the experimental design does not fit wonderfully.

$$\text{MOR} = 149 - 0.775 \text{ PKSA} - 0.894 \text{ Al} - \text{Mg} - \text{Si} \quad (8)$$

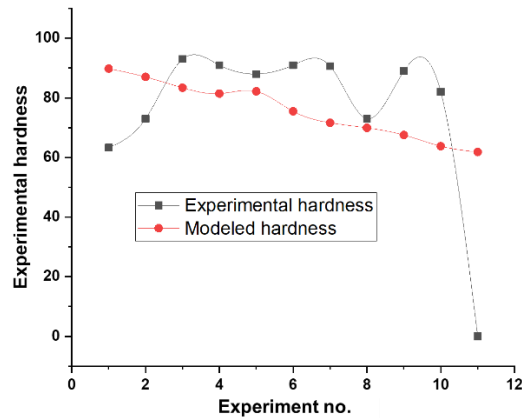


Fig 1. Experimental and Modeled Hardness

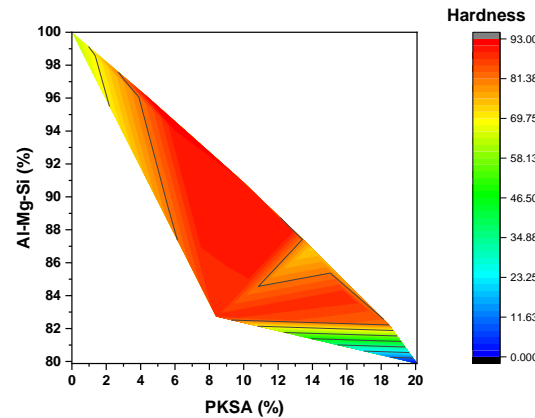


Fig 2. Interaction Plot for Hardness

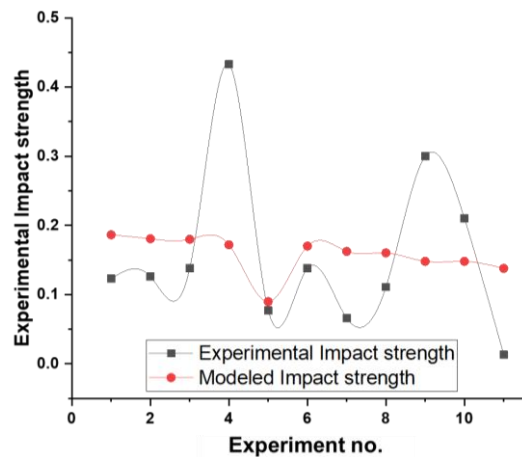


Fig 3. Experimental and Modeled Impact Strength

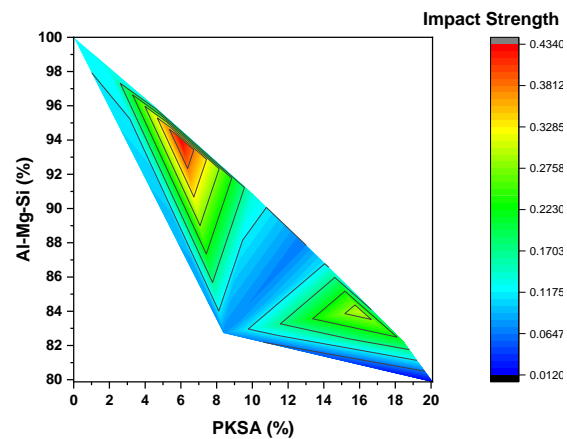


Fig 4. Interaction Plot for Impact Strength

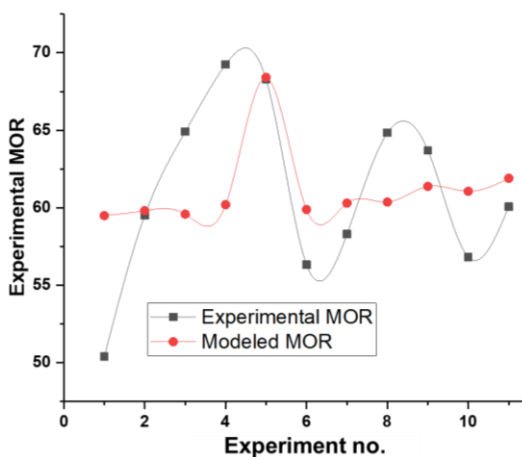


Fig 5. Experimental and Modeled MOR

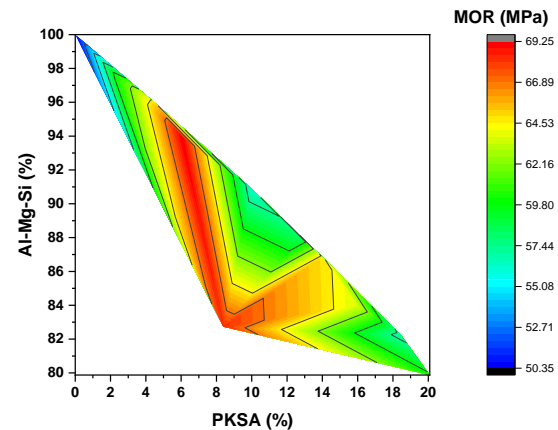


Fig 6. Interaction Plot for MOR

Table 10. Experimental MOR

Experiment no.	PKSA	Al-Mg-Si	MOR
1	0	100	50.4
2	2.034	97.874	59.51
3	4.451	96.023	64.91
4	6.0323	93.9677	69.25
5	8.3902	82.7341	68.28
6	9.989	90.8879	56.32
7	12.781	88.0023	58.3
8	13.985	86.8745	64.84
9	15.997	83.9978	63.71
10	18.453	82.2348	56.81
11	20.0842	79.8765	60.07

Table 11. Analysis of Variance for MOR

Source	DF	SS	MS	% of Contribution
Regression	2	64.15	32.07	50.02
Residual Error	8	256.31	32.04	49.98
Total	10	320.45	64.11	

The modeling of MOR presented in Figure 5 showed a better fitness of the experiment as compared hardness and impact strength of the composite. However, it is important to note that the residual errors contributed significantly on MOR of the composite. The ANOVA analysis in Table 11 gave a quantitative contribution of the residual error to be 49.98%. As it is recommended in other mechanical properties analysis, further study should be conducted on essential factors responsible on the mechanical properties of Al-Mg-Si composite.

The interaction plot of the compositions showing their corresponding MOR is shown in Figure 6. The results showed an L curve pattern of the composition that gave better with the red color. The presented interaction plot also highlights different compositions of Al-Mg-Si and PKSA with different resultant MOR.

5. Conclusion

Mechanical analysis and modeling of Al-Mg-Si-PKSA composite have been successfully done in this study. It was found that the mechanical properties of the composite are inconsistent with variation in the composition. The mathematical and graphical modeling of the mechanical properties of the composite have been presented. The modeling revealed that the experimental mechanical properties are influenced by some external factors that were not considered in this study. Analysis of variance further substantiate the modeling with quantitative analysis. The interaction study of the analyzed mechanical properties showed a broader view of different combination of the compositions with their resultant mechanical properties. It also showed some specific compositions that could result to better mechanical properties. It is strongly recommended that further analysis should be conducted on other essential factors that may be responsible on the mechanical properties of the composite.

Acknowledgement

The authors will like to acknowledge the support provided by the Departments of Mechanical Engineering and Metallurgical and Materials Engineering, Ahmadu Bello University, Zaria, Nigeria. The data can be made available on a reasonable request.

Appendix: Nomenclature

Symbol	Description
FSP	Friction stir processing
UFG	Ultrafine-grained
MMC	Metal Matrix Composite

HMMC	Hybrid Metal Matrix Composite
PMMCs	Particulate Metal Matrix Composites
GRA	Grey Relational Analysis
PKSA	Palm Kernel Shell Ash
ASTM	American Society for Testing and Materials
ISO	International Organization for Standardization
m	Meters
s	Seconds
mm	Millimetre
°C	Degree Celsius
ANOVA	Analysis of Variance
MPa	Mega-Pascal
MOR	Modulus of Rupture
J	Joules
$x_i(k)$	Preprocessed data/similarity arrangements
$X_o(k)$	Reference arrangements
$y_i(k)$	Response estimation
$\Delta_{oi}(k)$	Difference in absolute value between $x_o(k)$ and $x_i(k)$
ζ	Distinguishing coefficient of Deng's GRA model
$\Delta_{min}, \Delta_{max}$	The base of every reaction variable
GRC	Grey Relationship Coefficient
GRG	Grey Relational Grade
P_{ij}	Partial positive probability index
\square_j	Normalized factor
j^{th}	utility index of the performance characteristic indicator
x_{ij}	j^{th} beneficial utility index of the sample's characteristic performance measurement
n	Number of samples in the study
m	Number of utility indices for each sample involved
x_i	Sample characteristics performance indicator's arithmetic mean utility index
DF	Degree of Freedom
SS	Sum of Squares
MS	Mean Squares

References

- Abifarin, J. K., Olubiyi, D. O., Dauda, E. T., & Oyedepi, E. O. (2021). Taguchi Grey Relational Optimization of the Multi-mechanical Characteristics of Kaolin Reinforced Hydroxyapatite: Effect of Fabrication Parameters. *International Journal of Grey Systems*, 1(2), 20–32. <https://doi.org/10.52812/ijgs.30>
- Chakravarthy, C. H. N., Kumar, S. S., Muthalagu, R., & Ramasamy, M. (2020). Experimental investigation and optimization on surface parameters of ZrO₂ nano particles reinforced Al-7050 metal matrix composites for aeronautical applications. *Materials Today: Proceedings*, 37(Part 2), 2406–2414. <https://doi.org/10.1016/j.matpr.2020.08.265>
- Chaudhary, S., & Tak, R. K. (2022). Natural corrosion inhibition and adsorption characteristics of tribulus terrestris plant extract on aluminium in hydrochloric acid environment. *Biointerface Research in Applied Chemistry*, 12(2), 2603–2617. <https://doi.org/10.33263/BRIAC122.26032617>
- Chou, T., Kelly, A., & Okura, A. (1985). Fibre-reinforced metal-matrix composites. *Composites*, 16(3), 187–206. [https://doi.org/10.1016/0010-4361\(85\)90603-2](https://doi.org/10.1016/0010-4361(85)90603-2)
- Edalati, K., Imamura, K., Kiss, T., & Horita, Z. (2012). Equal-channel angular pressing and high-pressure torsion of pure copper: Evolution of electrical conductivity and hardness with strain. *Materials Transactions*, 53(1), 123–127. <https://doi.org/10.2320/matertrans.MD201109>
- Engler, O. (2022). Effect of precipitation state on plastic anisotropy in sheets of the age-hardenable aluminium alloys AA 6016 and AA 7021. *Materials Science and Engineering A*, 830, 142324. <https://doi.org/10.1016/j.msea.2021.142324>
- Girish, B. M., Siddesh, H. S., & Satish, B. M. (2019). Taguchi grey relational analysis for parametric optimization of severe plastic deformation process. *SN Applied Sciences*, 1(8), 1–11. <https://doi.org/10.1007/s42452-019-0982-6>
- Kazemi-Navaei, A., Jamaati, R., & Aval, H. J. (2021). Asymmetric cold rolling of AA7075 alloy: The evolution of microstructure, crystallographic texture, and mechanical properties. *Materials Science and Engineering A*, 824, 141801. <https://doi.org/10.1016/j.msea.2021.141801>
- Kordijazi, A., Zhao, T., Zhang, J., Alrfou, K., & Rohatgi, P. (2021). A Review of Application of Machine Learning in Design, Synthesis, and Characterization of Metal Matrix Composites: Current Status and Emerging Applications. *Jom*, 73(7), 2060–2074. <https://doi.org/10.1007/s11837-021-04701-2>
- Kulekci, M. K. (2008). Magnesium and its alloys applications in automotive industry. *International Journal of Advanced Manufacturing Technology*, 39(9–10), 851–865. <https://doi.org/10.1007/s00170-007-1279-2>
- Li, Q., Xue, S., Wang, J., Shao, S., Kwong, A. H., Giwa, A., Fan, Z., Liu, Y., Qi, Z., Ding, J., Wang, H., Greer, J. R., Wang, H., & Zhang, X. (2018). High-Strength Nanotwinned Al Alloys with 9R Phase. *Advanced Materials*, 30(11), 1704629. <https://doi.org/10.1002/adma.201704629>
- Miracle, D. B. (2005). Metal matrix composites - From science to technological significance. *Composites Science*

- and Technology, 65(15-16 SPEC. ISS.), 2526–2540. <https://doi.org/10.1016/j.compscitech.2005.05.027>
- Oyedede, A. N., Umar, A. U., Kuburi, L. S., & Apeh, I. O. (2020). Trend of Harvesting of Oil Palm Fruit; The Mechanisms, and Challenges. *International Journal of Scientific Research and Engineering Development*, 3(3), 1053–1063. <http://www.ijred.com/volume3/issue3/IJSRED-V3I3P138.pdf>
- Oyedede, A., Umar, U. A., & Shettima, K. L. (2021a). Investigation of the Allometry of Oil Palm Trees in Nigeria for Mechanization of the Farming Process. *Atbuftejoste.Com*, 9(2), 123–130. <http://www.atbuftejoste.com/index.php/joste/article/view/1205>
- Oyedede, E., Dauda, M., Yaro, S., & Abdulwahab, M. (2021b). Palm Kernel Shell Ash Particle Reinforcement on Al-Mg-Si and its Effect on the Mechanical and Thermal Behaviour. *Journal of Experimental Research*, 9(2), 57–66.
- Oyedede, E. O., Dauda, M., Yaro, S. A., & Abdulwahab, M. (2022). The effect of palm kernel shell ash reinforcement on microstructure and mechanical properties of Al-Mg-Si metal-matrix composites. *Proceedings of the Institution of Mechanical Engineers, Part C: Journal of Mechanical Engineering Science*, 236(3), 1666–1673. <https://doi.org/10.1177/09544062211014535>
- Oyedede, Elijah O, Dauda, M., Yaro, S. A., & Abdulwahab, M. (2021c). Influence of Particle Size and Particle Range Distribution on the Microstructure of Al–Mg–Si/PKSA Composite for Amateur Solid Rocket Chamber. *FUOYE Journal of Engineering and Technology*, 6(1), 88-91. <https://doi.org/10.46792/fuoyej.v6i1.580>
- Pandya, V. J., & Rathod, P. P. (2020). Optimization of mechanical properties of green composites by gray relational analysis. *Materials Today: Proceedings*, 27, 19–22. <https://doi.org/10.1016/j.matpr.2019.08.166>
- Rakhmonov, J., Liu, K., Rometsch, P., Parson, N., & -Grant Chen, X. (2021). Effects of Al (MnFe) Si dispersoids with different sizes and number densities on microstructure and ambient/elevated-temperature mechanical properties of extruded Al. *Journal of Alloys and Compounds*, 861, 157937. <https://doi.org/10.1016/j.jallcom.2020.157937>
- Ramu, I., Srinivas, P., & Vekatesh, K. (2018). Taguchi based grey relational analysis for optimization of machining parameters of CNC turning steel 316. *IOP Conference Series: Materials Science and Engineering*, 377(1), 012078. <https://doi.org/10.1088/1757-899X/377/1/012078>
- Reddy, S., & Chalamalasetti, S. R. (2021). Optimization of drilling parameters during machining of Al-Mg-Si alloys by Taguchi method coupled with grey relational analysis and validated by FEA based deform - 3D. *Strojnický Casopis*, 71(2), 221–238. <https://doi.org/10.2478/scjme-2021-0032>
- Sanchez, J. M., Pascual, A., Vicario, I., Albizuri, J., Guraya, T., & Galarraga, H. (2021). Microstructure and phase formation of novel Al80Mg5Sn5Zn5X5 lightweight complex concentrated aluminum alloys. *Metals*, 11(12), 1944. <https://doi.org/10.3390/met11121944>
- Sharma, S., Singh, J., Gupta, M. K., Mia, M., Dwivedi, S. P., Saxena, A., Chattopadhyaya, S., Singh, R., Pimenov, D. Y., & Korkmaz, M. E. (2021). Investigation on mechanical, tribological and microstructural properties of Al-Mg-Si-Ti6/SiC/muscovite-hybrid metal-matrix composites for high strength applications. *Journal of Materials Research and Technology*, 12, 1564–1581. <https://doi.org/10.1016/j.jmrt.2021.03.095>
- Soorya Prakash, K., Gopal, P. M., & Karthik, S. (2020). Multi-objective optimization using Taguchi based grey relational analysis in turning of Rock dust reinforced Aluminum MMC. *Measurement: Journal of the International Measurement Confederation*, 157, 107664. <https://doi.org/10.1016/j.measurement.2020.107664>
- Sumesh, K. R., & Kanthavel, K. (2020). Optimizing various parameters influencing mechanical properties of banana/coir natural fiber composites using grey relational analysis and artificial neural network models. *Journal of Industrial Textiles*. <https://doi.org/10.1177/1528083720930304>
- Yin, M. S. (2013). Fifteen years of grey system theory research: A historical review and bibliometric analysis. *Expert Systems with Applications*, 40(7), 2767–2775. <https://doi.org/10.1016/j.eswa.2012.11.002>

Evaluation of Barriers to Electric Vehicle Adoption in Indonesia through Grey Ordinal Priority Approach

Cliford Septian Candra^{1,*}

¹*Binjiang College of Nanjing University of Information Science and Technology, Wuxi, China*

*Corresponding author: clifordseptianc@gmail.com

Received 23 April 2022; Revised 28 July 2022; Accepted 29 July 2022

Abstract: Emissions from vehicles are a major contributor to greenhouse gases, and thus climate change. Electric vehicles (EVs) provide a promising solution to deal with this problem. Even though in the emerging economies like China and Europe, the adoption of EVs is praiseworthy, the pace of the EV rollout in Indonesia is slow. The Indonesian electric vehicle market has remained stagnant due to the country's low adoption rate of electric vehicles, which is currently less than 0.3%. This is because electric vehicle adoption has been stymied in Indonesia for a variety of reasons. As such, the purpose of this study is to determine the factors influencing electric vehicle adoption in Indonesia and to rank the barriers to widespread EV rollout in the country using the Grey Ordinal Priority Approach (OPA-G). It is found that high initial purchase price, insufficient amount of charging infrastructure, and a lack of government incentives are key barriers to the EV adoption in Indonesia.

Keywords: Electric Vehicle; Barriers; Grey Ordinal Priority Approach; Multiple Criteria Decision Analysis; Indonesia

1. Introduction

Transportation is an essential component of contemporary civilization; it is necessary for economic development, provision of a living wage for the masses, and the creation of various micro and macroeconomic benefits (Krishna, 2021); however, the transportation sector is also one of the largest and fastest-growing carbon dioxide emitters, accounting for 16.2 percent of total global carbon dioxide (CO₂) emissions in 2020 (Ritchie, 2020), which hurt the environment and human health (Degirmenci & Breitner, 2017). Countries sought a solution to reduce carbon emissions produced in this sector, and Khalili *et al.*, (2019) found that alternative energy sources have the potential to replace fossil fuels which currently provide energy for almost 92 percent of transportation fleets/vehicles. To reduce reliance on fossil fuel energy, electric vehicles (EVs) offer a promising opportunity for countries to replace their transportation sector, which is primarily powered by fossil fuel energy, with more environmentally friendly alternative energy (electricity).

An electric vehicle (EV) is a vehicle that is propelled by one or more traction motors or electric motors, with electrical energy stored in batteries or other energy storage (Rudatyo & Tresya, 2021). Electric vehicles have the potential to become a viable solution to the growing environmental, economic, and energy concerns in transportation such as air quality, climate change, and growing urbanization (Haddadian *et al.*, 2015) because they emit fewer greenhouse gases and pollutants into

the atmosphere than gasoline or diesel vehicles do (Ehrenberger *et al.*, 2019). However, in a world where developed countries like the USA have faced setbacks in the adoption of the EV (Bakker, 2021), the challenges that the developing countries (excluding China) are facing are no small. Currently, more than 94% of the vehicles in Indonesia, a major developing country in East Asia, are fossil-fuel vehicles (PWYP, 2019) while EVs account for only 0.2% of them (Grupta & Hansmann, 2021).

According to the World Population Review (2022), Indonesia is in the 11th position as the largest emitter of greenhouse gases by contributing around 2.09% of total greenhouse gas emissions. To address this issue, Indonesia intends to transition from internal combustion engines to more environmentally friendly electric vehicles, a long-term goal that is supported by actions such as the issuance of Presidential Regulation No. 55 of 2019, which includes an incentive to encourage the transition process. Replacing ICEVs with EVs is also underway in several cities, most notably Jakarta, Indonesia's capital, which is routinely included on lists of cities with poor air quality, even ranking among the top 6 cities with the worst air quality in 2019 (IQAir, 2022).

Indonesia is one of the largest emitters of greenhouse gases, one of the primary causes of climate change; as Southeast Asia's largest economy and second-largest car manufacturing nation, Indonesia is attempting to switch the transportation sector away from fossil fuel-powered vehicles and toward more environmentally friendly electric vehicles; however, the challenges Indonesia faces are significant, making adoption of electric vehicles in Indonesia extremely slow. Numerous studies have identified barriers to the adoption of electric vehicles in Indonesia, but few have identified and prioritized the predominant barriers to the adoption of electric vehicles in Indonesia. The current study will fill this gap in the literature by identifying the drivers and barriers to electric vehicle adoption in Indonesia followed by the weighting of these drivers and barriers based on the opinions of the respondents. The current study recognizes the following research questions:

- (1) What is the current status of the electric vehicle (EV) industry in Indonesia?
- (2) Which are the most significant barriers (and drivers) to EV adoption in Indonesia?
- (3) How Indonesia can overcome challenges and improve EV adoption?

This is the first study where the OPA-G is being employed for the evaluation of barriers to electric vehicle adoption. The rest of the study is organized as: The second section reviews the past literature on the EV and the status of its current popularity in Indonesia. The third section presents the model. The fourth section presents the research methodology. The fifth section presents data analysis and discussion. In the last section conclusion and recommendations are reported.

2. Literature review

2.1 Overview of electric vehicle industry in developed countries

Electric Vehicle development is accelerating; after a decade of rapid growth, there are now over 16 million electric vehicles (EVs) on the road worldwide (Lambert, 2022) of which 90 percent of EVs are concentrated in China, Europe, and the United States (IEA, 2020). Several countries, particularly developed countries, have made significant strides toward mass EV adoption. According to Fortuna (2019), the top 15 countries with the highest EVs uptake in terms of market share are all European countries, with Norway leading the pack with 82.7 percent market share in the first half of 2021, followed by Iceland (55.6%), Sweden (39.9%), Finland (28.3%), Denmark (26.8%), Germany (22.1%), Netherlands (19.7%), Luxembourg (18.3%), Switzerland (18.2%), Austria (17.2%), France (15.5%), Portugal (15.4%), Belgium (15.3%), UK (14.9%), and Ireland (13.4%). Although the United States (US) is not among the top 15 countries in terms of market share of electric vehicles, it ranks third in terms of market size, trailing China and Europe. By 2020, Europe has surpassed China as the region that has consistently dominated the world's largest electric vehicle market in terms of sales growth since 2012 (Perkins, 2021).

In addition, in the process of transitioning from internal combustion engine vehicle (ICEV) to more environmentally friendly EVs, almost all countries still face no small obstacles except for Norway. Scholars (Carranza *et al.*, 2014; D'Egmont, 2015; Olson, 2018) studied EVs in Norway

and discovered that while the country faced some obstacles, such as higher EVs costs relative to ICEVs and limited charging infrastructure, the Norwegian government can overcome these obstacles through incentives and a clear objective plan to build adequate charging infrastructure. Biresselioglu *et al.* (2018) performed research on electric mobility in Europe and identified hurdles to widespread EV adoption as a scarcity of charging infrastructure, growing electric vehicle prices, lengthy charging times, higher EV electricity consumption, and a scarcity of battery raw materials. Greene *et al.*, (2014) investigated the EV transition in the United States and concluded that reasons inhibiting the shift include the uncertainties around EVs technology and the limited impact of governmental regulations. Additionally, they stressed the significance of future studies on EV hurdles to remove associated uncertainties and provide a framework for policy development. Vassileva and Campillo (2017) concluded that a lack of a strong incentive scheme was a potential adoption barrier for Sweden in their analysis of EVs barriers.

2.2 Overview of electric vehicle industry in developing countries

Between 2015 and 2020, the data of market share of new electric vehicle sales in "other countries" (excluding China, Europe, and the United States) was less than 2%, indicating that the majority of countries, particularly developing countries, continue to face barriers to EV adoption (IEA, 2021). The absence of a developed country's market structure, network infrastructure, and economy are the primary reasons for developing countries' EV adoption to lag behind developed countries (Asif *et al.*, 2021).

Prakash *et al.* (2018) examined the impediments to widespread EV adoption in India and identified insufficient charging infrastructure, a lack of government incentives, and customer characteristics as significant barriers. Asadi *et al.* (2021) conducted a study on the factors influencing electric vehicle adoption and discovered that range anxiety, after-sales support, and a lack of charging infrastructure in Malaysia were the primary impediments to EV adoption progress. Bigot (2020) studied electric vehicles in Russia and discovered that the slow adoption of EVs is primarily due to the high cost of EVs, harsh winter weather conditions, and a lack of charging infrastructure; however, Russia's charging infrastructure is expanding and will overcome this barrier in the future (Habich-Sobiegalla *et al.*, 2018) concluded a study on the purchase intentions of electric vehicles in Brazil and discovered the high cost of EVs in comparison to ICEVs and the lack of public infrastructure in Brazil. Moeletsi (2021) surveyed EV barriers in Gauteng, South Africa, and discovered that the primary factors influencing people's unwillingness to purchase an electric vehicle were the vehicle's high purchase price and high battery costs.

However, although the process of EV adoption in developing countries is arguably slow to non-existent, even research on EV adoption in developing countries is still scarce (Asif *et al.*, 2021), some developing countries have set serious goals and long-term plans for EV adoption like India which has set ambitious goals to replace all ICEVs with EVs by 2030 (Chhikara *et al.*, 2021; Das *et al.*, 2019). Malaysia has plans to install 125,000 charging stations by 2030, while Thailand has established a long-term EV policy with a goal of 1.2 million operational EVs by 2036 and 690 charging stations (Schröder *et al.*, 2021), and Africa is targeting to generate 1% of global EVs in South Africa (Wilberforce, 2021).

2.3 Overview of electric vehicle industry in Indonesia

According to CSRI (2019) the Indonesian government has set a target for mass production of electric vehicles (EV) of 20% of total vehicle production by 2025, followed by a policy to stop sales of internal combustion engines (ICEV) by 2040 to achieve net-zero emissions by 2060 (Haryanto *et al.*, 2020), but the progress of electric vehicles in Indonesia is very slow compared to other countries (Yuniza *et al.*, 2021). To help accelerate the transition to electric vehicles in Indonesia, President Joko Widodo issued Presidential Regulation No. 55 of 2019 in the form of incentives to assist the transition from internal combustion engines to an electric vehicle (Maghfiroh *et al.*, 2021). However, there was only 0.15 percent of EVs on the road at the end of September 2020 (IESR,

2021). According to Yuniza *et al.* (2021), the incentives offered by the government in the presidential regulation were not enough to attract the attention of EVs in the Indonesian market. Apart from the lack of attractive government incentives, there are other barriers to the adoption of electric vehicles in Indonesia, including the high price of electric vehicles, a scarcity of spare parts and repair and maintenance services, an insufficient amount of charging infrastructure, limited battery life, a lack of public awareness, slow charging speeds, range anxiety, and a scarcity of models (Haryanto *et al.*, 2020; Huda *et al.*, 2019; Natalia *et al.*, 2020; Sidabutar, 2020; Sirait, 2020; Utami *et al.*, 2020).

However, the challenge of high electric vehicle prices will not be a major issue in Indonesia in the future (Thorn, 2021), as Indonesia is abundant in raw materials such as nickel and cobalt, which are the primary components of electric vehicle batteries. Unfortunately, the technology and infrastructure required to process these raw materials remain extremely limited, forcing Indonesia to continue importing them from abroad (Setiawan, 2021).

2.4 Identifications of drivers and barriers of electric vehicles adoption in Indonesia

2.4.1 High up-front purchase price: The high initial purchase price is one of the impediments to electric vehicle adoption in Indonesia (Sidabutar, 2020). The average purchasing power of cars in Indonesia is around 200 million (Prasetyo, 2021), while the cheapest electric vehicle in Indonesia, the DFSK Gelora E, costs 480 million Rupiah (Zigwheels, 2022), or more than 200 percent higher than the average purchasing power of cars in Indonesia. This results in consumers in Indonesia preferring internal combustion engines as their primary choice. The high price of electric vehicles in Indonesia is a result of high battery prices, as Indonesia continues to import batteries from China, which serve as the primary raw material for electric vehicles (Umah, 2021).

2.4.2 Range anxiety: Numerous studies have identified consumer range anxiety as one of the significant barriers to the adoption of electric vehicles (Liao *et al.*, 2017; Maghfiroh *et al.*, 2021; Marciano & Christian, 2020). This is undoubtedly true when the drivers notice power depletion while driving are unsure how far they can travel on their remaining battery charge, or when trips are suddenly extended (Graham-Rowe *et al.*, 2012). The uncertainty about the range of an electric vehicle's single charge or remaining battery forces drivers to reconsider using electric vehicles for lengthy trips (She *et al.*, 2017).

2.4.3 Insufficient amount of charging infrastructure: The lack of charging infrastructure is a major impediment to the adoption of electric vehicles in Indonesia (Raksodewanto, 2020). As the infrastructure that facilitates the primary fuel source for electric vehicles, charging stations are critical to the adoption of electric vehicles. However, Indonesia is still far short of the target of 25,000 gas stations by 2030, with only 200 charging stations in total currently operational due to the high cost of gas station installation in Indonesia. The charging infrastructure installed in Indonesia is currently insignificant in comparison to the number of gas stations, leading potential buyers of Indonesian electric vehicles to assume that Indonesia is still not fully prepared to transition to electric vehicles (Jati, 2021).









2.4.4 Low availability of spare parts and, repairing and maintenance services: The availability of dealers, suppliers, and electric vehicle services is still extremely limited in Indonesia (GEM INDONESIA, 2020; Khadafi, 2018), owing to the fact that electric vehicle adoption is still in the "early adopter" phase, which encourages dealers to sell ICEVs rather than EVs due to the longer anticipated sales time, lack of knowledge and competence required to sell, lower profitability for dealers, lower after-sales revenue from services, and the complexity required to install charging points (SEAI, 2020).

2.4.5 Limited battery life: A hurdle to the widespread adoption of electric vehicles is limited battery life, as stated (GEM INDONESIA, 2020) during an Electric Vehicles Indonesia webinar. Batteries are the main source of power for electric vehicles, but these batteries can only last 8 to 10 years of

use. When the battery capacity drops below 80%, the user must replace it with a new battery as it is deemed insufficient for transportation applications (Pelletier *et al.*, 2014) and it requires additional costs for battery replacement.

2.4.6 Fewer electric vehicle models: Another barrier to the widespread adoption of electric vehicles is the narrow market for EV models (Haddadian *et al.*, 2015). The limited number of electric vehicle models (lack of variety) circulating in Indonesia makes the electric vehicle market unable to meet all consumer needs and preferences. At the moment, there are only 18 different electric vehicle models scattered throughout Indonesia. Table 1 shows some of the popular EV brands in Indonesia.

Table 1. Popular brands selling EVs in Indonesia

Brand	Models	Years of Active	Type of EV	Logo	Country
Tesla	Tesla Model S	2012 - Present	BEV		The United States
	Tesla Model X	2015 – Present	BEV		
	Tesla Model 3	2017 - Present	BEV		
BMW	BMW i3s	2013 - Present	ER-EV		Germany
	BMW i8	2014 - 2020	PHEV		
	X5 Plug-in Hybrid	2014 – Present	PHEV		
Hyundai	Hyundai IONIQ Prime	2016 – Present	BEV		South Korea
	Hyundai Kona Electric	2017 - Present	HEV		
Nissan	Nissan LEAF	2010 - Present	BEV		Japan
	Nissan kicks-e POWER	2016 - Present	BEV		
Porsche	Porsche Taycan Turbo S	2019 - Present	BEV		Germany
DFSK	DFSK Gelora E	2021 - Present	BEV		China
Mitsubishi	Mitsubishi Outlander	2021 - Present	PHEV		Japan
Toyota	C-HR Hybrid	2016 - Present	HEV		Japan
	Corolla Altis	2018 - Present	HEV		
	Camry	2019 - Present	HEV		
	Lexus UX 300e	2019 - Present	BEV		
	Corolla Cross Hybrid	2020 - Present	HEV		

2.4.7 Lack of public awareness: A lack of public awareness is one of the issues leading to the delayed adoption of electric vehicles (Fortuna, 2019; Lambert, 2017). Although electric car development is still in its infancy, the reality is that many Indonesians are unfamiliar with the technology and some are unaware of the possibility to drive an electric vehicle (EV) (Aziz *et al.*, 2020). This illustrates that public awareness of electric vehicles in Indonesia is extremely low.

2.4.8 Lack of government incentives and support: To encourage the adoption of electric vehicles in Indonesia, President Joko Widodo issued Presidential Regulation Number 55 of 2019 concerning the Battery Electric Vehicle Acceleration Program for Road Transportation (BEV Regulation). The Presidential Regulation contains provisions aimed at accelerating vehicle adoption. Although articles 19 and 20 of the Presidential Regulation include fiscal and non-fiscal incentives, the fact is that the number of electric vehicles in Indonesia remains low, this is due to the lack of attractive incentives from the government to accelerate the adoption of electric vehicles (Yuniza *et al.*, 2021). Of the 17 fiscal and non-fiscal incentives, only four are directed to consumers, while the rest are directed to companies. Table 2 shows both fiscal and non-fiscal incentives contained in Presidential Regulation No. 55 of 2019 on electric vehicles.

These fiscal and non-fiscal incentives are deemed less attractive and are unlikely to result in a significant change in the absence of a subsidy policy for vehicle prices (Yuniza *et al.*, 2021). It is unfortunate because some incentive policies, like purchasing subsidies and tax exemptions, are more effective than others, particularly when some incentive policies are targeted at particular groups (Li *et al.*, 2019). As a result, the primary point of contention is the EV's exclusivity. Additionally, the cost of a single electric vehicle unit remains high in comparison to conventional vehicles. Several countries, including China, the United States, and France, have implemented price reductions or subsidies as a central policy (Volkswagen, 2019). For instance, China has an incentive system in place that entails the waiver of certain prohibitions. In major Chinese cities, electric vehicles are exempt from registration requirements and driving restrictions that apply to vehicles with combustion engines on certain days. The United States utilizes tax credits and exemptions. By purchasing an electric vehicle, users can avoid all federal taxes associated with gasoline

Table 2. Electric Vehicle Incentives in Presidential Regulation No. 55 of 2019

Fiscal Incentives (Article 19)	Non-fiscal incentives (Article 20)
<ul style="list-style-type: none"> - Import duty incentives for BEV imports; - Sales tax breaks for high-end goods; - Central and local tax incentives or reductions; - Incentives for import duties on machinery, goods, and materials in the context of investment; - Duty suspension in the context of export; - Government-funded duty incentives on the import of raw materials and/or auxiliary materials used in the production line; - Incentives for the manufacture of charging station equipment; - Export financing incentives; - Fiscal incentives for research, development, and technological innovation activities, as well as industrial vocational components, for Battery-Powered Electric Vehicles; - Parking rates at areas designated by the Regional Government; - Cost-cutting measures for charging electricity at charging stations; - Assistance with the construction of charging station infrastructure; - Professional competency certification for resource-based electric vehicle industry personnel; and - Product certification and/or technical standards for battery-based electric vehicle industry companies and component manufacturers. 	<ul style="list-style-type: none"> - Exemptions from certain road usage restrictions; - Delegation of production rights for BEV-related technology for which the Central Government and/or Regional Governments have obtained a patent license; - Promoting security and/or ensuring the industrial sector's operational activities in order to maintain the continuity or reliable performance of logistics and/or manufacturing operations for particular industrial enterprises that are critical to the national economy.

Source: Presiden Republik Indonesia (2019)

consumption. France offers an incentive program to encourage the purchase of electric vehicles. The maximum amount eligible for subsidy is 8,500 euros per electric vehicle purchase (Volkswagen, 2019). Table 3 summarizes important literature on drivers and barriers to electric vehicle adoption.

3. Grey ordinal priority approach

Multiple attribute decision-making techniques are frequently used for evaluation and assessment of multiple factors against multiple conflicting attributes. The Ordinal Priority Approach (OPA) is a new technique for multiple attribute decision-making that was proposed in 2020 by Amin Mahmoudi and colleagues and is a very useful tool to help make complex decisions confidently (Mahmoudi & Javed, 2022a). It has seen several applications in just a short span of time. For instance, Quarthey-Papafio *et al.* (2021) used the OPA to evaluate healthcare suppliers. Mahmoudi and Javed (2022b) used the OPA to evaluate Iranian construction sub-contractors. Bah and Tulkinov (2022) used the OPA to rank the automotive parts suppliers. Mahmoudi *et al.* (2021c) showed the feasibility of the OPA for handling big data. Scholars have attempted to extend the OPA to solve new problems. Mahmoudi *et al.* (2021a) proposed the fuzzy Ordinal Priority Approach to evaluate green and resilient suppliers. Pamucar *et al.* (2022) also extended OPA in fuzzy environment to prioritize transport planning strategies. Abdel-Basset *et al.* (2022) extended OPA under neutrosophic environment for evaluation of robots.

One of the major breakthroughs in the OPA theory was the development of Grey Ordinal Priority Approach (OPA-G), which was proposed by Mahmoudi *et al.* (2021b). The model combined the benefits of the grey number theory and the OPA. Later, Shajedul (2022) validated the OPA-G model by evaluating sustainable agricultural technologies. The OPA-G model does

Table 3. The summary of drivers and barriers to electric vehicle adoption

Year	Description	Region of focus	Methodology	Reference
2014	The study identified the relationship between financial incentives and other socio-economic factors to EV adoption	N/A	Multiple Linear Regression (MLR) analysis	Sierzechula <i>et al.</i> (2014)
2017	The study identified the barriers that can hamper the transition to EV in BRICS Countries	Brazil, Russia, India, China, and South Africa	Descriptive Study (Case Analysis)	Pratiwi (2016)
2019	The Study explores barriers to the uptake of plug-in Electric Vehicles (EV)	Ireland	Descriptive Study (Case study)	O'Neill <i>et al.</i> (2019)
2020	The study identified the challenges and rank the barriers to the use of Electric Vehicles (EV)	Nepal	Analytical Hierarchy Process (AHP)	Adhikari <i>et al.</i> (2020)
2020	The study identified the strategies and challenges in Electrical Vehicles (EV) adoption	Indonesia	System dynamics	Natalia <i>et al.</i> (2020)
2020	The study identified the drivers and barriers to different types of Electric Vehicle (EV) adoption	Developing countries	Preferred Reporting Items for Systematic Reviews and Meta-analysis (PRISMA)	Rajper and Albrecht (2020)
2021	The study identified the drivers, barriers, and support mechanisms of transition from ICE to EVs	India	Qualitative approach	Chhikara <i>et al.</i> (2021)
2021	The study identified the contextual preferential set of EV barriers	India	Best-Worst Method (BWM) and Interpretive Structural Modeling (ISM)	Tarei <i>et al.</i> (2021)
2022	The Study identified the factors which affect consumer's intention to EV	Malaysia	Decision-Making Trials and Evaluation Laboratory (DEMATEL)	Asadi <i>et al.</i> (2022)
2022	This study will identify the drivers and barriers to Electric Vehicle (EV) adoption	Indonesia	Grey Ordinal Priority Approach (OPA-G)	The current study

not require input data to be linguistic variables or pairwise comparisons, but it can present expert, criteria, and alternative weights. Defining sets, indexes, variables, and parameters is necessary prior to introduce OPA-G. As a result, Table 4 includes all necessary sets, indexes, and variables for comprehending the proposed model.

3.1 Definitions

The following definitions and operations are integral part of the Grey Ordinal Priority Approach (OPA-G) and have been borrowed from Mahmoudi *et al.* (2021b).

DEFINITION 1. Assume we have the grey value $\otimes A$. When no distribution exists for the grey number $\otimes A$, the kernel of the grey number A should be determined as follows.

$$\otimes \hat{A} = \frac{1}{2}(\bar{A} + \underline{A}) \quad (1)$$

DEFINITION 2. Suppose that we have crisp number A . Therefore, $\otimes A$ has a grey rank in the interval $[Rank(A) - 0.5, Rank(A) + 0.5]$. To convert crisp rank n to grey rank $\otimes n$, Equation 2 can be employed.

$$Rank \otimes n = [n - 0.5, n + 0.5] \quad (2)$$

DEFINITION 3. If the respondent(s) has reservations about choosing between the ranks C and D for a barrier while $C < D$, then the following relation should be used for the grey rank.

$$Rank(\otimes C, \otimes D) = [Rank(C) - 0.5, Rank(D) + 0.5] \quad (3)$$

DEFINITION 4. Let $\otimes A = [\bar{A}, \underline{A}]$ and $\otimes B = [\bar{B}, \underline{B}]$. The main operations between $\otimes A$ and $\otimes B$ have been presented in Equations 4 to 7.

$$\otimes A + \otimes B = [\underline{A} + \underline{B}, \bar{A} + \bar{B}], \quad (4)$$

$$\otimes A - \otimes B = \otimes A + (-\otimes B) = [\underline{A} - \bar{B}, \bar{A} - \underline{B}], \quad (5)$$

$$\otimes A \times \otimes B = [Min\{\underline{A}\underline{B}, \bar{A}\bar{B}, \bar{A}\underline{B}, \underline{A}\bar{B}\}, Max\{\underline{A}\underline{B}, \bar{A}\bar{B}, \bar{A}\underline{B}, \underline{A}\bar{B}\}], \quad (6)$$

$$\frac{\otimes A}{\otimes B} = \otimes A \times \otimes B^{-1} = [Min\{\frac{\underline{A}}{\underline{B}}, \frac{\underline{A}}{\bar{B}}, \frac{\bar{A}}{\underline{B}}, \frac{\bar{A}}{\bar{B}}\}, Max\{\frac{\underline{A}}{\underline{B}}, \frac{\underline{A}}{\bar{B}}, \frac{\bar{A}}{\underline{B}}, \frac{\bar{A}}{\bar{B}}\}] \quad (7)$$

3.2 Algorithm

The steps to extract the weights and ranking of the respondents and the barriers to EV adoption in Indonesia are listed below.

STEP 1. Identify the barriers to electric vehicle adoption in Indonesia.

STEP 2. Identify the respondents based on their knowledge of the problem.

Table 4. Sets, indexes, and variables for OPA-G method

Sets	
I	Sets of respondents $\forall i \in I$
J	Sets of barriers $\forall j \in J$
Indexes	
I	Index of the respondents (A, ..., K)
J	Index of barriers (1, ..., 8)
Variables	
$\otimes Z$	Grey objective function
$\otimes W_{ij}$	Grey weight(importance) of J^{th} barrier based on respondent at I^{th} rank
Parameters	
$\otimes i$	Grey rank of the respondent i
$\otimes j$	Grey rank of the barrier j

STEP 3. Ranking the barriers: In this stage, the respondent(s) should specify the priorities of barriers, and Definitions 2 and 3 should be employed to convert the crisp ranks to grey ranks. Also, Definition 1 can be used to sort grey numbers.

STEP 4. Solving the OPA-G model, finding the weights of the barriers, and ranking the barriers: Based on the collected data in Steps 1 to 3, the linear model 8 should be formed.

$$\begin{aligned}
 & \text{Max } \otimes Z \\
 & \text{S.t:} \\
 & \otimes Z \leq \otimes i (\otimes j (\otimes r (\otimes W_{ij}^r - \otimes W_{ij}^{r+1})) \quad \forall i, j \text{ and } r \\
 & \otimes Z \leq \otimes i \otimes j \otimes m \otimes W_{ij}^m \quad \forall i \text{ and } j \\
 & \sum_{i=1}^p \sum_{j=1}^n \otimes W_{ij} = [0.8, 1.2] \\
 & \otimes W_{ij} \geq 0 \quad \forall i \text{ and } j
 \end{aligned} \tag{8}$$

where $\otimes Z$ is unrestricted in sign.

After solving the grey model 8, Equations 9 and 10 should be used to obtain the grey weight of the respondents and barriers. The grey weight of the barriers can be determined using Equation 9.

$$\otimes W_j = \sum_{i=1}^p \otimes W_{ij}, \forall j \tag{9}$$

To calculate the grey weights of the respondents, Equation (10) should be utilized.

$$\otimes W_i = \sum_{j=1}^n \otimes W_{ij}, \forall i \tag{10}$$

STEP 5. In this step both Grey Possibility Degree and kernel can be used. The current study will use the kernel, which is much easier to calculate. The kernel is given by.

$$\otimes W = \frac{1}{2} (\underline{W} + \overline{W}) \tag{11}$$

4. Results and discussion

4.1 The research instrument

The questionnaire was divided into two parts; the first section aimed to gather demographic information of the respondents. In the second part, respondents were asked fundamental questions about their perceptions of the barriers to electric vehicle adoption in Indonesia. The eight barriers came from section 2.4. The 7-point Likert scale, which is an ordinal scale, was used to collect data where 1 indicated “1st Priority” and 7 indicated “7th Priority”. Respondents were asked to assign ranks to each barrier, and were given freedom to assign any rank to any factor based on their viewpoint.

4.2 Data collection

The data collection instrument for this study, a questionnaire, was created and distributed through Google Form targeted at Indonesian citizens. The data was collected from March to April 2022. Thirteen respondents filled the questionnaire but eleven of them knew driving while holding valid driving license. These eleven respondents formed our sample size. The demographic profile of the respondents is shown in Table 5. After converting all data to OPA-G specifications, Lingo software was used to build the OPA-G model and its implementation.

Table 5. The demographic profile of the respondents (N = 11)

Characteristics	Level	Number	%
Age	21 to 30	6	54.5
	31 to 39	2	18.1
	40 to 49	2	18.1
	50 to 59	1	9.1
Marital status	Single	6	54.5
	Married	4	36.3
	Did not answer	1	9.1
City	Jakarta	3	27.2
	Surabaya	2	18.1
	Banyuwangi	1	9.1
	Palembang	1	9.1
	Malang	1	9.1
	Bekasi	1	9.1
	Yogyakarta	1	9.1
	Bandung	1	9.1
Gender	Male	8	72.7
	Female	3	27.2
Educational background	Bachelor (4 year degree)	10	90.9
	High School Diploma	1	9.1
Driving intensity	At least 1 day per week	3	27.2
	At least 4 days per week	2	18.1
	At least 5 days per week	2	27.2
	At least 7 days per week	2	27.2
Purpose of driving	Work, Personal, and Family	6	54.5
	Personal and Family	2	18.1
	Work and Personal	1	9.1
	Work	1	9.1
	Family	1	9.1
Knowledge of Government incentives to support EVs	Know some of the incentives	7	63.6
	Know most of the incentives	2	18.1
	Have no idea of the incentives	2	18.2
Awareness on environmental and pollution-related issues	Aware with the most of the issues	6	54.5
	Aware with the some of the issues	4	36.3
	Have no idea about the issues	1	9.1

4.3 The model

In the current study, eleven respondents and eight barriers/factors were involved and the complete model was very lengthy, and thus is shown in the Appendix. The model was run on LINGO software.

5. Data, results and discussion

The study surveyed eleven respondents with eight separate variables as mentioned in Table 6. It is critical to highlight that all respondents were treated equally in the study. Nonetheless, the the Grey Ordinal Priority Approach (OPA-G) is still capable of calculating the weight of each respondent as well. Tables 7 and 8 indicate the weights and rankings for the barriers and respondents. Equations (9) and (10) are used to determine the barrier and respondent weights. In these tables, A, B, ..., K are the respondents/experts, and B1, B2, ..., B8 are our barriers. The complete definitions of the barriers are listed below:

Barrier 1 (B1) = High up-front purchase price;

Barrier 2 (B2) = Low availability of spare parts, and repairing and maintenance services;

Barrier 3 (B3) = Insufficient amount of charging infrastructure;

Barrier 4 (B4) = Limited battery life;

Barrier 5 (B5) = Lack of public awareness;

Table 6. Opinion of respondents for factors to electric vehicle adoption in Indonesia

Respondents	Rank Type	B1	B2	B3	B4	B5	B6	B7	B8
A	CR	1	3	1	4	2	2	5	1
	GR	[0.5,1.5]	[2.5,3.5]	[0.5,1.5]	[3.5,4.5]	[1.5,2.5]	[1.5,2.5]	[4.5,5.5]	[0.5,1.5]
B	CR	1	2	2	4	3	3	5	4
	GR	[0.5,1.5]	[1.5,2.5]	[1.5,2.5]	[3.5,4.5]	[2.5,3.5]	[2.5,3.5]	[4.5,5.5]	[3.5,4.5]
C	CR	4	3	4	3	4	4	2	3
	GR	[3.5,4.5]	[2.5,3.5]	[3.5,4.5]	[2.5,3.5]	[3.5,4.5]	[3.5,4.5]	[1.5,2.5]	[2.5,3.5]
D	CR	1	7	4	1	1	1	6	1
	GR	[0.5,1.5]	[6.5,7.5]	[3.5,4.5]	[0.5,1.5]	[0.5,1.5]	[0.5,1.5]	[5.5,6.5]	[0.5,1.5]
E	CR	3	1	3	2	3	4	2	2
	GR	[2.5,3.5]	[0.5,1.5]	[2.5,3.5]	[1.5,2.5]	[2.5,3.5]	[3.5,4.5]	[1.5,2.5]	[1.5,2.5]
F	CR	1	1	1	1	6	1	7	1
	GR	[0.5,1.5]	[0.5,1.5]	[0.5,1.5]	[0.5,1.5]	[5.5,6.5]	[0.5,1.5]	[6.5,7.5]	[0.5,1.5]
G	CR	3	4	5	3	3	3	4	2
	GR	[2.5,3.5]	[3.5,4.5]	[4.5,5.5]	[2.5,3.5]	[2.5,3.5]	[2.5,3.5]	[3.5,4.5]	[1.5,2.5]
H	CR	2	2	1	2	2	2	2	2
	GR	[1.5,2.5]	[1.5,2.5]	[0.5,1.5]	[1.5,2.5]	[1.5,2.5]	[1.5,2.5]	[1.5,2.5]	[1.5,2.5]
I	CR	1	3	1	4	2	2	7	3
	GR	[0.5,1.5]	[2.5,3.5]	[0.5,1.5]	[3.5,4.5]	[1.5,2.5]	[1.5,2.5]	[6.5,7.5]	[2.5,3.5]
J	CR	1	1	2	6	2	5	4	2
	GR	[0.5,1.5]	[0.5,1.5]	[1.5,2.5]	[5.5,6.5]	[1.5,2.5]	[4.5,5.5]	[3.5,4.5]	[1.5,2.5]
K	CR	2	2	2	2	2	2	2	2
	GR	[1.5,2.5]	[1.5,2.5]	[1.5,2.5]	[1.5,2.5]	[1.5,2.5]	[1.5,2.5]	[1.5,2.5]	[1.5,2.5]

Table 7. Weight and ranking of barriers

Barriers	\bar{W}	\overline{W}	$\otimes W$	Rank
High up-front purchase price	0.159	0.211	0.185	1
Low availability of spare parts, and repairing and maintenance services	0.108	0.159	0.133	4
Insufficient amount of Charging infrastructure	0.125	0.176	0.151	2
Limited battery life	0.078	0.120	0.099	7
Lack of public awareness	0.082	0.141	0.111	6
Range anxiety	0.087	0.136	0.112	5
Fewer Electric Vehicles models	0.045	0.085	0.065	8
Lack of government incentives	0.116	0.173	0.145	3

Table 8. Weights and ranks of the respondents

Respondents	\bar{W}	\overline{W}	$\otimes W$	Rank
A	0.111	0.164	0.138	1
B	0.070	0.119	0.094	6
C	0.033	0.063	0.048	11
D	0.102	0.128	0.115	2
E	0.070	0.114	0.092	7
F	0.104	0.116	0.110	5
G	0.046	0.091	0.069	8
H	0.052	0.073	0.063	9
I	0.088	0.137	0.112	3
J	0.086	0.135	0.111	4
K	0.038	0.060	0.049	10

Barrier 6 (B6) = Range anxiety;

Barrier 7 (B7) = Fewer Electric Vehicles (EVs) models;

Barrier 8 (B8) = Lack of government incentives.

As shown in Table 7, The high upfront purchase price of electric vehicles is the most significant constraint in Indonesia, followed by an insufficient amount of charging infrastructure in second place and a lack of government incentives in third place, while limited battery life and a lack of

electric vehicle models are the two lowest barriers to electric vehicle adoption in Indonesia. Additionally, as shown in Table 8, the OPA-G was successful in determining the rank of each respondent. Whereas respondent 'K' and respondent 'C' are the two least reliable respondents and rank in the bottom two, this is because respondent 'K' answered all core questions with the same answer while respondent 'C' answered all core questions with two consecutively repeated answers. The ranking and weights of the eight barriers to the electric vehicle adoption in Indonesia are shown in Figure 1.

Transportation is critical for connecting people, places, goods, and services, as well as for community development, improving people's quality of life and the economy's overall health. However, it is also a significant source of greenhouse gases. The world, including Indonesia, is attempting to address these issues by shifting to more environmentally friendly energy sources and shifting away from fossil fuel-powered vehicles toward electric vehicles. However, Indonesia is having difficulty adopting electric vehicles; barriers such as a lack of charging infrastructure, the high cost of electric vehicles, and a lack of public awareness all contributed to the slow adoption of EVs. Recognizing the most significant drivers and barriers to electric vehicle adoption can help Indonesia choose the best method to overcome these barriers as well as improve the EVs adoption. Therefore, the current study identified the factors of electric vehicle adoption in Indonesia and applied the OPA-G method to evaluate those factors. After analyzing the responses of all respondents, Table 7 was created. The results indicate that the top three barriers to electric vehicle adoption in Indonesia are a high initial purchase price, an insufficient amount of charging infrastructure, and a lack of government incentives for EVs, followed by a lack of spare parts and repair and maintenance services, range anxiety, a lack of public awareness, a limited battery life, and a lack of EV models.

However, the current study discovered that there is no literature suggesting an uncertain ranking for the barriers to electric vehicle adoption in Indonesia. As a result, the current study used the OPA-G model to account for the uncertainty associated with barriers to electric vehicle adoption and to determine the relative importance of various barriers. With the OPA-G method, decision-makers can truly benefit from a high degree of flexibility when dealing with a variety of electric vehicle-related factors and uncertainties. Additionally, the OPA-G method eliminates the need for data normalization, a pairwise comparison matrix, and opinion aggregation.

6. Conclusion

Climate change and greenhouse gas emissions have become increasingly serious in recent years. While transportation is an integral part of any country, it cannot be denied that it is also a significant



Fig 1. The weights and ranks of the barriers to EV adoption

contributor to greenhouse gases, and Indonesia, as one of the largest emitters, takes this issue seriously. Indonesia is following developed countries' lead in addressing the issue of greenhouse gases by transitioning to electric vehicles that are more environmentally friendly than fossil fuel vehicles. However, the barriers to the adoption of electric vehicles are not insignificant; even Indonesia, Southeast Asia's largest economy, has less than 0.3 percent of electric vehicles due to barriers such as the high cost of electric vehicles in Indonesia, insufficient number of charging infrastructure, and a lack of government incentives. This pushes Indonesia to re-identify and prioritizes the barriers to electric vehicle adoption. There are numerous Multi-Criteria Decision-Making approaches available in the literature to assist decision-makers, but several of these methods are incapable of dealing with information ambiguity. Thus, the Grey Ordinal Priority Approach (OPA-G) was used in this study, a current multi-attribute decision-making technique that assists decision-makers in identifying the barriers to electric car adoption. In Indonesia, choose the best feasible solution for the adoption of electric vehicles.

To combat climate change and greenhouse gas emissions and to achieve carbon neutrality, there is no doubt that transitioning to electric vehicles is one of the best steps the world can take, regardless of the various challenges associated with each country's stage of electric vehicle adoption. This study identified several drivers and barriers to electric vehicle adoption in Indonesia and determined that the high cost of EVs, a lack of charging infrastructure, and a lack of government incentives were the top three barriers to EV adoption. These top three barriers are inextricably linked; by offering more attractive incentives for EVs, such as price subsidies comparable to those offered in China, the United States, and Europe, as well as incentives to boost infrastructure installation, it is possible to increase the number of EVs in Indonesia.

In the future, the OPA-G model can be used to prioritize barriers to EV adaption in other countries as well. In the current study, only one criterion was involved. In the future, more criteria can be considered. Also, barriers like low charging speed can be included in the future.

Acknowledgement

The work is a derivative of the undergraduate thesis of the author submitted to Nanjing University of Information Science and Technology, China, and written under the supervision of Dr. Saad Ahmed Javed. The work is supported by the Natural Science Foundation of the Jiangsu Higher Education Institutions of China (No. 21KJB480011).

Appendix

In the OPA-G model built below, L denotes upper limit, U denotes lower limit and W denotes weights. A, B, ... K denotes respondents/experts. The program was written and run on LINGO software.

MAX=1/2*ZU+1/2*ZL;		
! RESPONDENT A;	! RESPONDENT C;	1.5*4.5*(WLD3-WLD7)>=ZL;
1.5*1.5*(WLA1-WLA5)>=ZL;	1.5*2.5*(WLC7-WLC2)>=ZL;	0.5*3.5*(WUD3-WUD7)>=ZU;
0.5*0.5*(WUA1-WUA5)>=ZU;	0.5*1.5*(WUC7-WUC2)>=ZU;	1.5*6.5*(WLD7-WLD2)>=ZL;
1.5*1.5*(WLA3-WLA5)>=ZL;	1.5*2.5*(WLC7-WLC4)>=ZL;	0.5*5.5*(WUD7-WUD2)>=ZU;
0.5*0.5*(WUA3-WUA5)>=ZU;	0.5*1.5*(WUC7-WUC4)>=ZU;	1.5*7.5*(WLD2)>=ZL;
1.5*1.5*(WLA8-WLA5)>=ZL;	1.5*2.5*(WLC7-WLC8)>=ZL;	0.5*6.5*(WUD2)>=ZU;
0.5*0.5*(WUA8-WUA5)>=ZU;	0.5*1.5*(WUC7-WUC8)>=ZU;	! RESPONDENT E;
1.5*1.5*(WLA1-WLA6)>=ZL;	1.5*3.5*(WLC2-WLC1)>=ZL;	1.5*1.5*(WLE2-WLE4)>=ZL;
0.5*0.5*(WUA1-WUA6)>=ZU;	0.5*2.5*(WUC2-WUC1)>=ZU;	0.5*0.5*(WUE2-WUE4)>=ZU;
1.5*1.5*(WLA3-WLA6)>=ZL;	1.5*3.5*(WLC4-WLC1)>=ZL;	1.5*1.5*(WLE2-WLE7)>=ZL;
0.5*0.5*(WUA3-WUA6)>=ZU;	0.5*2.5*(WUC4-WUC1)>=ZU;	0.5*0.5*(WUE2-WUE7)>=ZU;
1.5*1.5*(WLA8-WLA6)>=ZL;	1.5*3.5*(WLC8-WLC1)>=ZL;	1.5*1.5*(WLE2-WLE8)>=ZL;
0.5*0.5*(WUA8-WUA6)>=ZU;	0.5*2.5*(WUC8-WUC1)>=ZU;	0.5*0.5*(WUE2-WUE8)>=ZU;
1.5*2.5*(WLA5-WLA2)>=ZL;	1.5*3.5*(WLC2-WLC3)>=ZL;	1.5*2.5*(WLE4-WLE1)>=ZL;
0.5*1.5*(WUA5-WUA2)>=ZU;	0.5*2.5*(WUC2-WUC3)>=ZU;	0.5*1.5*(WUE4-WUE1)>=ZU;
1.5*2.5*(WLA6-WLA2)>=ZL;	1.5*3.5*(WLC4-WLC3)>=ZL;	1.5*2.5*(WLE7-WLE1)>=ZL;
0.5*1.5*(WUA6-WUA2)>=ZU;	0.5*2.5*(WUC4-WUC3)>=ZU;	0.5*1.5*(WUE7-WUE1)>=ZU;
1.5*3.5*(WLA2-WLA4)>=ZL;	1.5*3.5*(WLC8-WLC3)>=ZL;	1.5*2.5*(WLE8-WLE1)>=ZL;
0.5*2.5*(WUA2-WUA4)>=ZU;	0.5*2.5*(WUC8-WUC3)>=ZU;	0.5*1.5*(WUE8-WUE1)>=ZU;
1.5*4.5*(WLA4-WLA7)>=ZL;	1.5*3.5*(WLC2-WLC5)>=ZL;	

0.5*3.5*(WUA4-WUA7)>=ZU;	0.5*2.5*(WUC2-WUC5)>=ZU;	1.5*2.5*(WLE4-WLE3)>=ZL;
1.5*5.5*(WLA7)>=ZL;	1.5*3.5*(WLC4-WLC5)>=ZL;	0.5*1.5*(WUE4-WUE3)>=ZU;
0.5*4.5*(WUA7)>=ZU;	0.5*2.5*(WUC4-WUC5)>=ZU;	1.5*2.5*(WLE7-WLE3)>=ZL;
	1.5*3.5*(WLC8-WLC5)>=ZL;	0.5*1.5*(WUE7-WUE3)>=ZU;
! RESPONDENT B;	0.5*2.5*(WUC8-WUC5)>=ZU;	1.5*2.5*(WLE8-WLE3)>=ZL;
	1.5*3.5*(WLC2-WLC6)>=ZL;	0.5*1.5*(WUE8-WUE3)>=ZU;
1.5*1.5*(WLB1-WLB2)>=ZL;	0.5*2.5*(WUC2-WUC6)>=ZU;	1.5*2.5*(WLE4-WLE5)>=ZL;
0.5*0.5*(WUB1-WUB2)>=ZU;	1.5*3.5*(WLC4-WLC6)>=ZL;	0.5*1.5*(WUE4-WUE5)>=ZU;
1.5*1.5*(WLB1-WLB3)>=ZL;	0.5*2.5*(WUC4-WUC6)>=ZU;	1.5*2.5*(WLE7-WLE5)>=ZL;
0.5*0.5*(WUB1-WUB3)>=ZU;	1.5*3.5*(WLC8-WLC6)>=ZL;	0.5*1.5*(WUE7-WUE5)>=ZU;
1.5*2.5*(WLB2-WLB5)>=ZL;	0.5*2.5*(WUC8-WUC6)>=ZU;	1.5*2.5*(WLE8-WLE5)>=ZL;
0.5*1.5*(WUB2-WUB5)>=ZU;	1.5*4.5*(WLC1)>=ZL;	0.5*1.5*(WUE8-WUE5)>=ZU;
1.5*2.5*(WLB3-WLB5)>=ZL;	0.5*3.5*(WUC1)>=ZU;	1.5*3.5*(WLE1-WLE6)>=ZL;
0.5*1.5*(WUB3-WUB5)>=ZU;	1.5*4.5*(WLC3)>=ZL;	0.5*2.5*(WUE1-WUE6)>=ZU;
1.5*2.5*(WLB2-WLB6)>=ZL;	0.5*3.5*(WUC3)>=ZU;	1.5*3.5*(WLE3-WLE6)>=ZL;
0.5*1.5*(WUB2-WUB6)>=ZU;	1.5*4.5*(WLC5)>=ZL;	0.5*2.5*(WUE3-WUE6)>=ZU;
1.5*2.5*(WLB3-WLB6)>=ZL;	0.5*3.5*(WUC5)>=ZU;	1.5*3.5*(WLE5-WLE6)>=ZL;
0.5*1.5*(WUB3-WUB6)>=ZU;	1.5*4.5*(WLC6)>=ZL;	0.5*2.5*(WUE5-WUE6)>=ZU;
1.5*3.5*(WLB5-WLB4)>=ZL;	0.5*3.5*(WUC6)>=ZU;	1.5*4.5*(WLE6)>=ZL;
0.5*2.5*(WUB5-WUB4)>=ZU;		0.5*3.5*(WUE6)>=ZU;
1.5*3.5*(WLB6-WLB4)>=ZL;	! RESPONDENT D;	
0.5*2.5*(WUB6-WUB4)>=ZU;		! RESPONDENT F;
1.5*3.5*(WLB5-WLB8)>=ZL;	1.5*1.5*(WLD1-WLD3)>=ZL;	
0.5*2.5*(WUB5-WUB8)>=ZU;	0.5*0.5*(WUD1-WUD3)>=ZU;	1.5*1.5*(WLF1-WLF5)>=ZL;
1.5*3.5*(WLB6-WLB8)>=ZL;	1.5*1.5*(WLD4-WLD3)>=ZL;	0.5*0.5*(WUF1-WUF5)>=ZU;
0.5*2.5*(WUB6-WUB8)>=ZU;	0.5*0.5*(WUD4-WUD3)>=ZU;	1.5*1.5*(WLF2-WLF5)>=ZL;
1.5*4.5*(WLB4-WLB7)>=ZL;	1.5*1.5*(WLD5-WLD3)>=ZL;	0.5*0.5*(WUF2-WUF5)>=ZU;
0.5*3.5*(WUB4-WUB7)>=ZU;	0.5*0.5*(WUD5-WUD3)>=ZU;	1.5*1.5*(WLF3-WLF5)>=ZL;
1.5*4.5*(WLB8-WLB7)>=ZL;	1.5*1.5*(WLD6-WLD3)>=ZL;	0.5*0.5*(WUF3-WUF5)>=ZU;
0.5*3.5*(WUB8-WUB7)>=ZU;	0.5*0.5*(WUD6-WUD3)>=ZU;	1.5*1.5*(WLF4-WLF5)>=ZL;
1.5*5.5*(WLB7)>=ZL;	1.5*1.5*(WLD8-WLD3)>=ZL;	0.5*0.5*(WUF4-WUF5)>=ZU;
0.5*4.5*(WUB7)>=ZU;	0.5*0.5*(WUD8-WUD3)>=ZU;	1.5*1.5*(WLF6-WLF5)>=ZL;
0.5*0.5*(WUF6-WUF5)>=ZU;	! RESPONDENTS H;	0.5*0.5*(WUI3-WUI6)>=ZU;
1.5*1.5*(WLF8-WLF5)>=ZL;		1.5*2.5*(WLI5-WLI2)>=ZL;
0.5*0.5*(WUF8-WUF5)>=ZU;	1.5*1.5*(WLH3-WLH1)>=ZL;	0.5*1.5*(WUI5-WUI2)>=ZU;
1.5*6.5*(WLF5-WLF7)>=ZL;	0.5*0.5*(WUH3-WUH1)>=ZU;	1.5*2.5*(WLI6-WLI2)>=ZL;
0.5*5.5*(WUF5-WUF7)>=ZU;	1.5*1.5*(WLH3-WLH2)>=ZL;	0.5*1.5*(WUI6-WUI2)>=ZU;
1.5*7.5*(WLF7)>=ZL;	0.5*0.5*(WUH3-WUH2)>=ZU;	1.5*2.5*(WLI5-WLI8)>=ZL;
0.5*6.5*(WUF7)>=ZU;	1.5*1.5*(WLH3-WLH4)>=ZL;	0.5*1.5*(WUI5-WUI8)>=ZU;
	0.5*0.5*(WUH3-WUH4)>=ZU;	1.5*2.5*(WLI6-WLI8)>=ZL;
! RESPONDENT G;	1.5*1.5*(WLH3-WLH5)>=ZL;	0.5*1.5*(WUI6-WUI8)>=ZU;
	0.5*0.5*(WUH3-WUH5)>=ZU;	1.5*3.5*(WLI2-WLI4)>=ZL;
1.5*2.5*(WLG8-WLG1)>=ZL;	1.5*1.5*(WLH3-WLH6)>=ZL;	0.5*2.5*(WUI2-WUI4)>=ZU;
0.5*1.5*(WUG8-WUG1)>=ZU;	0.5*0.5*(WUH3-WUH6)>=ZU;	1.5*3.5*(WLI8-WLI4)>=ZL;
1.5*2.5*(WLG8-WLG4)>=ZL;	1.5*1.5*(WLH3-WLH7)>=ZL;	0.5*2.5*(WUI8-WUI4)>=ZU;
0.5*1.5*(WUG8-WUG4)>=ZU;	0.5*0.5*(WUH3-WUH7)>=ZU;	1.5*4.5*(WLI4-WLI7)>=ZL;
1.5*2.5*(WLG8-WLG5)>=ZL;	1.5*1.5*(WLH3-WLH8)>=ZL;	0.5*3.5*(WUI4-WUI7)>=ZU;
0.5*1.5*(WUG8-WUG5)>=ZU;	0.5*0.5*(WUH3-WUH8)>=ZU;	1.5*7.5*(WLI7)>=ZL;
1.5*2.5*(WLG8-WLG6)>=ZL;	1.5*2.5*(WLH1)>=ZL;	0.5*6.5*(WUI7)>=ZU;
0.5*1.5*(WUG8-WUG6)>=ZU;	0.5*1.5*(WUH1)>=ZU;	
1.5*3.5*(WLG1-WLG2)>=ZL;	1.5*2.5*(WLH2)>=ZL;	! RESPONDENT J;
0.5*2.5*(WUG1-WUG2)>=ZU;	0.5*1.5*(WUH2)>=ZU;	
1.5*3.5*(WLG4-WLG2)>=ZL;	1.5*2.5*(WLH4)>=ZL;	1.5*1.5*(WLJ1-WLJ3)>=ZL;
0.5*2.5*(WUG4-WUG2)>=ZU;	0.5*1.5*(WUH4)>=ZU;	0.5*0.5*(WUJ1-WUJ3)>=ZU;
1.5*3.5*(WLG5-WLG2)>=ZL;	1.5*2.5*(WLH5)>=ZL;	1.5*1.5*(WLJ2-WLJ3)>=ZL;
0.5*2.5*(WUG5-WUG2)>=ZU;	0.5*1.5*(WUH5)>=ZU;	0.5*0.5*(WUJ2-WUJ3)>=ZU;
1.5*3.5*(WLG6-WLG2)>=ZL;	1.5*2.5*(WLH6)>=ZL;	1.5*1.5*(WLJ1-WLJ5)>=ZL;
0.5*2.5*(WUG6-WUG2)>=ZU;	0.5*1.5*(WUH6)>=ZU;	0.5*0.5*(WUJ1-WUJ5)>=ZU;
1.5*3.5*(WLG1-WLG7)>=ZL;	1.5*2.5*(WLH7)>=ZL;	1.5*1.5*(WLJ2-WLJ5)>=ZL;
0.5*2.5*(WUG1-WUG7)>=ZU;	0.5*1.5*(WUH7)>=ZU;	0.5*0.5*(WUJ2-WUJ5)>=ZU;
1.5*3.5*(WLG4-WLG7)>=ZL;	1.5*2.5*(WLH8)>=ZL;	1.5*1.5*(WLJ1-WLJ8)>=ZL;
0.5*2.5*(WUG4-WUG7)>=ZU;	0.5*1.5*(WUH8)>=ZU;	0.5*0.5*(WUJ1-WUJ8)>=ZU;
1.5*3.5*(WLG5-WLG7)>=ZL;		1.5*1.5*(WLJ2-WLJ8)>=ZL;
0.5*2.5*(WUG5-WUG7)>=ZU;	! RESPONDENTS I;	0.5*0.5*(WUJ2-WUJ8)>=ZU;
1.5*3.5*(WLG6-WLG7)>=ZL;		1.5*2.5*(WLJ3-WLJ7)>=ZL;
0.5*2.5*(WUG6-WUG7)>=ZU;	1.5*1.5*(WLI1-WLI5)>=ZL;	0.5*1.5*(WUJ3-WUJ7)>=ZU;
1.5*4.5*(WLG2-WLG3)>=ZL;	0.5*0.5*(WUI1-WUI5)>=ZU;	1.5*2.5*(WLJ5-WLJ7)>=ZL;
0.5*3.5*(WUG2-WUG3)>=ZU;	1.5*1.5*(WLI3-WLI5)>=ZL;	0.5*1.5*(WUJ5-WUJ7)>=ZU;
1.5*4.5*(WLG7-WLG3)>=ZL;	0.5*0.5*(WUI3-WUI5)>=ZU;	1.5*2.5*(WLJ8-WLJ7)>=ZL;
0.5*3.5*(WUG7-WUG3)>=ZU;	1.5*1.5*(WLI1-WLI6)>=ZL;	0.5*1.5*(WUJ8-WUJ7)>=ZU;
1.5*5.5*(WLG3)>=ZL;	0.5*0.5*(WUI1-WUI6)>=ZU;	1.5*4.5*(WLJ7-WLJ6)>=ZL;
0.5*4.5*(WUG3)>=ZU;	1.5*1.5*(WLI3-WLI6)>=ZL;	0.5*3.5*(WUJ7-WUJ6)>=ZU;

1.5*5.5*(WLJ6-WLJ4)>=ZL;
 0.5*4.5*(WUJ6-WUJ4)>=ZU;
 1.5*6.5*(WLJ4)>=ZL;
 0.5*5.5*(WUJ4)>=ZU;

 ! RESPONDENT K;

 1.5*2.5*(WLK1)>=ZL;
 0.5*1.5*(WUK1)>=ZU;

 1.5*2.5*(WLK2)>=ZL;
 0.5*1.5*(WUK2)>=ZU;

 1.5*2.5*(WLK3)>=ZL;
 0.5*1.5*(WUK3)>=ZU;

 1.5*2.5*(WLK4)>=ZL;
 0.5*1.5*(WUK4)>=ZU;

 1.5*2.5*(WLK5)>=ZL;
 0.5*1.5*(WUK5)>=ZU;

 1.5*2.5*(WLK6)>=ZL;
 0.5*1.5*(WUK6)>=ZU;

 1.5*2.5*(WLK7)>=ZL;
 0.5*1.5*(WUK7)>=ZU;

 1.5*2.5*(WLK8)>=ZL;
 0.5*1.5*(WUK8)>=ZU;

 ZL>=ZU;

 WUA1+WUA2+WUA3+WUA4+WUA5+WUA6+WUA7+WUA8+WUB1+WUB2+WUB3+WUA4+WUB5+WUB6+WUB7+WUB8+WUC1+WUC2+WUC3+WUC4+WUC5+WUC6+WUC7+WUC8+WUD1+WUD2+WUD3+WUD4+WUD5+WUD6+WUD7+WUD8+WUE1+WUE2+WUE3+WUE4+WUE5+WUE6+WUE7+WUE8+WUF1+WUF2+WUF3+WUF4+WUF5+WUF6+WUF7+WUF8+WUG1+WUG2+WUG3+WUG4+WUG5+WUG6+WUG7+WUG8+WH1+WH2+WH3+WH4+WH5+WH6+WH7+WH8+WUI1+WUI2+WUI3+WUI4+WUI5+WUI6+WUI7+WUI8+WUJ1+WUJ2+WUJ3+WUJ4+WUJ5+WUJ6+WUJ7+WUJ8+WUK1+WUK2+WUK3+WUK4+WUK5+WUK6+WUK7+WUK8=0.8;

 WLA1+WLA2+WLA3+WLA4+WLA5+WLA6+WLA7+WLA8+WLB1+WLB2+WLB3+WLA4+WLB5+WLB6+WLB7+WLB8+WLC1+WLC2+WLC3+WLC4+WLC5+WLC6+WLC7+WLC8+WLD1+WLD2+WLD3+WLD4+WLD5+WLD6+WLD7+WLD8+WLE1+WLE2+WLE3+WLE4+WLE5+WLE6+WLE7+WLE8+WLF1+WLF2+WLF3+WLF4+WLF5+WLF6+WLF7+WLF8+WLG1+WLG2+WLG3+WLG4+WLG5+WLG6+WLG7+WLG8+WLH1+WLH2+WLH3+WLH4+WLH5+WLH6+WLH7+WLH8+WLJ1+WLJ2+WLJ3+WLJ4+WLJ5+WLJ6+WLJ7+WLJ8+WLK1+WLK2+WLK3+WLK4+WLK5+WLK6+WLK7+WLK8=1.2;

 WLA1>=WUA1; WLA2>=WUA2; WLA3>=WUA3; WLA4>=WUA4; WLA5>=WUA5; WLA6>=WUA6; WLA7>=WUA7; WLA8>=WUA8; WLB1>=WUB1; WLB2>=WUB2; WLB3>=WUB3; WLB4>=WUB4; WLB5>=WUB5; WLB6>=WUB6; WLB7>=WUB7; WLB8>=WUB8; WLC1>=WUC1; WLC2>=WUC2; WLC3>=WUC3; WLC4>=WUC4; WLC5>=WUC5; WLC6>=WUC6; WLC7>=WUC7; WLC8>=WUC8; WLD1>=WUD1; WLD2>=WUD2; WLD3>=WUD3; WLD4>=WUD4; WLD5>=WUD5; WLD6>=WUD6; WLD7>=WUD7; WLD8>=WUD8; WLE1>=WUE1; WLE2>=WUE2; WLE3>=WUE3; WLE4>=WUE4; WLE5>=WUE5; WLE6>=WUE6; WLE7>=WUE7; WLE8>=WUE8; WLF1>=WUF1; WLF2>=WUF2; WLF3>=WUF3; WLF4>=WUF4; WLF5>=WUF5; WLF6>=WUF6; WLF7>=WUF7; WLF8>=WUF8; WLJ1>=WUJ1; WLJ2>=WUJ2; WLJ3>=WUJ3; WLJ4>=WUJ4; WLJ5>=WUJ5; WLJ6>=WUJ6; WLJ7>=WUJ7; WLJ8>=WUJ8; WLK1>=WUK1; WLK2>=WUK2; WLK3>=WUK3; WLK4>=WUK4; WLK5>=WUK5; WLK6>=WUK6; WLK7>=WUK7; WLK8>=WUK8;

 WUA1>=0; WUA2>=0; WUA3>=0; WUA4>=0; WUA5>=0; WUA6>=0; WUA7>=0; WUA8>=0; WUB1>=0; WUB2>=0; WUB3>=0; WUB4>=0; WUB5>=0; WUB6>=0; WUB7>=0; WUB8>=0; WUC1>=0; WUC2>=0; WUC3>=0; WUC4>=0; WUC5>=0; WUC6>=0; WUC7>=0; WUC8>=0; WUD1>=0; WUD2>=0; WUD3>=0; WUD4>=0; WUD5>=0; WUD6>=0; WUD7>=0; WUD8>=0; WUE1>=0; WUE2>=0; WUE3>=0; WUE4>=0; WUE5>=0; WUE6>=0; WUE7>=0; WUE8>=0; WUF1>=0; WUF2>=0; WUF3>=0; WUF4>=0; WUF5>=0; WUF6>=0; WUF7>=0; WUF8>=0; WUG1>=0; WUG2>=0; WUG3>=0; WUG4>=0; WUG5>=0; WUG6>=0; WUG7>=0; WUG8>=0; WH1>=0; WH2>=0; WH3>=0; WH4>=0; WH5>=0; WH6>=0; WH7>=0; WH8>=0; WUI1>=0; WUI2>=0; WUI3>=0; WUI4>=0; WUI5>=0; WUI6>=0; WUI7>=0; WUI8>=0; WUJ1>=0; WUJ2>=0; WUJ3>=0; WUJ4>=0; WUJ5>=0; WUJ6>=0; WUJ7>=0; WUJ8>=0; WUK1>=0; WUK2>=0; WUK3>=0; WUK4>=0; WUK5>=0; WUK6>=0; WUK7>=0; WUK8>=0;

References

- Abdel-Basset, M., Mohamed, M., Abdel-Monem, A., & Elfattah, M. A. (2022). New extension of ordinal priority approach for multiple attribute decision-making problems: design and analysis. *Complex & Intelligent Systems*. <https://doi.org/10.1007/s40747-022-00721-w>
- Adhikari, M., Ghimire, L. P., Kim, Y., Aryal, P., & Khadka, S. B. (2020). Identification and analysis of barriers against electric vehicle use. *Sustainability*, 12(12), 1–20. <https://doi.org/10.3390/SU12124850>
- Asadi, S., Nilashi, M., Iranmanesh, M., Ghobakhloo, M., Samad, S., Alghamdi, A., Almulihi, A., & Mohd, S. (2022). Drivers and barriers of electric vehicle usage in Malaysia: A DEMATEL approach. *Resources, Conservation and Recycling*, 177, 105965. <https://doi.org/10.1016/j.resconrec.2021.105965>
- Asadi, S., Nilashi, M., Samad, S., Abdullah, R., Mahmoud, M., Alkinani, M. H., & Yadegaridehkordi, E. (2021). Factors impacting consumers' intention toward adoption of electric vehicles in Malaysia. *Journal of Cleaner Production*, 282, 124474. <https://doi.org/10.1016/j.jclepro.2020.124474>
- Asif, M., Jajja, M. S. S., & Searcy, C. (2021). A Review of Literature on the Antecedents of Electric Vehicles Promotion: Lessons for Value Chains in Developing Countries. *IEEE Transactions on Engineering Management*. <https://doi.org/10.1109/tem.2021.3099070>
- Aziz, M., Marcellino, Y., Rizki, I. A., Ikhwanuddin, S. A., & Simatupang, J. W. (2020). Analysis of Technological Developments and Indonesian Government Support for Electric Cars [Studi Analisis Perkembangan Teknologi Dan Dukungan Pemerintah Indonesia Terkait Mobil Listrik]. *TESLA: Jurnal Teknik Elektro*, 22(1), 45. <https://doi.org/10.24912/tesla.v22i1.7898>
- Bah, M. K., & Tulkinov, S. (2022). Evaluation of Automotive Parts Suppliers through Ordinal Priority Approach and TOPSIS. *Management Science and Business Decisions*, 2(1), 5–17. <https://doi.org/10.52812/msbd.37>
- Bakker, G. (2021). Infrastructure killed the electric car. *Nature Energy*, 6(10), 947–948. <https://doi.org/10.1038/s41560-021-00902-w>
- Bigot, S. (2020). 8 things to know about electric cars in Russia. Eurasia Network. <https://eurasianetwork.eu/2017/08/19/7-things-to-know-about-electric-cars-in-russia/>
- Biresselioglu, M. E., Demirbag Kaplan, M., & Yilmaz, B. K. (2018). Electric mobility in Europe: A comprehensive review of motivators and barriers in decision making processes. *Transportation Research Part A: Policy and Practice*, 109, 1–13. <https://doi.org/10.1016/j.tra.2018.01.017>

- Carranza, F., Paturet, O., & Salera, S. (2014). *Norway, the most successful market for electric vehicles*. Proceedings of the 2013 World Electric Vehicle Symposium and Exhibition (EVS27). <https://doi.org/10.1109/EVS.2013.6915005>
- Chhikara, R., Garg, R., Chhabra, S., Karnatak, U., & Agrawal, G. (2021). Factors affecting adoption of electric vehicles in India: An exploratory study. *Transportation Research Part D: Transport and Environment*, 100, 103084. <https://doi.org/10.1016/j.trd.2021.103084>
- CSRI. (2019). *Gov't to Mass Produce EV By 2025, Minister Says*. Cabinet Secretariat of The Republic of Indonesia. <https://setkab.go.id/en/govt-to-mass-produce-ev-by-2025-minister-says/>
- D'Egmont, R. (2015). Electric Vehicles: The Norwegian Experience in Overcoming Barriers. *Bellona Europa*, 32(0), 2–5. https://bellona.org/assets/sites/4/Bellona-EV-Brief_The-Norwegian-Success-Story1.pdf
- Das, M. C., Pandey, A., Mahato, A. K., & Singh, R. K. (2019). Comparative performance of electric vehicles using evaluation of mixed data. *Opsearch*, 56(3), 1067–1090. <https://doi.org/10.1007/s12597-019-00398-9>
- Degirmenci, K., & Breitner, M. H. (2017). Consumer purchase intentions for electric vehicles: Is green more important than price and range? *Transportation Research Part D: Transport and Environment*, 51, 250–260. <https://doi.org/10.1016/j.trd.2017.01.001>
- Ehrenberger, S. I., Dunn, J. B., Jungmeier, G., & Wang, H. (2019). An international dialogue about electric vehicle deployment to bring energy and greenhouse gas benefits through 2030 on a well- to-wheels basis. *Transportation Research Part D: Transport and Environment*, 74, 245–254. <https://doi.org/10.1016/j.trd.2019.07.027>
- Fortuna, C. (2019). *If We Want To See More EV Adoption, We Need To Educate The Masses*. CleanTechnica. <https://cleantechnica.com/2019/03/31/if-we-want-to-see-more-ev-adoption-we-need-to-educate-the-masses/>
- GEM INDONESIA. (2020). *Electric Vehicle Indonesia Webinar 2020 - Part 1*. YouTube. https://www.youtube.com/watch?v=hRwREU6iskU&t=2574s&ab_channel=GEMINDONESIA
- Graham-Rowe, E., Gardner, B., Abraham, C., Skippon, S., Dittmar, H., Hutchins, R., & Stannard, J. (2012). Mainstream consumers driving plug-in battery-electric and plug-in hybrid electric cars: A qualitative analysis of responses and evaluations. *Transportation Research Part A: Policy and Practice*, 46(1), 140–153. <https://doi.org/10.1016/j.tra.2011.09.008>
- Greene, D. L., Park, S., & Liu, C. (2014). Analyzing the transition to electric drive vehicles in the U.S. *Futures*, 58, 34–52. <https://doi.org/10.1016/j.futures.2013.07.003>
- Gupta, R., & Hansmann, T. (2021). *Growing demand for electric vehicles a boost for Indonesia's economy – Opinion*. The Jakarta Post. <https://www.thejakartapost.com/academia/2021/05/27/growing-demand-for-electric-vehicles-a-boost-for-indonesias-economy.html>
- Habich-Sobiegalla, S., Kostka, G., & Anzinger, N. (2018). Electric vehicle purchase intentions of Chinese, Russian and Brazilian citizens: An international comparative study. *Journal of Cleaner Production*, 205, 188–200. <https://doi.org/10.1016/j.jclepro.2018.08.318>
- Haddadian, G., Khodayar, M., & Shahidehpour, M. (2015). Accelerating the Global Adoption of Electric Vehicles: Barriers and Drivers. *Electricity Journal*, 28(10), 53–68. <https://doi.org/10.1016/j.tej.2015.11.011>
- Haryanto, A. T., Utami, M. W. Dela, & Sutopo, W. (2020). Consumer perception analysis of electric car vehicle in Indonesia. *AIP Conference Proceedings*, 2217. <https://doi.org/10.1063/5.0000541>
- Huda, M., Aziz, M., & Tokimatsu, K. (2019). The future of electric vehicles to grid integration in Indonesia. *Energy Procedia*, 158(2018), 4592–4597. <https://doi.org/10.1016/j.egypro.2019.01.749>
- IEA. (2020). *Global EV Outlook 2020 – Analysis*. IEA. <https://www.iea.org/reports/global-ev-outlook-2020>
- IEA. (2021). *Global EV Outlook 2021 - Accelerating ambitions despite the pandemic*. Global EV Outlook 2021, 101. <https://iea.blob.core.windows.net/assets/ed5f4484-f556-4110-8c5c-4ede8bcb637/GlobalEVOutlook2021.pdf>
- IESR. (2021). *Indonesia Energy Transition Outlook 2021*. Institute for Essential Services Reform, 1–93. <https://iesr.or.id/en/pustaka/indonesia-energy-transition-outlook-ieto-2021>
- IQAir. (2022). *Indonesia Air Quality Index (AQI) and Air Pollution information* | AirVisual. IQAir. <https://www.iqair.com/indonesia>
- Jati, G. (2021). *The Government's Electric Vehicle Infrastructure Target is Still Creating Range Anxiety*. Institute for Essential Services Reform. <https://iesr.or.id/en/the-governments-electric-vehicle-infrastructure-target-is-still-creating-range-anxiety>
- Khadafi, M. (2018). *ELECTRIC VEHICLES: Spare Parts Industry Needs Incentives* [KENDARAAN LISTRIK: Industri Suku Cadang Butuh Insentif]. Otomotif.Bisnis. <https://otomotif.bisnis.com/read/20180703/275/811973/kendaraan-listrik-industri-suku-cadang-butuh-insentif>
- Khalili, S., Rantanen, E., Bogdanov, D., & Breyer, C. (2019). Global transportation demand development with impacts on the energy demand and greenhouse gas emissions in a climate-constrained world. *Energies*, 12(20). <https://doi.org/10.3390/en12203870>

- Krishna, G. (2021). Understanding and identifying barriers to electric vehicle adoption through thematic analysis. *Transportation Research Interdisciplinary Perspectives*, 10, 100364. <https://doi.org/10.1016/j.trip.2021.100364>
- Lambert, F. (2017). *Lack of awareness is surprisingly still the biggest problem for electric vehicle adoption*. Electrek. <https://electrek.co/2017/01/03/electric-vehicle-adoption-awareness/>
- Lambert, F. (2022, February 2). *Global market share of electric cars more than doubled in 2021 as the EV revolution gains steam*. Electrek. <https://electrek.co/2022/02/02/global-market-share-of-electric-cars-more-than-doubled-2021/>
- Li, W., Long, R., Chen, H., Chen, F., Zheng, X., & Yang, M. (2019). Effect of policy incentives on the uptake of electric vehicles in China. *Sustainability*, 11(12), 1–20. <https://doi.org/10.3390/su10023323>
- Liao, F., Molin, E., & van Wee, B. (2017). Consumer preferences for electric vehicles: a literature review. *Transport Reviews*, 37(3), 252–275. <https://doi.org/10.1080/01441647.2016.1230794>
- Maghfiroh, M. F. N., Pandyaswargo, A. H., & Onoda, H. (2021). Current readiness status of electric vehicles in indonesia: Multistakeholder perceptions. *Sustainability*, 13(23), 1–25. <https://doi.org/10.3390/su132313177>
- Mahmoudi, A., & Javed, S. A. (2022a). Probabilistic Approach to Multi-Stage Supplier Evaluation: Confidence Level Measurement in Ordinal Priority Approach. *Group Decision and Negotiation*. <https://doi.org/10.1007/s10726-022-09790-1>
- Mahmoudi, A., & Javed, S.A. (2022b). Performance Evaluation of Construction Sub-contractors using Ordinal Priority Approach. *Evaluation and Program Planning*, 91, 102022. <https://doi.org/10.1016/j.evalprogplan.2021.102022>
- Mahmoudi, A., Deng, X., Javed, S. A., & Yuan, J. (2021c). Large-Scale Multiple Criteria Decision-Making with Missing Values: Project Selection through TOPSIS-OPA. *Journal of Ambient Intelligence and Humanized Computing*, 12, 9341–9362. <https://doi.org/10.1007/s12652-020-02649-w>
- Mahmoudi, A., Deng, X., Javed, S. A., & Zhang, N. (2021b). Sustainable Supplier Selection in Megaprojects through Grey Ordinal Priority Approach. *Business Strategy and The Environment*, 30, 318–339. <https://doi.org/10.1002/bse.2623>
- Mahmoudi, A., Javed, S.A., & Mardani, A. (2021a). Gresilient Supplier Selection through Fuzzy Ordinal Priority Approach: Decision-making in Post-COVID era. *Operations Management Research*. <https://doi.org/10.1007/s12063-021-00178-z>
- Marciano, I., & Christian, J. A. (2020). *The Role of Electric Vehicles in Decarbonizing Indonesia's Road Transport Sector*. Institute for Essential Services Reform. <https://iesr.or.id/en/pustaka/the-role-of-electric-vehicles-in-decarbonizing-indonesias-road-transport-sector>
- Moeletsi, M. E. (2021). Socio-economic barriers to adoption of electric vehicles in South Africa: Case study of the gauteng province. *World Electric Vehicle Journal*, 12(4), 1–11. <https://doi.org/10.3390/wevj12040167>
- Natalia, Y., Rahman, I., & Hidayatno, A. (2020). Conceptual Model for Understanding the Policy Challenges of Electric Vehicle Adoption in Indonesia. *PervasiveHealth: Pervasive Computing Technologies for Healthcare*, 113–117. <https://doi.org/10.1145/3429551.3429557>
- O'Neill, E., Moore, D., Kelleher, L., & Brereton, F. (2019). Barriers to electric vehicle uptake in Ireland: Perspectives of car-dealers and policy-makers. *Case Studies on Transport Policy*, 7(1), 118–127. <https://doi.org/10.1016/j.cstp.2018.12.005>
- Olson, E. L. (2018). Lead market learning in the development and diffusion of electric vehicles. *Journal of Cleaner Production*, 172, 3279–3288. <https://doi.org/10.1016/j.jclepro.2017.10.318>
- Pamucar, D., Deveci, M., Gokasar, I., Martínez, L., & Köppen, M. (2022). Prioritizing Transport Planning Strategies for Freight Companies Towards Zero Carbon Emission Using Ordinal Priority Approach. *Computers & Industrial Engineering*, 108259. <https://doi.org/10.1016/j.cie.2022.108259>
- Pelletier, S., Jabali, O., & Laporte, G. (2014). *Battery Electric Vehicles for Goods Distribution: A Survey of Vehicle Technology, Market Penetration, Incentives and Practices* (CIRRELT-2014-43). CIRRELT, September, 51. <https://www.cirrelt.ca/documentstravail/cirrelt-2014-43.pdf>
- Perkins, R. (2021). *Europe overtakes China in EV sales growth in 2020*. S&P Global. <https://www.spglobal.com/platts/en/market-insights/latest-news/coal/012021-europe-overtakes-china-in-ev-sales-growth-in-2020>
- Prakash, S., Dwivedy, M., Poudel, S. S., & Shrestha, D. R. (2018). *Modelling the barriers for mass adoption of electric vehicles in Indian automotive sector: An Interpretive Structural Modeling (ISM) approach*. 2018 5th International Conference on Industrial Engineering and Applications, ICIEA 2018, 458–462. <https://doi.org/10.1109/IEA.2018.8387144>
- Prasetyo, W. B. (2021). *The Price of Electric Cars Is Expensive, There Needs To Be Incentives* [Harga Mobil Listrik Mahal, Perlu Ada Insentif]. Beritasatu. <https://www.beritasatu.com/otomotif/862807/harga-mobil-listrik-mahal-perlu-ada-insentif>

- Pratiwi, L. (2016). Barriers and Strategies for Transition to Electric Vehicles in BRICS Countries. TU Delft Library. <https://repository.tudelft.nl/islandora/object/uuid%3A0b25e361-31ec-4cbf-9653-1e8764ce1864>
- Presiden Republik Indonesia. (2019). *Presidential Regulation Number 55 of 2019 concerning the Acceleration Program for Battery Electric Vehicles for Road Transportation* [Peraturan Presiden Nomor 55 Tahun 2019 Tentang Percepatan program Kendaraan Bermotor Listrik Berbasis Baterai] (Battery Electric Vehicle) Untuk Transportasi Jalan. Republik Indonesia, 55.
- PWYP. (2019). *Energy Efficiency in the Transportation Sector, Case Studies in Indonesia and the European Union*. PWYP Indonesia. <https://pwypindonesia.org/en/energy-efficiency-in-the-transportation-sector-case-studies-in-indonesia-and-the-european-union/>
- Quartey-Papafio, T. K., Shajedul, I., & Dehaghani, A. R. (2021). Evaluating Suppliers for Healthcare Centre using Ordinal Priority Approach. *Management Science and Business Decisions*, 1(1), 5-11. <https://doi.org/10.52812/msbd.12>
- Rajper, S. Z., & Albrecht, J. (2020). Prospects of electric vehicles in the developing countries: A literature review. *Sustainability*, 12(5). <https://doi.org/10.3390/su12051906>
- Raksodewanto, A. A. (2020). *Compare Electric Car With Conventional Car* [Membandingkan mobil listrik dengan mobil konvensional], 89–92. <http://technopex.iti.ac.id/ocs/index.php/tpx20/tpx20/paper/viewFile/331/192>
- Ritchie, H. (2020). *Sector by sector: where do global greenhouse gas emissions come from?*. OurWorldInData. <https://ourworldindata.org/ghg-emissions-by-sector>
- Rudaty, & Tresya, R. (2021). *Construction of Electric Vehicle Policies in Indonesia, Types, and Prices*. International Conference For Democracy and National Resilience (ICDNR 2021). <http://dx.doi.org/10.2991/assehr.k.211221.016>
- Schröder, M., Iwasaki, F., & Kobayashi, H. (2021). *Promotion of Electromobility in ASEAN: States, Carmakers, and International Production Networks*. Economic Research Institute for ASEAN and East Asia (ERIA). <https://www.eria.org/uploads/media/Research-Project-Report/2021-03-Promotion-Electromobility-ASEAN/Promotion-of-Electromobility-in-ASEAN.pdf>
- SEAI. (2020). *Driving Purchases of Electric Vehicles in Ireland – Behavioural insights for policy series*. Sustainable Energy Authority of Ireland. <https://www.seai.ie/publications/Driving-Purchases-of-Electric-Vehicles-in-Ireland.pdf>
- Setiawan, V. N. (2021). *RI Imports Raw Materials for Electric Batteries Despite Abundance of Nickel, Why?* [RI Impor Bahan Baku Baterai Listrik Meski Nikel Melimpah, Mengapa?] - Pertambangan Katadata.co.id. Katadata. <https://katadata.co.id/happyfajrian/berita/61441bcc1ff03/ri-impor-bahan-baku-baterai-listrik-meski-nikel-melimpah-mengapa>
- Shajedul, I. (2021). Evaluation of Low-Carbon Sustainable Technologies in Agriculture Sector through Grey Ordinal Priority Approach. *International Journal of Grey Systems*, 1(1), 5-26. <https://doi.org/10.52812/ijgs.3>
- She, Z. Y., Qing Sun, Ma, J. J., & Xie, B. C. (2017). What are the barriers to widespread adoption of battery electric vehicles? A survey of public perception in Tianjin, China. *Transport Policy*, 56, 29–40. <https://doi.org/10.1016/j.tranpol.2017.03.001>
- Sidabutar, V. T. P. (2020). A study of the development of electric vehicles in Indonesia: prospects and constraints. [Kajian pengembangan kendaraan listrik di Indonesia: prospek dan hambataannya]. *Jurnal Paradigma Ekonomika*, 15(1), 21–38. <https://doi.org/10.22437/paradigma.v15i1.9217>
- Sierzechula, W., Bakker, S., Maat, K., & Van Wee, B. (2014). The influence of financial incentives and other socio-economic factors on electric vehicle adoption. *Energy Policy*, 68, 183–194. <https://doi.org/10.1016/j.enpol.2014.01.043>
- Sirait, S. (2020). *7 Factors Challenging the Implementation of Electric Vehicles in Indonesia* [7 Faktor yang Menjadi Tantangan Implementasi Kendaraan Listrik di Indonesia]. Carmudi. <https://www.carmudi.co.id/journal/7-faktor-yang-menjadi-tantangan-implementasi-kendaraan-listrik-di-indonesia/>
- Tarei, P. K., Chand, P., & Gupta, H. (2021). Barriers to the adoption of electric vehicles: Evidence from India. *Journal of Cleaner Production*, 291, 125847. <https://doi.org/10.1016/j.jclepro.2021.125847>
- Thorn, M. (2021). *Indonesia on Thorny Path to Electric Vehicles*. Jakarta Globe. <https://jakartaglobe.id/business/indonesia-on-thorny-path-to-electric-vehicles>
- Umah, A. (2021, September 21). *This is the reason electric cars are still expensive in Indonesia*. [Ini lho Alasan Mobil Listrik Masih Mahal di RI]. CNBC. <https://www.cnbcindonesia.com/news/20210921093008-4-277837/ini-lho-alasan-mobil-listrik-masih-mahal-di-ri>
- Utami, M. W. Dela, Yuniaristanto, & Sutopo, W. (2020). Adoption Intention Model of Electric Vehicle in Indonesia. *Jurnal Optimasi Sistem Industri*, 19(1), 70. <https://doi.org/10.25077/josi.v19.n1.p70-81.2020>
- Vassileva, I., & Campillo, J. (2017). Adoption barriers for electric vehicles: Experiences from early adopters in Sweden. *Energy*, 120, 632–641. <https://doi.org/10.1016/j.energy.2016.11.119>

- Volkswagen. (2019). *How electric car incentives around the world work*. Volkswagen.
<https://www.volkswagenag.com/en/news/stories/2019/05/how-electric-car-incentives-around-the-world-work.html>
- Wilberforce W, C. (2021). *Electric vehicles market Intelligence Report*. GreenCape.
<https://www.readkong.com/page/electric-vehicles-market-intelligence-report-greencape-2289456>
- World Population Review. (2022). *Greenhouse Gas Emissions by Country 2022*. World Population Review.
<https://worldpopulationreview.com/country-rankings/greenhouse-gas-emissions-by-country>
- Yuniza, M. E., Pratama, I. W. B. E., & Ramadhianti, R. C. (2021). Indonesias incentive policies on electric vehicles: the questionable effort from the government. *International Journal of Energy Economics and Policy*.
[https://doi.org/OI: https://doi.org/10.32479/ijeep.11453](https://doi.org/OI:https://doi.org/10.32479/ijeep.11453)
- Zigwheels. (2022). *20 New Electric Cars for Sale March 2022*. Zigwheels.
<https://www.zigwheels.co.id/en/mobil-baru/elektrik/>



publish.thescienceinsight.com
manager@thescienceinsight.com